

# **NUCLEAR MAGNETIC RESONANCE STUDIES OF MOLECULAR MOTIONS IN LIQUIDS**

*A Thesis Submitted*  
In Partial Fulfilment of the Requirements  
for the Degree of  
**DOCTOR OF PHILOSOPHY**

by  
**PRASANNA KUMAR MISHRA**

8781

to the

**DEPARTMENT OF PHYSICS**  
**INDIAN INSTITUTE OF TECHNOLOGY KANPUR**  
**1977 JUNE**

सर्वेदं आपोऽहं

To

*Dasharathi and Bhagabati*

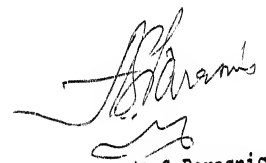
PHY-1977-D-MIS-NUC


LIBRARY  
CENTRAL LIBRARY  
No. A 54879.

19 AUG 1978

This is to certify that the work reported in this thesis has been carried out under my supervision in this Department. No part of this work has been submitted elsewhere for a degree.

1977.10.02  
Gandhi Jayanti

  
(A S Parasnis)  
Professor of Physics

POST GRADUATE OFFICE  
This thesis has been approved  
for the award of the Degree of  
Doctor of Philosophy (Ph.D.)  
in accordance with the  
regulations of the Indian  
Institute of Technology, Bombay  
Dated: 17. 4. 78 

## ACKNOWLEDGEMENTS

It has been a great privilege to have worked with Professors Arawind Shripad Parasnis and Bhagavatula Durga Nageswara Rao. It is but quite natural to find shades of them in all the endeavour. I treasure their examples on courage, fortitude, striving for excellence and truth. I am highly grateful to them.

I am deeply indebted to Professors T.M. Srinivasan and Gyan Mohan for their kind concern and encouragements during the course of the work. I am thankful to Professor Rajat Kumar Ray, who dispelled many a blues on and off the research and teaching laboratories which were rejuvenating, and Professors J. Mahanty, and P.T. Narasimhan for their kind interest in the work.

Many technicians who parted with their inimitable secret rites are Sarva Shri Pratap Singh, B.K. Jain, V.K. Sharma in Pumps and Compressors, J.S. Sharma in the Machine Shop, R.L. Arora, A.L. Athawale, H. Fatima Naqvi in the Electronics Shop, and J.N. Sharma and Piar Singh in Glass Blowing. Shri S.L. Kanaujia helped keeping the laboratory in good order. Sarva Shri H.K. Panda and Lalloo Singh rendered able office assistance. Shri S.L. Rathore did careful typing work. Shri G. Kameswara Rao gave some of his valuable time for proof reading. Dr K.N. Swamy Rao was a dear friend philosopher. To these I am indeed deeply grateful.

## TABLE OF CONTENTS

LIST OF TABLES	7
LIST OF FIGURES	8
SYMBOLS AND ABBREVIATIONS	11
SYNOPSIS	12
CHAPTER 1. INTRODUCTION	18
1. Basic Principle	20
2. Some Salient Points on the Review of Others Work	39
3. Scope of the present work	48
CHAPTER 2. EXPERIMENTAL METHODS	53
1. Spin Echo	53
2. Transmitter	63
3. Pulse Programmer	63
4. Receiver	68
5. Tank Coil	72
6. Transmitter-Tank Coil-Receiver Connection	72
7. Magnet	72
8. Field Gradient	73
9. Thermostat	73
10. Sample Preparation	75
11. Spectrometer Tuning	78
12. Signal Display and Measurement	79

13. $T_1$ Measurement	79
14. $D$ Measurement	80
15. Test Sample Runs	82
CHAPTER 3. SPIN-ROTATION RELAXATION IN LIQUIDS FOR DYNAMICALLY COHERENT REORIENTATION	85
CHAPTER 4. STUDIES IN SOME METHYL GROUP CONTAINING MOLECULAR LIQUIDS	97
1. $\text{CH}_3\text{I}$ and $\text{CH}_3\text{CN}$	125
2. $\text{CH}_3\text{NO}_2$	129
3. $\text{CH}_3\text{COCH}_3$ and $\text{CH}_3\text{SOCH}_3$	130
CHAPTER 5. STUDIES IN A GROUP OF ASSORTED MOLECULAR LIQUIDS	133
1. $\text{CH}_2\text{Cl}_2$ and $\text{CH}_2\text{I}_2$	150
2. $\text{C}_6\text{H}_5\text{OCH}_3$	156
3. $\text{C}_6\text{H}_5\text{CF}_3$	158
CHAPTER 6. SUMMARY AND CONCLUSIONS	161
APPENDIX ON THE ESTIMATION OF MOLECULAR RADIUS AND DIFFUSION COEFFICIENTS IN MOLECULAR LIQUIDS	167
LIST OF REFERENCES	179

## LIST OF TABLES

TABLE 4.1	THE ACTIVATION ENERGIES OF THE VARIOUS PARAMETERS IN THE METHYL GROUP CONTAINING COMPOUNDS	108
TABLE 4.2	THE CORRELATION TIMES IN THE METHYL GROUP CONTAINING COMPOUNDS	122
TABLE 4.3	SOME MOLECULAR PARAMETERS IN THE METHYL GROUP CONTAINING COMPOUNDS	124
TABLE 5.1	THE ACTIVATION ENERGIES OF THE VARIOUS PARAMETERS IN A GROUP OF ASSORTED COMPOUNDS	143
TABLE 5.2	THE CORRELATION TIMES IN A GROUP OF ASSORTED COMPOUNDS	151
TABLE 5.3	SOME MOLECULAR PARAMETERS IN A GROUP OF ASSORTED COMPOUNDS	152
TABLE APP.1	THE EXPERIMENTAL VALUES OF $D\eta/T$ AT DIFFERENT TEMPERATURES FOR VARIOUS COMPOUNDS	171
TABLE APP.2	COMPARISON OF MOLECULAR RADII OF SEVERAL COMPOUNDS BY VARIOUS METHODS	172
TABLE APP.3	DIFFUSION COEFFICIENTS IN SOME MOLECULAR LIQUIDS	177

# LIST OF FIGURES

FIGURE 1.	ECHO FORMATION WITH $90^{\circ}$ - $180^{\circ}$ PULSE SEQUENCE	55
FIGURE 2.	BLOCK DIAGRAM OF THE PULSED NMR ARRANGEMENT	62
FIGURE 3.	GATED OSCILLATOR	64
FIGURE 4.	PULSE PROGRAMMER	65
FIGURE 5.	DIFFERENTIATOR-INVERTER	66
FIGURE 6.	MIXER-INVERTER	67
FIGURE 7.	PULSE SHAPER	69
FIGURE 8.	RECEIVER	70
FIGURE 9.	RECEIVER LINEARITY CHECK. SIGNAL AMPLITUDE vs SPIN DENSITY PLOT	71
FIGURE 10.	FIELD GRADIENT ARRANGEMENT	74
FIGURE 11.	SAMPLE TUBE	77
FIGURE 12.	TEMPERATURE DEPENDENCE OF PROTON SPIN-LATTICE RELAXATION TIME ( $T_1$ ) AND SELF-DIFFUSION COEFFICIENT ( $D$ ) IN DISTILLED WATER	83
FIGURE 13.	TEMPERATURE DEPENDENCE OF PROTON SPIN-LATTICE RELAXATION TIME ( $T_1$ ) AND SELF-DIFFUSION COEFFICIENT ( $D$ ) IN BENZENE	84
FIGURE 14.	TEMPERATURE DEPENDENCE OF PROTON SPIN-LATTICE RELAXATION TIME ( $T_1$ ) AND SELF-DIFFUSION COEFFICIENT ( $D$ ) IN METHYL IODIDE	100
FIGURE 15.	TEMPERATURE DEPENDENCE OF PROTON SPIN-LATTICE RELAXATION TIME ( $T_1$ ) AND SELF-DIFFUSION COEFFICIENT ( $D$ ) IN ACETONITRILE	101
FIGURE 16.	TEMPERATURE DEPENDENCE OF PROTON SPIN-LATTICE RELAXATION TIME ( $T_1$ ) IN NITROMETHANE	102
FIGURE 17.	TEMPERATURE DEPENDENCE OF SELF-DIFFUSION COEFFICIENT ( $D$ ) IN NITROMETHANE	103

FIGURE 18.	TEMPERATURE DEPENDENCE OF PROTON SPIN-LATTICE RELAXATION TIME ( $T_1$ ) IN ACETONE	104
FIGURE 19.	TEMPERATURE DEPENDENCE OF SELF-DIFFUSION COEFFICIENT ( $D$ ) IN ACETONE	105
FIGURE 20.	TEMPERATURE DEPENDENCE OF PROTON SPIN-LATTICE RELAXATION TIME ( $T_1$ ) IN DIMETHYL SULFOXIDE	106
FIGURE 21.	TEMPERATURE DEPENDENCE OF SELF-DIFFUSION COEFFICIENT ( $D$ ) IN DIMETHYL SULFOXIDE	107
FIGURE 22.	PLOTS OF THE VARIATION OF THE VARIOUS RELAXATION RATES WITH TEMPERATURE IN METHYL IODIDE	111
FIGURE 23.	PLOTS OF THE VARIATION OF THE VARIOUS RELAXATION RATES WITH TEMPERATURE IN ACETONITRILE	112
FIGURE 24.	PLOTS OF THE VARIATION OF THE VARIOUS RELAXATION RATES WITH TEMPERATURE IN NITROMETHANE	113
FIGURE 25.	PLOTS OF THE VARIATION OF THE VARIOUS RELAXATION RATES WITH TEMPERATURE IN ACETONE	114
FIGURE 26.	PLOTS OF THE VARIATION OF THE VARIOUS RELAXATION RATES WITH TEMPERATURE IN DIMETHYL SULFOXIDE	115
FIGURE 27.	PLOTS OF THE VARIATION OF $\tau_{02 \text{ eff}}$ , THE EFFECTIVE REORIENTATIONAL CORRELATION TIMES, WITH TEMPERATURE OF THE VARIOUS COMPOUNDS STUDIED	117
FIGURE 28.	TEMPERATURE DEPENDENCE OF PROTON SPIN-LATTICE RELAXATION TIME ( $T_1$ ) IN METHYLENE CHLORIDE	135
FIGURE 29.	TEMPERATURE DEPENDENCE OF SELF-DIFFUSION COEFFICIENT ( $D$ ) IN METHYLENE CHLORIDE	136
FIGURE 30.	TEMPERATURE DEPENDENCE OF PROTON SPIN-LATTICE RELAXATION TIME ( $T_1$ ) IN METHYLENE IODIDE	137
FIGURE 31.	TEMPERATURE DEPENDENCE OF SELF-DIFFUSION COEFFICIENT ( $D$ ) IN METHYLENE IODIDE	138
FIGURE 32.	TEMPERATURE DEPENDENCE OF PROTON SPIN-LATTICE RELAXATION TIME ( $T_1$ ) IN ANISOLE	139
FIGURE 33.	TEMPERATURE DEPENDENCE OF SELF-DIFFUSION COEFFICIENT ( $D$ ) IN ANISOLE	140
FIGURE 34.	TEMPERATURE DEPENDENCE OF PROTON ( $^1\text{H}$ ) AND FLUORINE ( $^{19}\text{F}$ ) SPIN-LATTICE RELAXATION TIME ( $T_1$ ) IN $\alpha$ -TRIFLUORO TOLUENE	141

FIGURE 35.	TEMPERATURE DEPENDENCE OF SELF-DIFFUSION COEFFICIENT ( $D$ ) IN $\alpha$ -TRIFLUORO TOLUENE	142
FIGURE 36.	PLOTS OF THE VARIATION OF THE VARIOUS RELAXATION RATES WITH TEMPERATURE IN METHYLENE CHLORIDE	146
FIGURE 37.	PLOTS OF THE VARIATION OF THE VARIOUS RELAXATION RATES WITH TEMPERATURE IN METHYLENE IODIDE	147
FIGURE 38.	PLOTS OF THE VARIATION OF THE VARIOUS RELAXATION RATES WITH TEMPERATURE IN ANISOLE	148
FIGURE 39.	PLOTS OF THE VARIATION OF THE VARIOUS RELAXATION RATES WITH TEMPERATURE IN $\alpha$ -TRIFLUORO TOLUENE	149
FIGURE 40.	PLOTS OF THE VARIATION OF THE EFFECTIVE REORIENTATIONAL CORRELATION TIMES ( $\tau_{02}$ eff) WITH TEMPERATURE IN METHYLENE CHLORIDE AND METHYLENE IODIDE	155

## SYMBOLS AND ABBREVIATIONS

The work presented here follow the symbols and units as described in the second edition of the booklet, *Quantities, Units, and Symbols* prepared and published by the Symbols Committee of the Royal Society in the year 1975 A.D. In labeling the figure axes and giving the column headings in the tables the prescription of the aforementioned booklet is followed.

The journal abbreviations are according to the American Institute of Physics' *Style Manual* published in April 1973. Other abbreviations follow the recommendations therein except that the term nuclear magnetic resonance is abbreviated as nmr.

A deviation from the prescribed SI units is the use of the traditional  $H$  for the magnetic induction or magnetic flux density rather than the prescribed  $B$  and also to loosely call it the magnetic field.

## SYNOPSIS

PRASANNA KUMAR MISHRA  
Ph.D  
INDIAN INSTITUTE OF TECHNOLOGY KANPUR  
NUCLEAR MAGNETIC RESONANCE STUDIES  
OF MOLECULAR MOTIONS IN LIQUIDS

In understanding the liquid state the study of the motion of the constituent atoms and molecules is of great importance. The translational and rotational motions of the constituents modulate the various interactions, and also the positional and motional autocorrelations which are amenable to nmr. Other advantages of the nmr technique are that it is a non-destructive method of investigation of the substance *in situ* and that although the help of models is required to be taken due to unsuitable time scales involved, the information obtained through nmr is quite significant in view of the present state of knowledge about the molecular dynamics in molecular liquids. Measurement of spin-lattice relaxation time and of self-diffusion coefficient of various neat compounds by using pulsed nmr technique as a function of molecular kinetic energy and their analysis provides valuable information such as the translational, reorientational, rotational and exchange correlation times, the extent of translation-rotation coupling, the effect of intramolecular group motion on

the entire molecular motion, the effect of molecular shape, size, inertia (mass, moment of inertia), dipole moment on the various motions *etc.*.

A brief account of the principle of nmr with emphasis on the pulsed nmr measurable parameters is given in Chapter 1 of this thesis. The various relaxation mechanisms discernible are described. The importance of the spin-rotation interaction and the magnificent ability of the nmr technique to give information about the angular momentum correlation time are particularly emphasised. Self-diffusion coefficient, a measure of the linear velocity autocorrelation function, measured by the nmr technique is contrasted with the radioactive tracer diffusion and other techniques. The relevance of correlation function method is emphasised. Such a method leads to the problem of various molecular models and the various estimates of the molecular parameters. Under these premises other workers' study of the liquid state is reviewed. The nature of an Arrheniuslike equation is discussed. With these in view, the purpose of the work described in this Thesis has been to study the molecular motion of small, simple molecules with fairly simple intermolecular potential and a few possibilities in internal mobility in neat phase, along their liquid-vapour co-existence curve. Such a study would give us an idea about how far the belief, that even the motion of non-symmetrical molecules is inertial and coherent, is true. The other purpose

has been to chart the various rotational and translational courses of the molecules in the high temperature region, namely from room temperature to say about 80 °C below the critical temperature. The effect of translation-rotation coupling and the influence of the molecular shape, size and dipole moment on the molecular motion is looked into. The self-diffusion coefficient and the coefficient of viscosity with their inter-relationships are especially looked into to discern the stamp of micro motions on them. The prevalent belief that a hard sphere model for the molecules is good enough to explain most of the experimental findings in the liquid state of matter is tested in the Appendix. Also discussed in the appendix are the various approaches to estimate the self-diffusion coefficients in molecular liquids,  $\chi$  parameter to test for the type of motion (diffusional and inertial) and the translation-rotation coupling are discussed there.

Chapter 2 consists of the description of the experimental set up for the measurement of fluorine ( $I=19$ ) and proton ( $I=1$ ) spin-lattice relaxation times and molecular self-diffusion coefficients in various compounds as a function of temperature by pulsed nmr technique. The salient features of the home-made 9.8 MHz pulsed nmr spectrometer and the experimental methods of data collection and the required parameter evaluation are given in this chapter. The scope and limitations of the spectrometer, tuning of the spectrometer, test sample run, reproducibility,

and limit of error in the experimental data are discussed. The bulk of  $T_1$  and  $\rho$  data thus obtained could be of help in understanding molecular liquids.

With a view to analyse data later, Chapter 3 is devoted to the theoretical aspects of rotational motions. It has been an observed fact that the translational motion of the molecules is most likely diffusional, *i.e.* the motion consists of short random steps. The rotational motions have been found to be highly characteristic of the molecules. Hence a detailed discussion of the diffusional (surrounding limited) and inertial (free) motions is given. In case of the coherent reorientational motion the angular velocity autocorrelation time varies directly as the square root of temperature. The surrounding dependent diffusive motion is strongly temperature dependent.

Chapters 4 and 5 contain respectively both data and analyses of results in simple molecules containing the methyl ( $\text{CH}_3$ ) group, *viz.*  $\text{CH}_3\text{I}$ ,  $\text{CH}_3\text{CN}$ ,  $\text{CH}_3\text{NO}_2$ ,  $\text{CH}_3\text{COCH}_3$ ,  $\text{CH}_3\text{SOCH}_3$  and some assorted molecules such as  $\text{CH}_2\text{Cl}_2$ ,  $\text{CH}_2\text{I}_2$ , anisole ( $\text{C}_6\text{H}_5\text{OCH}_3$ ), and  $\alpha$ -trifluoro toluene ( $\text{C}_6\text{H}_5\text{CF}_3$ ).

The basic feature of the simple methyl group compounds except dimethyl sulfoxide studied in Chapter 4 is the slow variation of the spin-lattice relaxation time with temperature. In all except  $\text{CH}_3\text{SOCH}_3$ , the reorientational motion is characterised

by the inertial nature. The good deal of reorientational coherence in  $\text{CH}_3\text{NO}_2$  does not seem to be getting affected by the large dipole moments of the molecules of such a highly polar liquid. The reorientational motion in  $\text{CH}_3\text{SOCH}_3$  is diffusive in nature. In the molecular dynamics of  $\text{CH}_3\text{SOCH}_3$ , there seems to be a strong translation-rotation coupling. Liquid  $\text{CH}_2\text{Cl}_2$  and  $\text{CH}_2\text{I}_2$  although belong to the same family of halogen derivatives and though are structurally similar, the reorientational process in the former is inertial, whereas that in the later is diffusional. In addition to this,  $\text{CH}_2\text{I}_2$  also shows fairly strong translation-rotation coupling and that the motion about the parallel symmetry axis of  $\text{CH}_2\text{Cl}_2$  is somewhere between inertial and diffusional limits - but close to the diffusion end. Anisole and  $\alpha$ -trifluorotoluene have mobile groups within the molecules. A simple analysis of anisole data leads to the observation of a correlation time characteristic of a free motion which might arise due to the intramolecular  $\text{CH}_3$  group rotation. In  $\alpha$ -trifluorotoluene the  $^{19}\text{F}$  relaxation shows large, highly temperature sensitive spin-rotation interaction which seemingly arises because of the  $\text{CF}_3$  rotation, and seems to be temperature activated.  $^1\text{H}$  intramolecular interaction is modulated by the overall diffusive reorientation of the  $\text{C}_6\text{H}_5\text{CF}_3$  molecule.

In the concluding chapter (Chap. 6) a summary of the work presented in this thesis is given and it is felt that molecular liquids will be better understood combining all the ancillary experimental data.

*The Walrus said, "Let us talk of many things ...*

## CHAPTER 1

### INTRODUCTION

Of all the branches of magnetic resonance nuclear magnetic resonance has come a long way in looking ably into the static and dynamic behaviour of molecules in matter. It has a special place of pride so far as the dynamical studies in fluids are concerned. Liquids, the awkward in-between of the solid and gas phases (Powles (1974)), have proven difficult for comprehension. With the success achieved in understanding atomic liquids molecular liquids are gradually engaging the attention of the investigators. NMR has established itself as a good experimental tool in the study of molecular liquids.

The microscopic study of matter often boils down in practice to the study of their constituents: molecules and atoms. So far as molecular physics is concerned the research interest falls into two distinct categories. First, the study of the static properties of the molecules, arising because of the charge distribution within, gives an idea about the molecule *per se*. Chemical and biological scientists exult in such information. Second, the study of the dynamic properties of the molecules lets us know how they behave as a community with mutual interactions. This is of immense interest to those who wish to know about the molecular dynamics

in that state of matter, matter in various phases of existence and the like. The subject of our study is a part of the second.

The study of liquids from the time of van der Waals to the present has given workers in this field a very hard time. Liquids are neither as orderly as solids nor as random as gases. There exists only a short range order.

In the study of molecular dynamics two important aspects come to the fore. First, the molecule moves as a whole body translating, rotating, reorientating. Second, there are inner convulsions within the molecule where the various parts which make the molecule, can sometimes rotate relative to one another, reorientate or get exchanged with the surrounding. If the whole and the segmental motions are responsive to each other because of the coupling between them, the dynamical study becomes complicated and more challenging. NMR rises to the occasion in exploring into molecular motion in fluids and particularly scores high so far as its contribution to the understanding of molecular rotation is concerned. Although nmr times and molecular motion characteristic times are vastly different ( $10^{-8}$ s vs  $10^{-12}$ s) the systematics of temperature and pressure variations of nmr parameters have enabled one to make models and infer about the dynamics.

## I.1 Basic Principle

A collection of nuclear spins each of spin  $I$  in a zero external magnetic field has all its  $(2I+1)$  levels equally populated. When an external magnetic field  $H_0$  is applied the Zeeman type interaction given by

$$E = - \vec{\mu} \cdot \vec{H}_0 , \quad (1.1)$$

(where  $E$  is the energy of the magnetic dipole of moment  $\vec{\mu}$ ) lifts the degeneracy of the system. The spins interacting with the other degrees of freedom, called the lattice or reservoir, will tend to come to thermal equilibrium with the lattice. As the lattice is taken as a classical system the population distribution in the various nondegenerate levels will be governed by the Boltzmann statistics. The rate at which a net macroscopic Magnetization  $M_0 = \chi_0 H_0$  (where  $\chi_0$  is the bulk static susceptibility) is established is called the spin-lattice relaxation rate. The rate at which the coherence existing between the spins is lost, i.e. the rate at which the spin system in bulk matter attains thermal equilibrium within itself is called the spin-spin relaxation rate. Such relaxations in bulk matter are given by the Bloch's phenomenological equation (see Abragam (1961)),

$$\frac{d\vec{M}}{dt} = \gamma(\vec{M} \times \vec{H}) - \hat{x} \frac{M_x}{T_2} - \hat{y} \frac{M_y}{T_2} - \hat{z} \frac{M_z - M_0}{T_1} , \quad (1.2)$$

where  $\gamma$  is the gyromagnetic ratio of the nucleus under consideration and  $M_x$ ,  $M_y$ ,  $M_z$  are the components of the bulk

magnetization  $\underline{M}$ , and the magnetic field  $\underline{H}$  is set along the z-direction. In solids the spins are coupled more tightly to each other than to the lattice, which makes the spin-spin relaxation times much shorter than the spin-lattice relaxation times. Thus, spins in solids are said to have a spin temperature distinct from the lattice temperature and also the system is visualized as one with many degrees of freedom. In liquids the spin-spin interaction is quite weak and is of the same magnitude of strength as the spin-lattice interaction. Therefore it is assumed that the nuclei in a molecule (and some time groups of nuclei too) see the lattice independently of other spins or group(s) of spins. Both the relaxation times are of the same order of magnitude unless special cases like quadrupolar interactions, exchange of the resonating nuclei between nonequivalent sites, coupling to a quadrupolar nucleus and presence of paramagnetic nuclei occur. Due to the rapid molecular motions in liquids the local fields which are an index of the strength of interaction experienced by the nuclear spin get very much weakened leading to the observed narrow resonance line widths: in the magnetic field equivalent, of the order of a fraction of a milligauss. This motional narrowing coupled with the relative heaviness of the nuclei enable us to express in classical terms the very cumbersome quantum mechanical expressions for the molecular motions in a liquid. The density matrix (Wangsness and Bloch (1953), Redfield (1965) and the linear response methods

(Kubo (1957a, 1957b, 1966), Deutch and Oppenheim (1968), Kivelson and Ogan (1974)) are most suitable for this purpose. In the case of weak coupling of the nuclear spin to the lattice although both the methods give the same result, the density matrix method is more conventionally used. Further, this method obviates the consideration of the limitations of the phenomenological Bloch equation which is valid in liquids because of a number of generally realizable conditions. The molecular motions do not produce any shifts in the energy levels of the spin system but they affect relaxation mechanisms.

Molecular motions in liquids can be of two extreme kinds: The diffusional motions are attributes of asymmetric large molecules. Here, the molecular motion greatly depends on the forces and torques exerted by the surrounding molecules. Therefore in such asymmetric molecular liquids it is natural to expect the viscosity parameter to be a good indicator of molecular dynamics. In small spherical molecules the intermolecular forces and torques will be of less consequence as the potentials are expected to be small, symmetric. The molecular motion then is more or less oblivious of the surroundings, and the molecular inertial parameters, *viz.* mass and moment of inertia, chiefly determine the translational and rotational motions and therefore such characteristic motions are called inertial. The wide variety of molecular symmetry and inertia ensures a spectrum o

possibilities between these two extreme models. Cases of isotropic and anisotropic motion arise depending on whether the motions of and about the molecular axes are similar or otherwise. Sometimes one could expect the motion of a molecule as a whole to be diffusional but the motion of its segment(s) to be inertial. A case to the point is the overall diffusive motion of biggish organic molecules and the facile motion of the segmental  $-CH_3$  group which is quite free or inertial. The internal rotational motions can be of various kinds as described in the following:

1. In the 'Free Rotation' kind the internal rotation is free or inertial.
2. In the 'Rotational Diffusive' kind the internal motion is such that a vector fixed to the internal group changes in small angular steps.
3. When the rotational motion of such a vector takes place in large angular steps with fixed molecular orientation between jumps, such motions are called 'Jump Diffusive'.
4. Random large angle jumps in angular position with free rotation during the time between them entails the name 'Free Diffusive'.

The microdynamic behaviour of liquid molecules, namely their translation and rotation, leave their signatures on the measurable 'dynamic' parameters like the relaxation times and self-diffusion coefficients. It has been an interesting exercise theoretically to relate the micromotions to macroparameters and infer about the molecular dynamics from the observed macroparameters in liquids. (See Powles (1966), Waugh (1966), Hertz (1967), Zeidler (1971a) and Jonas (1973).) Gordon (1968) shows

how the correlation functions can be related to the micro-dynamics and how the correlation functions can be extracted from the Fourier transformation of the various spectroscopically observed macroparameters. The mathematical ground work required for a quantitative appreciation is given below which shows how the spin relaxation measurements and self-diffusion coefficients can convey some information about molecular motion.

In liquids, because of the rapid molecular motion the spins are very weakly coupled to the lattice. Such a time-dependent coupling can be given by a Hamiltonian

$$H_1(t) = \sum_{q=-2}^2 (-1)^q F^q(t) A^{-q}, \quad (1.3)$$

where  $F^q(t)$  is the lattice operator, a stationary random function of time which carries the molecular time development information;  $A^q$  is the space-quantized spin operator. The irreducible operators  $F^q$  and  $A^q$  transform exactly like the spherical harmonics. The contribution of an interaction of the type cited above to the spin-lattice relaxation rate is

$$1/T_1 \propto J(\omega) = \int_0^\infty e^{-i\omega\tau} G(\tau) d\tau, \quad (1.4)$$

where  $G(\tau)$ , the correlation function of the lattice parameters, is given by

$$\begin{aligned} G(\tau) &= \sum_q G_q(\tau) \\ &= \sum_q \langle F^{q*}(t) F^q(t+\tau) \rangle_{av} \\ &= \sum_q \langle F^{q*}(0) F^q(\tau) \rangle_{av}, \quad (1.5) \end{aligned}$$

with  $\langle \dots \rangle_{av}$  standing for the ensemble average, and  $J(\omega)$  is the spectral density at angular frequency  $\omega$ . For a stationary process the decay of the correlation function is given by an exponential relation with characteristic time  $\tau_c$ , the correlation time for the analogous fluctuation (molecular motion) under consideration, such as

$$\langle F^q(0) F^q(\tau) \rangle_{av} = \langle |F^q(0)|^2 \rangle_{av} e^{-|\tau|/\tau_c}. \quad (1.6)$$

Hence the relaxation rate for such a motion would be

$$1/T_1 \propto \Sigma \langle |F^q(0)|^2 \rangle_{av} \tau_c / (1 + \omega^2 \tau_c^2). \quad (1.7)$$

In the present studies of molecular dynamics we have to simply pin-point the fluctuations contributing to relaxation and then try writing down the lattice and spin functions. All except  $\tau_c$  in the foregoing equation being known, it is a small step further to have a glimpse of the characteristic time of the fluctuation under consideration. One great simplification in the calculation of  $\tau_c$  occurs as the molecular motional processes are extremely rapid (the motional characteristic times are of the order of  $10^{-11}$  to  $10^{-14}$ s) thus making for nmr experiments  $\omega \tau_c \ll 1$  (as the usual working frequency ranges from 1 to 300 MHz). This, popularly known as extreme narrowing condition, gives

$$1/T_1 \propto J(0) = \sum_q \langle |F^q(0)|^2 \rangle_{av} \tau_c ,$$

$$\text{or} \quad \tau_c = \int_0^\infty \sum_q \langle F^q(0) F^q(\tau) \rangle_{av} d\tau / \sum_q \langle |F^q(0)|^2 \rangle_{av} \quad (1.8)$$

The integral on the right hand side shows that the correlation time is related to the area enclosed by the correlation function but not to the actual shape of the correlation function. Light scattering and infrared methods (Gordon (1968) Berne and Pecora (1976)) give information about the correlation function *per se*. The correlation function obtained from such experiments integrated appropriately (Steele (1963a, 1963b)) can serve as a check on the nmr results. Further, the importance of the integrals of the correlation functions is no less in that they can also be related to appropriate macroscopic transport coefficients (see Chester (1963), Zwanzig (1965), Kubo (1966), Eglestaff (1967) and Steele (1969)). A frequency dependent relaxation rate measurement (Noack (1971)) can surely provide more information about the molecular dynamics.

The same kind of molecular motion can simultaneously modulate several interactions leading to spin relaxation. With each kind of the motion a characteristic motional correlation time is associated. Therefore the analysis of the various relaxation rates leads to the determination of the motional correlation times.

The translational correlation time is a measure of the persistence of the translational motion. It is natural to expect

the self-diffusion coefficient and intermolecular dipolar interaction, which are predominantly intermolecular spin separation dependent, to be governed by translational correlation time  $\tau_t$ .

The persistence of molecular orientation in the laboratory frame will be a measure of the reorientational correlation time  $\tau_\theta$ . It is natural to expect a relation between  $\tau_\theta$  and rotational diffusion coefficient ( $\mathcal{D}_{\text{rot}}$ ). Since an intramolecular dipolar vector, because of the molecular motion, can have different orientations relative to an external magnetic field, the intramolecular dipolar relaxation rate can give an idea of  $\tau_\theta$ . In the case of the quadrupolar nuclei the relaxation is due to the strong coupling between the quadrupole moment and the intramolecular field gradient. Molecular tumbling (i.e. orientational changes) modulates this interaction and hence a study of the quadrupolar relaxation rate could finally lead to a knowledge of  $\tau_\theta$ . The chemical shielding at a resonating nucleus arises because of the bilinear coupling between the resonating spin and the external field through the surrounding molecular electrons. If the coupling is isotropic the chemical shift or equivalently the local magnetic field is not modulated by the molecular orientation. However anisotropic chemical shift leads to a fluctuation of the local field at the resonating spin and therefore to spin relaxation. Thus an estimate of the contribution of anisotropic chemical shift to relaxation can also give information about  $\tau_\theta$ .

The characteristic time for angular momentum correlation  $\tau_J$  is a very important parameter. *A priori*, the persistence of the rotational motion  $\tau_J$  is expected to be determined by the molecular moment of inertia and the intermolecular frictional torques. Along with the molecular rotation, the molecular electrons too rotate and give rise to a local magnetic field at the resonating spin persisting as long. The local field fluctuates with the fluctuation of the molecular rotation. The coupling between this fluctuating local field and the resonating spin is responsible for the spin-rotation relaxation. The determination of the spin-rotation relaxation rate would thus lead to  $\tau_J$  evaluation.

The molecular free rotational correlation time ( $\tau_{\text{free}}$ ), determined by the thermal kinetic energy and the moment of inertia is another rotational parameter useful for understanding the dynamics.

A nuclear spin type under observation, if migrating from one molecular site to another gives rise to a small residence time at a site which suitably modulates the nmr relaxation rate. The rate studies can therefore yield such average residence times. Sometimes the resonating nuclear spins, though static in a molecule, if coupled to an exchanging spin or a fast relaxing spin bear the mark of the prevalent process. Rotating frame experiments (Farrar and Becker (1971)) proved convenient to determine such 'exchange correlation times'  $\tau_e$ .

Although  $\tau_\theta$  and  $\tau_J$  are the characteristic times related to the general rotational motion of the molecule they must be properly differentiated. The molecular collisions set in torques which affect the molecular rotation. Therefore it is the molecular collisions which determine  $\tau_J$ . In a classical rotational random walk having short free rotations interrupted by hard collisions (the diffusion limit) short  $\tau_J$ s are found. The average angle of rotation  $\bar{\theta}$  if short, many random walk steps will then be necessary for a sizeable orientational change (say by 1 radian) and therefore  $\tau_\theta$  is much longer than  $\tau_J$ . This is the diffusion limit. For small, symmetric molecules the angular velocity is quite large and therefore  $\bar{\theta}$  is large during  $\tau_J$  and hence  $\tau_\theta \sim \tau_J$ . This is the inertial situation. In the free gas situation the collisions are few and far between, although during the interval between collisions there may be sizeable orientational change thus making  $\tau_J > \tau_\theta$ . The relative values of  $\tau_J$  and  $\tau_\theta$  and the systematics of their variation with external constraints like temperature and pressure would yield a picture about the molecular dynamics. In the following the relationships between the correlation times, relaxation rates and self-diffusion coefficient is discussed.

The self-diffusion coefficient is a measure of the linear velocity autocorrelation. The characteristic time of the linear velocity autocorrelation is directly related to the self-diffusion coefficient. The Bloembergen, Purcell and Pound (1948) correlation function approach for a spherical body of radius 'a' finally

leads to the relation

$$\tau_t = 2a^2/D, \quad (1.9)$$

where  $\tau_t$  is the translational correlation time, and  $D$  the self-diffusion coefficient. As the self-diffusion coefficient and the intermolecular dipolar interaction arise because of the translational motion of the molecules, it has been gainfully shown by Torrey (1953) that in the random flight model of the molecules undergoing isotropic translational diffusion, in the limit of small mean squared flight paths and small times between the jumps,

$$(1/T_1)_{\text{inter}} = \pi \gamma^4 \hbar^2 N_A n \rho / (5 M_r a D), \quad (1.10)$$

where  $(1/T_1)_{\text{inter}}$  is the intermolecular dipolar contribution to the relaxation rate,  $n$  is the number of resonating spins per molecule,  $N_A$  is the Avogadro number,  $\rho$  is the density of the liquid sample under consideration,  $M_r$  is the molecular weight of the compound under study, and  $a$  is the average hard sphere radius. This result has the explicit assumption that the resonating spin is situated at the centre of the molecule. Hubbard (1963a), however, estimated that the consideration of off-centre resonating spins increases the relaxation rate estimation by only about 6%. Torrey's derivation also did not take into account the radial distribution function of the liquid. Consideration of the radial distribution function will increase the intermolecular relaxation rate estimation. The experimental method for estimating the intermolecular relaxation rate is through the dilution study in the perdeuterated analogue of the compound. The concentration dependent relaxation rate of the

substance in solution with its perdeuterated analogue is extrapolated to zero concentration to give the intramolecular relaxation rate (see for example, Bonera, Rigamonti (1965), Powles and Figgins (1965, 1967), Gillen, Schwartz and Noggle (1971)). Subtracting the intramolecular relaxation rate from the total relaxation rate of the normal substance gives the intermolecular relaxation rate. This method though very elaborate and accurate, is very often thwarted by the non-availability of the perdeuterated analogue compounds. However, Torrey's formula even without the inclusion of the purported corrections gives very good intermolecular relaxation rate estimates. Works which have also corroborated such a feeling are by Mitchell and Eisner (1960), Eisner and Mitchell (1961), Moniz, Steele and Dixon (1963), Powles and Figgins (1965), Muller (1966), Harmon and Muller (1969), Bull and Jonas (1970), Leblond *et al* (1971), Gillen *et al* (1971), Hwang and Freed (1975), Zeidler (1975), and Sandhu (1977). It is also realized that although a diffusion model predicts  $\tau_t$  well the prediction of  $\tau_\theta$  from the viscosity ( $\eta$ ) dependent Debye diffusion model,

$$\tau_\theta = 4\pi\eta a^3/3kT, \quad (1.11)$$

is many a times quite erroneous.

The molecular radius needed to estimate the intermolecular relaxation rate is obtained using the Stokes-Einstein relation,

$$a = kT/6\pi\eta D, \quad (.12)$$

where  $\eta$  is the coefficient of viscosity. The average molecular radius over the experimental temperature range is obtained using  $a$  and  $\eta$  values. It is usually seen that, 'a' is about constant

over the experimental temperature range. Although the validity of such a relation for microscopic bodies moving in a surrounding of its own kind is suspect (Edwards (1970)), the good intermolecular relaxation rate estimates arising thereof somewhat justifies the means. It is shown in the appendix that the molecular radius estimated using the Stokes-Einstein relation happens to be of lowest magnitude compared to the Lennard-Jones radius, van der Waals radius and the hexagonal close packing radius of the molecule in the liquid phase. This being so, the use of any molecular radius other than the one derived by the Stokes-Einstein relation underestimates the intermolecular dipolar relaxation rate. Further, it is also shown in the appendix that when the hexagonal close packing radius estimates are used for calculating the relaxation rates, translational and rotational microviscosity factors (Gierer and Wirtz (1953)) must be used so that the relaxation rates are not underestimated. This consideration is automatically accounted for by the use of Stokes-Einstein radius estimates as shown in the appendix. Therefore, in the present estimation of the intermolecular dipolar relaxation rate a two step process is involved: in first showing the about constancy of  $\eta/T$  and calculating the average molecular radius therefrom, and then using the Torrey's relation to calculate the intermolecular dipolar relaxation rate.

Bloembergen, Purcell and Pound (1948) following Debye's method (Debye (1929)) for isotropic rotational diffusion of the dipole moment vector of the polar molecules, related the

intramolecular relaxation rate to the reorientational correlation time of a vector joining two resonating spins. The theoretical estimates for the intramolecular relaxation rate obtained thus are much larger than those experimentally observed. Such discrepancy could arise because of the inherent limitation of the Stokes-Einstein relation incorporated into the Bloembergen-Purcell-Pound model and also because of not taking into consideration the possibility of anisotropic rotational diffusive or inertial motion. Some other works towards a better understanding of the rotational process and the consequent relaxation are: (1) random walk model championed by Ivanov (1964); (2) rotational diffusion equation as advanced by Furry (1957), Favro (1960), Woessner (1962), Shimizu (1962), Huntress (1968, 1970); and (3) the rotational Langevin equation as followed by Hubbard (1963b), Steele (1963), and Atkins (1967). The Steele's inertial model takes into account large step, free rotational motion. The inertial model is viscosity independent and obviates need for consideration of the limitations of the Stokes-Einstein relation. The anisotropic rotational diffusion model advanced by Huntress (1968, 1970) is fairly detailed one and it obtains  $\tau_0$  for the various rotor types like asymmetric planar and symmetric top molecules etc.. For a two-spin system the relation between the intramolecular dipolar relaxation rate and the reorientational correlation time is given by (Abragam (1961))

$$(1/T_1) = 3\gamma^4 \hbar^2 \tau_0 / 2r^6, \quad (1.13)$$

where  $r$  is the separation between the two resonating spins. One important thing to note here is that because of the  $r^{-6}$  dependence, spins other than the nearest neighbours will have negligibly small contribution to the relaxation rate and therefore in the analysis of the relaxation rate data one need only confine ones attention to the closest neighbours.

Significant spin-rotation contribution to  $^{19}\text{F}$  relaxation in liquid  $\text{CHFC}_2$  were first reported by Gutowsky, Lawrenson and Shimomura (1961), and Brown, Gutowsky and Shimomura (1963). Later observations (Green and Powles (1965), Krynicki and Powles (1965), and Powles and Figgins (1965)) in small symmetric molecules too showed dominant spin-rotation contribution to proton relaxation even at high temperatures. A distinctive feature for the spin-rotation interaction is that with the increasing temperature the molecules retain higher angular momentum values longer and thus have longer  $\tau_J$ . The persistence of the angular momentum for longer periods makes the spin-rotation relaxation rates larger. With the increasing temperature the translational and the orientational movements get faster and therefore the respective correlation times and the relaxation rates get smaller. Such an opposite temperature dependence of the spin-rotation relaxation is often of great help in separating the spin-rotation relaxation rate from the rest. (See, for example, Green and Powles (1965),

Powles and Figgins (1965).) The nmr has also the advantage over the molecular beam and microwave spectroscopy in giving small spin-rotation coupling constants in liquid state by non-destructive study of the experimental sample. Some salient relaxation expressions in the line of Huntress (1968) are as follows. In the diffusion limit ( $\tau_J < \tau_\theta$ , and therefore the rotational and reorientational motions are independent of each other), the rotational diffusion constant about the  $i$ th axis is related to the angular velocity autocorrelation time through the equation

$$D_i = (\tau_J)_i kT/I_i, \quad (1.14)$$

where  $(\tau_J)_i$  is the angular velocity autocorrelation time (also called the angular momentum correlation time) about the  $i$ th axis and  $I_i$  is the corresponding moment of inertia. In the principal co-ordinate system that diagonalizes the diffusion tensor

$$(1/T_1)_{SR} = 2/3\hbar^2 kT \sum_{i=x,y,z} [C_{ii}^2 - C_t(C_{ii} - C_t)] I_i (\tau_J)_i, \quad (1.15)$$

where  $C_t = 1/3 \text{ Tr } C$ ,  $C_{ii}$ s are the Cartesian components of the spin-rotation coupling tensor  $C$ , and the spin-rotation interaction hamiltonian is given by

$$H_{SR} = - \hbar \underline{I} \cdot \underline{C} \cdot \underline{J} \quad (1.16)$$

Spin-rotation coupling constant calculation, *ab initio*, is difficult as it requires the knowledge of all the excited levels of the molecule. Since the spin-rotation and chemical shift

effects originate from the molecular electrons, they are mutually related (Flygare and Goodisman (1968), Deverell (1970) and such relationship are often of great help in the relaxation data analysis.

In case of isotropic rotational diffusion of a spherical body of radius  $a$ , the friction torque  $\xi$  is given by the usual Stokes-Einstein relation

$$\xi = 8\pi\eta a^3 . \quad (1.17)$$

However, in the inertial limit (Steele (1963)) the rotational diffusion and viscosity dependence notions are discarded in favour of a friction tensor whose diagonal elements,  $\xi_i$ 's, are related to the intermolecular potential through the relation

$$\xi_i = \frac{2I_i}{\pi} < \frac{\partial^2 V(\tilde{R}^N)}{\partial \psi_i^2} > \quad (1.18)$$

where  $V(\tilde{R}^N)$  is the total intermolecular potential energy of  $N$  molecules in terms of  $6N$ -dimensional vector  $\tilde{R}^N$  specifying the positions and the orientations, and  $\psi_i$  is the angle of orientation about the  $i$ th molecular axis and the angular momentum correlation time is defined by

$$(\tau_J)_i = I_i / \xi_i . \quad (1.19)$$

It is further shown that for an inertial (Gaussian) reorientation the minimum possible value of the reorientational

correlation time is given by

$$\tau_L = 1/2 (\pi I / 3kT)^{1/2}. \quad (1.20)$$

The diffusional and the inertial models are extreme ones and a realistic model for molecular motion in liquids however remains intractable. Chapter 3 deals with the spin-rotation interaction and the dynamically coherent reorientational motion in greater detail.

The chemical shift anisotropy relaxation rate and the quadrupolar relaxation rates have been stated to be directly related to the reorientational correlation time. Large chemical shift anisotropy is expected in cases where large diamagnetic shielding by the surrounding electrons occur. Further, the relaxation rate due to the chemical shift anisotropy varies as the square of the magnetic field strength. Since the present work is concerned with  $^1\text{H}$ ,  $^{19}\text{F}$  relaxations which are known to have relatively low chemical shifts for any sizeable chemical shift anisotropy, and as low experimental magnetic fields are employed ( $\sim 0.23\text{T}$ ) in the present work the chemical shift anisotropy is not a matter of concern as a relaxation agency. Whenever quadrupolar interactions are present as relaxation agents they are usually so strong that other interactions contributing to relaxation are negligible in comparison. The predominant quadrupolar relaxation rate makes the data analysis simpler. Quadrupolar nuclei are not of direct concern in the present work.

The coupling of a resonating spin to a fast relaxing quadrupolar nucleus has very little contribution to the observed total spin-lattice relaxation rate although it affects the spin-spin relaxation. The scalar coupling between the resonating spin  $I$  and the quadrupolar spin  $S$  finally leads to

$$(1/T_1)_{SC} = 2/3 A^2 S(S+1) \{ \tau_S / [1 + (\omega_I - \omega_S)^2 \tau_S^2] \} , \quad (1.21)$$

$$\text{and } (1/T_2)_{SC} = 1/3 A^2 S(S+1) \{ \tau_S + \tau_S / [1 + (\omega_I - \omega_S)^2 \tau_S^2] \} , \quad (1.22)$$

where  $(1/T_1)_{SC}$  and  $(1/T_2)_{SC}$  are respectively the scalar coupling contributions to spin-lattice and spin-spin relaxation rates;  $\omega_I$ ,  $\omega_S$  are the Larmor frequencies of  $I$  and  $S$  spins respectively in the laboratory magnetic field and  $\tau_S$  is the relaxation time of the nucleus  $S$ . The Larmor frequencies of  $^1\text{H}$  and  $^{19}\text{F}$  are so high that  $(\omega_I - \omega_S)$  is usually several tens of megahertz. Since  $\tau_S$  is of the order of a few microseconds the quotient within the brackets of the right hand side of the equations (1.21 and 1.22) is small which gives  $(1/T_1)_{SC} \sim 0$  and  $(1/T_2)_{SC} \propto \tau_S$ . Thus, in the spin-lattice relaxation data analysis of the present work the scalar coupling as a relaxation mechanism need not be considered.

Paramagnetic compounds have large magnetic moments. Even when they are present in the experimental liquid sample in small quantities their interaction with the resonating spin is so strong as to obliterate other relaxation mechanisms. It is imperative that the paramagnetic impurities are scrupulously removed from the experimental sample.

In molecules with more than two spins if all the spins do not see dipolar interactions of the same strength, cross-correlation between the various pairwise dipolar interactions will result in a nonexponential relaxation process. Such cross-correlations seem to strongly affect the intramolecular dipolar relaxation, and an analogous spin relaxation nonexponential in time; and the simple two spin Eq. (1.13) needs modification. On the other hand the cross-correlation effects are small in intermolecular interaction and Eq (1.10) is quite valid (see, Hubbard (1958a, 1958b), Abragam (1961), Brooks *et al* (1968), Hubbard (1969), Kitchlew and Nageswara Rao (1972a, 1972b, 1973a), Cutnell *et al* (1975)).

## I.2 Some Salient Points on the Review of Others Work

The earliest approach to the study of molecular dynamics was through hydrodynamics. The self-diffusion coefficient  $D$  was related to the coefficient of friction  $\zeta$  through the relation

$$D = kT/\zeta \quad (1.23)$$

Stokes had earlier derived  $\zeta$  for macrospherical body motion in a liquid continuum. Einstein proposed the validity of the Stokes relation for molecules moving in a crowd of their own kind. Studies in molecular liquids in the line of Debye and others showed the Stokes-Einstein relation to predict a smaller diffusion coefficient than observed. Although the hydrodynamic theory was too crude to be valid for the molecules

an attempt was made to retain it by using empirical correction factors in the equations for translational and rotational diffusion. It was pointed out that the (macro)viscosity coefficient when used for molecular motions needs lessening by the 'microviscosity factor', of magnitude greater than one. These corrected Stokes-Einstein relations were somewhat successful in predicting the translational and reorientational correlation times. In the case of solutions the 'mutual viscosity' concept of Andrade (Hill (1954, 1955)) based on the kinetic theory was successful. This theory had built in inertial parameter dependence and pre-eminent rotational features at low concentration. For monomeric liquids formed by small spherical molecules it was observed that the hydrodynamics idea of viscous drag and stick must be discarded as the molecules are much freer to move about, oblivious of surrounding molecular attraction, than is a macrosolid body in a fluid. In the molecular motion there seems to be more 'slip' and less 'stick' than had been thought earlier. In this regard theoretical calculations *à la* Hu and Zwanzig (1974) and experimental studies by Bauer, Brauman and Pecora (1974) Bauer *et al* 1974 come to the fore. However, the primacy of a connection between the velocity autocorrelation and momentum transfer mechanisms of which statistical average measures respectively are the diffusion coefficient and shear viscosity coefficient, has always to be borne in mind in the mathematical constructs. The viscosity dependent spin-rotation relaxation study when extrapolated to zero viscosity if non-zero shows

the presence of internal motion (see, Bull, Barthel and Jonas (1971), Berne and Pecora (1976)).

The diffusional (collision limited) process is *a priori* expected to be strongly temperature dependent. The inertial (free) motions on the other hand are quite oblivious of the surrounding and thus have a slow temperature dependence.

An useful method of testing whether the rotational microdynamics is diffusional or inertial is through the ' $\chi$  test'. (See, Bopp (1967), Wallach and Huntress (1969), and Gillen and Noggle (1970).) The ratio of the reorientational correlation time  $\tau_\theta$  to the free rotational time ( $\tau_{\text{free}}$ ) is given by  $\chi$ . In the diffusion limit the small step collisions require much longer than the free rotational correlation time to change the molecular orientation sizeably - say by 1 radian. But in the inertial limit the orientational changes are through large steps and  $\tau_\theta$ ,  $\tau_J$ ,  $\tau_{\text{free}}$  being of the same order of magnitude,  $\chi$  is usually found to be within 1 and 3. In terms of the intermolecular potential  $V$ , and the reorientational angle ( $\psi_i$ ) about the molecular axis  $i$ , the  $\chi$  parameter given by Huntress (1969) is,

$$\chi_i = \frac{5}{18} \sqrt{\frac{2}{\pi kT} \frac{\partial^2 V}{\partial \psi_i^2}} \quad (1.23)$$

It is often that an anisotropic intermolecular potential is inferred from the observed diffusive nature of rotational motion.

A collisional efficiency parameter defined as the ratio of the rotational correlation time  $\tau_j$  to the reorientational correlation time  $\tau_\theta$  tells how good a rotation changing collision is in changing the orientation of the molecule. As the rotational and reorientational changes go almost hand in hand in the inertial limit the collisional efficiency is unity. But in case of the diffusional motion, as many a collisions are necessary to give a sizeable net orientational change the collisional efficiency is very low. (See pertinent discussions on dense gases by Gordon, Armstrong and Tward (1968) and that on liquids by Maryott, Malmberg and Gillen (1974).)

The greater is the asymmetry of a molecule, the greater will be the energy transfer between rotational and translational motion. In order to monitor the molecular asymmetry, a translation-rotation coupling parameter  $\kappa$  introduced by McClung and Kivelson (1968), is given as the ratio of the intermolecular torque on the solute molecule to the intermolecular force on the solvent molecule. In terms of the intermolecular potential energy  $V$ , the  $\kappa$  parameter is given by

$$\kappa_{ii} \propto \frac{1}{a^2} \left( \frac{\partial^2 V}{\partial \phi_i^2} / \nabla^2 V \right), \quad (1.24)$$

where  $a$  is the mean radius of the molecule and  $\phi_i$  is the angle of rotation about the molecular axis  $i$ . For spherical symmetric molecular potential, as does happen in spherical molecules, the

coupling is understandably zero. It was earlier thought that (Shimizu (1964), Wallach and Huntress (1969), Gillen and Noggle (1970)) large molecular dipole moments are responsible for the diffusive motion. The recent works of Bull and Jonas (1970), Assink and Jonas (1972), and Fury and Jonas (1976) show that it is the molecular shape which determines the extent of translation-rotation coupling. An interesting outcome of a good translation-rotation coupling is that the intermolecular and the intramolecular dipolar relaxation rates, which are dependent on the translational and reorientational motions respectively, will have similar temperature variation. Asymmetric molecules may be expected to show such a trend in their spin-lattice relaxation rates. As the asymmetric molecules will have to displace large volumes for orientational changes, pressure variation relaxation rate measurements will show large activation volumes. (See, McCall, Douglass and Anderson (1959), Bull and Jonas (1970).) The translation-rotation coupling has also been accounted for by bringing in a rough texture to the spheres of the hard sphere model (Chandler (1975)). Smooth spheres are germane to inertial motion. It is worthwhile pointing out that an implicit connection between the translation-rotation coupling and microviscosity idea exists. The molecular radius  $\sigma$  given by the relation (1.11),

$$\tau_0 = 4\pi\eta\sigma^3/3kT, \quad (1.11a)$$

is related to the hydrodynamic radius  $a$  given by the Eq (1.12),

through

$$\sigma^3 = \kappa a^3, \quad (1.25)$$

where  $0 < \kappa < 1$ . ( $\sigma$  and  $a$  can be viewed as rotational and translational radii respectively.) For most of the molecular liquids  $\kappa$  is seen to be between 0.1 and 0.3. From the foregoing relations (1.11a) and (1.25)  $\kappa$  is construed as one necessitated to retain the  $\tau_0 - a$  relationship. In microviscosity parlance this end was achieved by reducing the macroviscosity coefficient ( $\eta$ ) of the liquid by the microviscosity factor (see p. 40). Thus, an inverse relationship between  $\kappa$  and the microviscosity factor seems to exist. A recent work by Masood *et al* (1976) discusses anisotropic rotational motion and translation-rotation coupling in large polar molecules by an assorted relaxation studies.

The molecular volume and  $\eta$  dependence of the reorientational correlation time in the Debye model is an implicit result of the translation-rotation coupling. The greater is the molecular asymmetry, the greater will be the volume displaced as a molecule reorientates and  $\eta$ , which is an attribute of the translational motion in molecular physics, automatically determines the orientational motion. Sometimes (as in polar liquids), the good agreement of experimental results with the predictions from the Debye relation (Eq. 1.11) is highly misleading. It is shown by Cuckier and Lakatos-Lindenberg (1972), and Fung and McGaughy (1976) that two negative assumptions : (1) the Stokes law is

valid for microbody motion, and (2) the molecules even in highly polar liquids are monomeric; cancel each other in giving an apparently valid Debye picture. Therefore, in handling Debye relation due caution need be exercised.

The 'molecular dimension' in the liquid state has remained a very little understood parameter. The situation is complicated further by the molecular association, hydrogen bonding *etc.*. In gases the van der Waals idea and analogous Lennard-Jones parameters are good means to an understanding of the molecular dimensions. In solids the lattice structure gives a firm standing to the molecules and hence to the intermolecular distances, molecular dimensions *etc.*. But in liquids close neighbourliness and intermingling make it difficult to have a clear idea of the molecular dimension ~~as~~ the molecules, particularly nonspherical ones, can approach each other in a myriad of ways and inclinations. Sometimes the liquids are pictured with approximated spherical molecules hexagonally close packing the available volume. Although the various methods chosen for molecular dimension are of doubtful values, the one best suited for the work presented here is discussed in the appendix. (See comments by Abragam (1961) p. 326.)

It is also good to take note that the measured spin-echo nmr diffusion coefficients are single particle diffusion constants (Ahn, Jensen and Kivelson (1972)). The mutual diffusion constant through the tracer diffusion method Mills (1971)

claimed to be experimentally much more accurate than the nmr method (because of experimental refinements incorporated over the years) measures the concentration diffusion. However, if only very small amount of tracer is present the tracer diffusion and self-diffusion coefficients are identical. Such diffusion values for copiously investigated samples like benzene and water can be used as standard reference in diffusion measurements. The pulsed nmr self-diffusion measurement is, however, much superior to the methods of  $D$  estimation through the relation between translational correlation time and dubious value of molecular radius. (See, for example Bondi (1968).)

There are two salient aspects of data handling. First, the earlier classical frequency or energy domain work (the Schrödinger picture) is fraught with spectral width problems which arise mainly because of the experimental limitations. Time domain work (the Heisenberg picture), is more suitable where the time development of a physical system can be observed directly and the information available is with less uncertainty and noise. Nevertheless, Fourier transformation can take the result obtained in one domain to the other. Pulsed nmr experiment, which is pursued in the present work being a time domain work, time development and time correlation of the physical systems are directly and much more conveniently observed. Second, the validity of the linear response theory of

irreversible thermodynamics plays a subtle but major role in the understanding of the molecular microdynamics through the observed macroparameters. Situations slightly away from equilibrium, as do happen in the motion at the microlevel, can be comprehended through the correlation functions which give an average picture over the observed time and space interval. Such integration or averaging does not erase all the information of micromotion. The characteristic time which is a measure of the microdynamic rate is carried through the integration process. As the integral of the correlation function is intimately related to the macroparameters the macro and the microparameters get connected. For example Oppenheim (1971) shows how two such parameters of present interest  $T_1$  and  $D$  are related. Two things are to be clearly borne in mind. First, although the experimental time scale is longer than the molecular time scale (microseconds against picoseconds) one can still learn about the micromotion. Second, the molecular motional models have a relevance as long as the correlation functions are constructed first and then related to the macroparameter. The reverse approach namely the attempt to arrive at the validity of the models from macroparameters has very little significance. Models are necessary only so far as predicting the macroparameter is required. However, the systematics of the variation of macroparameters with external constraints like temperature and pressure reflect the character of the molecular dynamics.

### 1.3 Scope of the Present Work

The aim of the work presented in this thesis is to get a picture of the molecular dynamics in the liquid-vapour coexistence region of some molecular liquids through the *in situ* measurement and analyses of  $T_1$  and  $\rho$  data. The temperature variation work in a liquid sample in a sealed tube has the drawback that both the molecular kinetic energy and packing (density of the sample) change with temperature variation which are not accounted for in the data analysis. A better approach could be the simultaneous pressure and temperature variation study which could enable obtaining constant density  $T_1$  and  $\rho$  data which are more meaningful and better amenable to analyse à la Jonas group of workers. The maximum vapour pressure built on the experimental sample in the sample tube due to the temperature variation could be of the order of several tens of atmospheres which is not much as to deviate  $T_1$  and  $\rho$  from the normal pressure values. The  $T_1$  and  $\rho$  data are thus oblivious of the large vapour pressures, but are affected by the large convection currents in the sample.

A priori, the molecular shape, symmetry, mass, moment of inertia, dipole moment etc. seem to affect the molecular dynamics in liquid. The aim of such studies would be to ascertain the extent of influence<sup>of</sup> such agencies on the molecular dynamics. The two extreme kinds of molecular dynamics which ensue are diffusive and inertial types. In the Brownian diffusion kind of the

translational, reorientational or rotational dynamics the movement is collision limited, is through small steps, and is severely surrounding dependent. The strongly surrounding dependent dynamics reflects itself through a strong temperature and viscosity dependence of the corresponding parameters. The inertial kind of the dynamics is mostly determined by the molecular mass and moment of inertia, and has very little temperature and viscosity sensitivity. It is thus from the temperature variation of the parameters related either to the translational, reorientational, or the rotational motion the nature of the concomitant dynamics be known. Since building the microdynamic models from the microparameters are not definitive ones (p. 47) observation of the trends of variation of suitable parameters with temperature and pressure are very helpful.

The molecular dimensions are closely related to the dynamical parameters and there seems to be many approaches to determine such dimensions (see Appendix). In view of the nmr work and its data analysis the Stokes-Einstein method of finding the molecular radius from the experimental  $D$ , and  $\eta$  data seem to be best suited. Such an approach seems to naturally account for the microviscosity considerations and has important connection with several other works as stated in the Appendix.

The self-diffusion coefficient is translational motion dependent, collision limited and except in cases of highly

hydrogen bonded liquids like water, obeys an Arrheniuslike relation. The methods of estimation of the self-diffusion and rotational diffusion are also discussed in the Appendix.

In the asymmetric molecules the translation and orientational changes are well coupled as a collision would simultaneously and sizeably alter both. In such asymmetric molecules there will not be much scope for any reorientational coherence. Chapter 3 explores the outcome of the reorientational coherence as well as the diffusive process. The problem of the translation-rotation coupling is also touched on in the Appendix. An obvious outcome of the translation-rotation coupling is that the intermolecular relaxation rate and the intramolecular dipolar relaxation rate which depend respectively on the translational and reorientational motion vary similarly with temperature.

A coherent pulsed nmr spectrometer assembled for such temperature variation  $T_1$ ,  $D$  work and other ancillary experimental arrangements are described in Chapter 2. The procedure for data gathering, the data credibility (error etc.) and the test sample runs are also described. For the periodical spectrometer checks it seems very helpful to make use of two test samples, water and benzene, copiously studied otherwise.

The dynamical parameters  $D$  and  $\eta$  combined variouly with  $\rho$  and  $T$  have often been used to analyse the molecular dynamics. Several other parameters like the free rotational period of the

molecule, reorientational correlation time in the inertial (Gaussian) limit, reorientational correlation time in the diffusion limit,  $a_2^m(0)$  defined by Steele and associates (Steele (1963), and Moniz, Steele and Dixon (1963)), and the  $\chi$  parameter used to find the diffusion or inertial reorientation are also helpful for studying the molecular dynamics. The intermolecular relaxation, directly modulated by the translational motion, is estimated by using the Torrey's relation. The intermolecular relaxation rate separated from the observed relaxation rate gives the intramolecular relaxation rate carrying information about the orientational and rotational changes. As the orientational and rotational changes have opposite temperature dependence, these can be separated in suitable cases from the temperature variation work. In the event of absence of marked changes and a minimum in the intramolecular relaxation rate such separation is not possible. All these parameters are discussed in the context of the studied molecules presented in Chapters 4 and 5.

The work presented in Chapter 4 particularly looks into problem of molecular dynamics in some  $\text{CH}_3$  containing liquids. The  $\text{CH}_3$  group is particularly quite facile about the bond to the molecular skeleton. The large anisotropic rotational symmetric tops like  $\text{CH}_3\text{I}$  and  $\text{CH}_3\text{CN}$  give rise to spin-rotation interaction. In molecules like  $\text{CH}_3\text{NO}_2$  and  $\text{CH}_3\text{COCH}_3$ , the barrier to internal rotation is low and in the observed temperature range inertial reorientations are seen. The large dipole moments

CENTRAL LIBRARY

Acc. No. A 54879.

of  $\text{CH}_3\text{NO}_2$  and the consequent possible local structure does not seem to affect the reorientational motion. In case of  $\text{CH}_3\text{COCH}_3$  and  $\text{CH}_3\text{SOCH}_3$ , the small barrier to internal rotation in the former gives rise to inertial orientational changes whereas the structural asymmetry in the later gives rise to a translation-rotation coupling.

The work presented in Chapter 5 deals with a group of assorted molecules.  $\text{CH}_2\text{Cl}_2$  and  $\text{CH}_2\text{I}_2$  belong to a family of halogen derivatives with  $\text{CH}_2\text{I}_2$  more massive than  $\text{CH}_2\text{Cl}_2$ . Vestiges of inertial reorientations are seen in  $\text{CH}_2\text{Cl}_2$  whereas the reorientational process in  $\text{CH}_2\text{I}_2$  is diffusional. The liquid anisole has its molecules fairly asymmetric and with possibility of intramolecular rotation. The internal motion though not much prominent nevertheless makes itself felt in the analysis. The studies in  $\alpha$ -trifluoro toluene suggests that the internal rotation mostly contributes to the  $^{19}\text{F}$  relaxation which is spin-rotational in nature. The strong temperature dependence of the  $^{19}\text{F}$  intramolecular relaxation, however, hints at a temperature activated process.

The summary and conclusion of the work presented here are given in Chapter 6.

## CHAPTER 2

### EXPERIMENTAL METHODS

Pulsed nmr method is suitable for investigation of kinetic processes in the substances. The resonance is non-adiabatically, transiently stimulated. The observation of the re-establishment of the thermodynamic equilibriums permits the separation of the static and dynamic effects within the substances.

With an aim to study the molecular dynamics of liquids over the liquid-vapour coexistence region by means of the study of proton ( $Z=1$ ) and fluorine ( $Z=19$ ) relaxation time and of the molecular self-diffusion coefficient, a pulsed nmr spectrometer to work at a convenient radiofrequency ( $\sim 9.78$  MHz) is conceived. The method of spin echo and the experimental arrangement is described in the following.

#### 2.1 Spin Echo

In the spin echo method (Hahn (1950)), one observes the signals from the spin system when the excitation pulses are off. This is a time domain experiment. This time domain signal apart from being Fourier related to the frequency domain continuous wave (cw) spectrum has several advantages: (1) In contrast to the frequency domain signal

the time domain signals are easy to perceive. Direct analysis of the signals provides the relaxation times and the self-diffusion coefficients. (2) The excitation is off during the time the signal (echo) is observed. The observed signal, therefore, is free from the interference due to the excitation. (3) When the signal (echo) appears the receiving system is recovered from the excitation to normally receive the signal. (4) The same time domain signal from the repeated runs can be summed vectorially to average the non-periodic noise and give a better S/N. (5) The excitation and observation on the entire spin system is carried out in a time span much smaller than a cw experiment for the same amount of information (see Farrar and Becker (1971)) and therefore entails a good deal of time-saving.

To perceive the formation of the spin-echo let us first fix a set of Cartesian axes as follows. The static magnetic field direction defines the  $z$  axis of the static or laboratory frame of reference. The axis of the sample coil through which the rf excitation to the spin system is applied and which also record the subsequent response of the system; defines the  $x$  axis of the static reference frame. (See Fig.1a.) A right handed system of Cartesian axes fixes the remaining axis  $y$ .

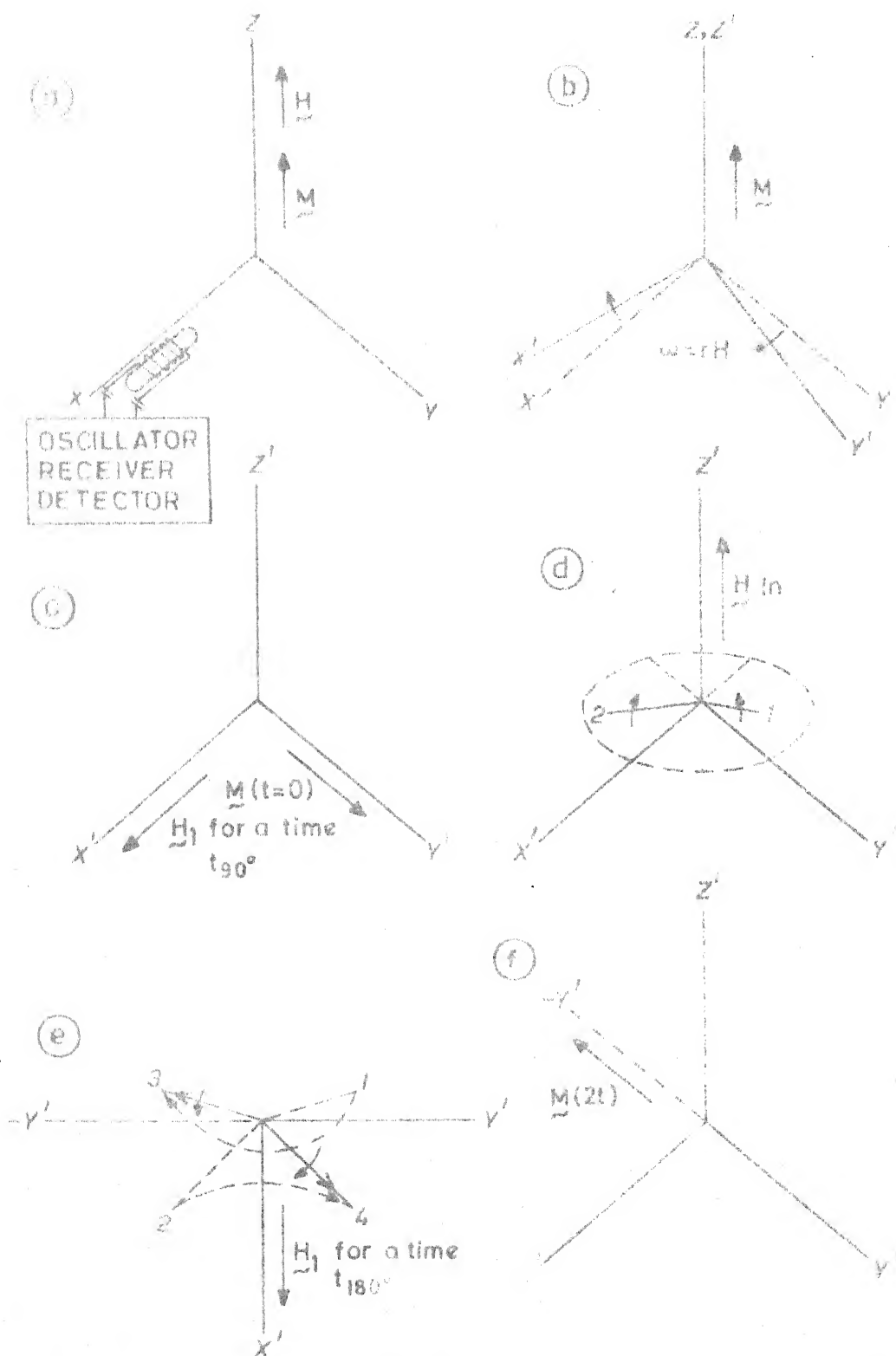


FIGURE 1. ECHO FORMATION WITH  $90^\circ$ - $180^\circ$  PULSE SEQUENCE

As mentioned in Chapter 1, a spin ( $I=1/2$ ) system placed in a static magnetic field  $\hat{k}H_0$  eventually in a time larger than the spin-lattice energy exchange time, attains thermal equilibrium (Boltzmann distribution of population amongst the Zeeman levels) amounting to a net magnetization along the static field. The dynamics of magnetic moment vector  $\underline{M}$  in a static homogeneous field  $\underline{H}_0$  can be given by (Abragam (1961))

$$\frac{d\underline{M}}{dt} = \gamma(\underline{M} \times \underline{H}_0) . \quad (2.1)$$

In a frame rotating at an angular velocity  $\underline{\omega}$  the time derivative of the magnetization is given by

$$\left( \frac{d\underline{M}}{dt} \right)_{\text{rot}} = \frac{d\underline{M}}{dt} + \gamma(\underline{M} \times \underline{\omega}) , \quad (2.2)$$

where the right hand terms in the expression are with respect to the static reference frame. Combining the Equations (2.1) and (2.2)

$$\left( \frac{d\underline{M}}{dt} \right)_{\text{rot}} = \gamma \underline{M} \left( \underline{H}_0 + \frac{\underline{\omega}}{\gamma} \right) . \quad (2.3)$$

The choice of  $\underline{\omega} = -\gamma \underline{H}_0$  leaves  $\underline{M}$  static in the rotating frame (see eq (2.3), Fig.1b). The rotating frame has its Cartesian axis  $z'$  coincident with the static frame  $z$  axis but rotates about the  $z$  axis with the Larmor frequency  $\omega = \gamma H_0$  in a sense apposite to  $\underline{H}_0$ .

The presence of an rf field at the Larmor frequency of the spin system under observation,

$$H_{\text{rf}} = 2\hat{i}H_1 \cos \omega t ,$$

can be resolved into two circularly polarized components one of which is a counter-clockwise rotating field

$$\hat{i}H_1 \cos \omega t + \hat{j}H_1 \sin \omega t ,$$

and the other a clockwise rotating field

$$\hat{i}H_1 \cos \omega t - \hat{j}H_1 \sin \omega t ,$$

both of the same amplitude  $H_1$ . The clockwise rotating field has the same sense of rotation as the previously mentioned rotating frame of reference. In this clockwise rotating frame the magnetization vector  $\underline{M}$  finds the field  $H_1$  static. Thus, in the rotating frame

$$\left( \frac{d\underline{M}}{dt} \right)_{\text{rot}} = \gamma(\underline{M} \times \underline{H}_1)_{\text{rot}} . \quad (2.4)$$

This equation suggests that the rotation of magnetization  $\underline{M}$  is about  $(\underline{H}_1)_{\text{rot}}$ . If the rf is kept on for a time  $t_{90^\circ}$  (a  $90^\circ$ -pulse) such that  $\gamma H_1 t_{90^\circ} = \pi/2$  the bulk magnetization is brought along  $y'$  axis (Fig.1c). Quantum mechanically this situation corresponds to a superposition of the two spin states. A  $180^\circ$ -pulse of duration  $t_{180^\circ}$  (such that  $\gamma H_1 t_{180^\circ} = \pi$ ) tips the net magnetization along the

z axis to -z axis which in quantum mechanical parlance is equivalent to inversion of the population of spin levels. The duration of the pulses must be so short that the spins do not have enough time to exchange energy and behave separately from the collective bulk magnetization.

The rotating frame Cartesian axis  $x'$  is imagined to be fixed along the clockwise rotating  $H_1$ . In a coherent oscillator the oscillation being always present (even in absence of the pulses) the rotating frame  $x'$  axis may be imagined to be present always. A right handed Cartesian axis system defines the remaining  $y'$  axis. In such a system the  $90^\circ$ -pulse tips the net magnetization to the  $y'$  axis. If the spins were free without interactions of any kind then they would stay coherently amongst themselves and therefore the bulk magnetization would stay put along  $y'$ . However, the interaction of the spins with the lattice leads to a thermal relaxation and growth of magnetization along  $H_0$ . Further, the mutual spin-spin interaction leads to an irreversible loss of the coherence in a characteristic time  $T_2$  and therefore an observed decay of the bulk magnetization in the transverse plane. For convenient observation of the net magnetization in the transverse plane at different times the decay of the magnetization is made reversible in the following ingenious way. In the presence of an inhomogeneous field  $\hat{H}_{in}(\vec{z})$ , (Fig.1d),

where  $H_{in}(z)$  is a function of the distance along the  $z$  axis, all the spins do not see the same field and therefore do not have the same Larmor period. As a result of this the isochromats (formed by the bunch of spin magnetizations seeing the same static magnetic field) fall apart from one another. The decay of spin coherence occurs in a characteristic time  $1/\gamma H_{in}$ , where  $H_{in}$  is the maximum inhomogeneous field over the sample. Ascertaining  $1/\gamma H_{in} > T_2$  the present inhomogeneous decay is made much faster than the homogeneous decay. The important thing to note here is that at time  $\tau < T_2$  although the isochromats may be fanned out and hence there may not be any transverse magnetization in the rotating frame, the memory of the inhomogeneous decay still persists in the isochromats. A second pulse at time  $\tau$  (such that  $T_2 > \tau > 1/\gamma H_{in}$ ) makes the isochromats regain their loss of relative phase due to inhomogeneous decay to come in phase (echo) at time  $\tau$  further. This is easily visualized in case of a second,  $180^\circ$ -pulse. The  $180^\circ$ -pulse applied along  $x'$  satisfying the foregoing condition takes two of the representatives of the fanned out isochromats positioned at 1 and 2 to positions 3 and 4 (see Fig. 1e). These newly positioned isochromats retain their sense of rotation about  $z'$  axis. Therefore in a time  $\tau$  further, except for the inhomogeneous spread, the isochromats will arrive in phase along  $-y'$  (see Fig 1f). The decay of magnetization and clustering of the isochromats

z axis to -z axis which in quantum mechanical parlance is equivalent to inversion of the population of spin levels. The duration of the pulses must be so short that the spins do not have enough time to exchange energy and behave separately from the collective bulk magnetization.

The rotating frame Cartesian axis  $x'$  is imagined to be fixed along the clockwise rotating  $H_1$ . In a coherent oscillator the oscillation being always present (even in absence of the pulses) the rotating frame  $x'$  axis may be imagined to be present always. A right handed Cartesian axis system defines the remaining  $y'$  axis. In such a system the  $90^\circ$ -pulse tips the net magnetization to the  $y'$  axis. If the spins were free without interactions of any kind then they would stay coherently amongst themselves and therefore the bulk magnetization would stay put along  $y'$ . However, the interaction of the spins with the lattice leads to a thermal relaxation and growth of magnetization along  $H_0$ . Further, the mutual spin-spin interaction leads to an irreversible loss of the coherence in a characteristic time  $T_2$  and therefore an observed decay of the bulk magnetization in the transverse plane. For convenient observation of the net magnetization in the transverse plane at different times the decay of the magnetization is made reversible in the following ingenious way. In the presence of an inhomogeneous field  $\hat{h}_{in}(\vec{z})$ , (Fig.1d),

where  $H_{in}(z)$  is a function of the distance along the  $z$  axis, all the spins do not see the same field and therefore do not have the same Larmor period. As a result of this the isochromats (formed by the bunch of spin magnetizations seeing the same static magnetic field) fall apart from one another. The decay of spin coherence occurs in a characteristic time  $1/\gamma H_{in}$ , where  $H_{in}$  is the maximum inhomogeneous field over the sample. Ascertaining  $1/\gamma H_{in} > T_2$  the present inhomogeneous decay is made much faster than the homogeneous decay. The important thing to note here is that at time  $\tau < T_2$  although the isochromats may be fanned out and hence there may not be any transverse magnetization in the rotating frame, the memory of the inhomogeneous decay still persists in the isochromats. A second pulse at time  $\tau$  (such that  $T_2 > \tau > 1/\gamma H_{in}$ ) makes the isochromats regain their loss of relative phase due to inhomogeneous decay to come in phase (echo) at time  $\tau$  further. This is easily visualized in case of a second,  $180^\circ$ -pulse. The  $180^\circ$ -pulse applied along  $x'$  satisfying the foregoing condition takes two of the representatives of the fanned out isochromats positioned at 1 and 2 to positions 3 and 4 (see Fig. 1e). These newly positioned isochromats retain their sense of rotation about  $z'$  axis. Therefore in a time  $\tau$  further, except for the inhomogeneous spread, the isochromats will arrive in phase along  $-y'$  (see Fig 1f). The decay of magnetization and clustering of the isochromats

(echo) in the rotating frame induces signals in the laboratory sample coil modulated at the relative frequency of the two frames. Ordinary amplitude detection of such signals in the laboratory frame gives the free induction decay and the spin echo. In a phase sensitive detection method, by properly referencing the laboratory frame signal with respect to the rotating frame (which, as mentioned earlier, is set by the oscillations of the coherent oscillator) one can distinguish between the sense of the decay of the  $y'$  magnetization and the sense of the echo formed along  $-y'$ . The height of the free induction decay after the  $90^\circ$ -pulsing of the equilibrium magnetization, is a measure of that magnetization. The echo formed at time  $2\tau$  from the first pulse is a measure of the transverse magnetization remaining after the irreversible loss for time  $2\tau$  and diffusion of spins during that time has taken place. The echo height, therefore, carries information about  $T_2$  and  $D$ .

Clark (1964), Farrar and Becker (1971) list elaborately the requirements for a good spinecho spectrometer. The salient conditions to be borne in mind are:

- (1)  $\gamma H_1 t_{90^\circ} = \pi/2$  and  $\gamma H_1 t_{180^\circ} = \pi$ .
- (2)  $t_{90^\circ}, t_{180^\circ} < T_1, T_2$ .
- (3)  $t_{90^\circ}, t_{180^\circ} > \tau > 1/\gamma H_{in}$ .
- (4)  $\tau > 1/\gamma H_{in} > t_{90^\circ}, t_{180^\circ}$ .
- (5)  $H_1$  must be much larger than the range of the chemical shift of the resonating spins so that all the spins are tipped about  $H_1$ .

Work on liquids needs only a moderate amount of pulse power (Clark (1964), Farrar and Becker (1971)). Therefore pulse level of about 300 V delivered at an impedance of  $50\Omega$  suffices. Typical pulse widths are a few microseconds. The space available for the sample between the poles of the magnet is restricted because of the arrangement for heating and for temperature measurement, and by the coil required for exciting the sample under study. A single coil sample circuit is preferred as it requires less space and obviates the need for tuning arrangement. It also obviates the need for electrostatic shielding which would be required for a double coil (crossed coil) system. The nmr signal is directly amplified in an rf amplifier of band width 1 MHz tuned to 9.78 MHz which is just about the requirement in view of the pulse rise time and signal width (Mansfield and Powles (1963), Clark (1964)). The nmr signal which is essentially an audio modulation of the rf carrier is finally detected and retained for measurement on a storage oscilloscope screen. As the signals in the samples of our interest are quite strong no phase sensitive detection is incorporated. The resonant magnetic field is provided by a 12" pole diameter Varian magnet (Model VFR 2703). The self-diffusion in liquids being as high as  $10^{-9}\text{m}^2\text{ s}^{-1}$  the use of a pulsed field gradient is unnecessary. A fresh dry cell gives the required steady, measurable field gradient. Figure 2 gives the block diagram of the experimental set up.

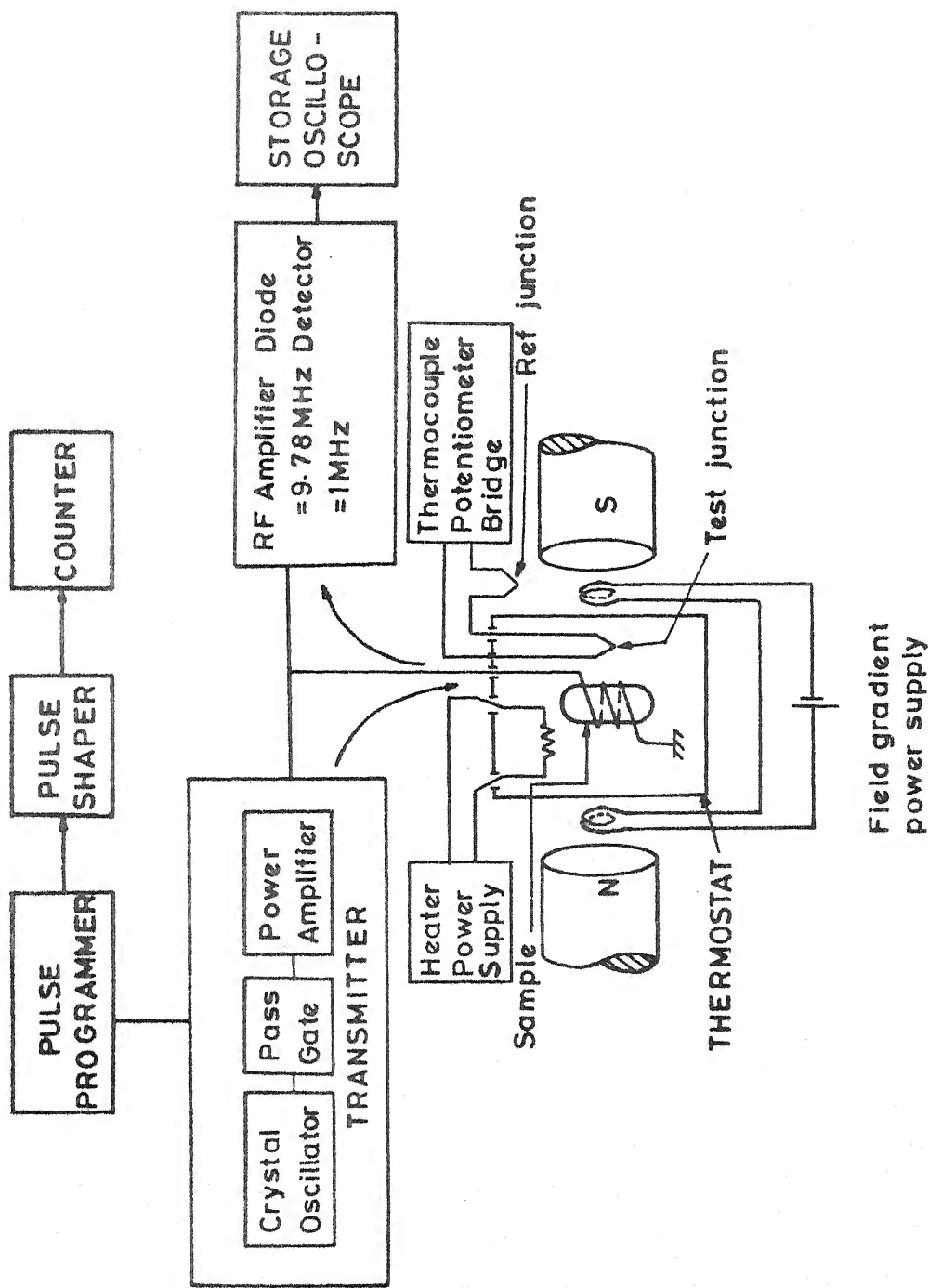


FIGURE 2. BLOCK DIAGRAM OF THE PULSED NMR ARRANGEMENT

## 2.2 Transmitter

Essentially Blume (1961)'s circuit for the transmitter (Figure 3) followed also by Kitchlew (1971) is used in the present work. The crystal oscillator works satisfactorily without an oven. The pass gate consists of the low leakage tube 7077 in order to give a very good carrier suppression. This tube often gets soft after a prolonged period of work. This is evidenced through a sizeable fraction of the rf carrier leaking to the receiver and giving undesired phase detection. Also then the plate cathode resistance is found to be low. Another trouble arises from the 5093 transmitter power tubes getting weak quickly. From time to time tuning of the coil-condenser arrangement in the transmitter has been necessary in order to maximise rf at the tank coil head (i.e. the sample head). The transmitter is properly rf-shielded lest spurious ringing and phase detected signals show up at the receiver output.

## 2.3 Pulse Programmer

The pulse programmer (Fig.4 ) consists of a number of units from Tektronix 160 series and conventional pulse shaping units for differentiation, inversion, mixing etc.. The detailed schematic of the circuits is given in the Figures 5 and 6. The programmer has the capability of giving one-, two-, or three-pulse sequence in continuous or manual triggered mode. The Carr-Purcell sequence can be had in the manual triggered mode

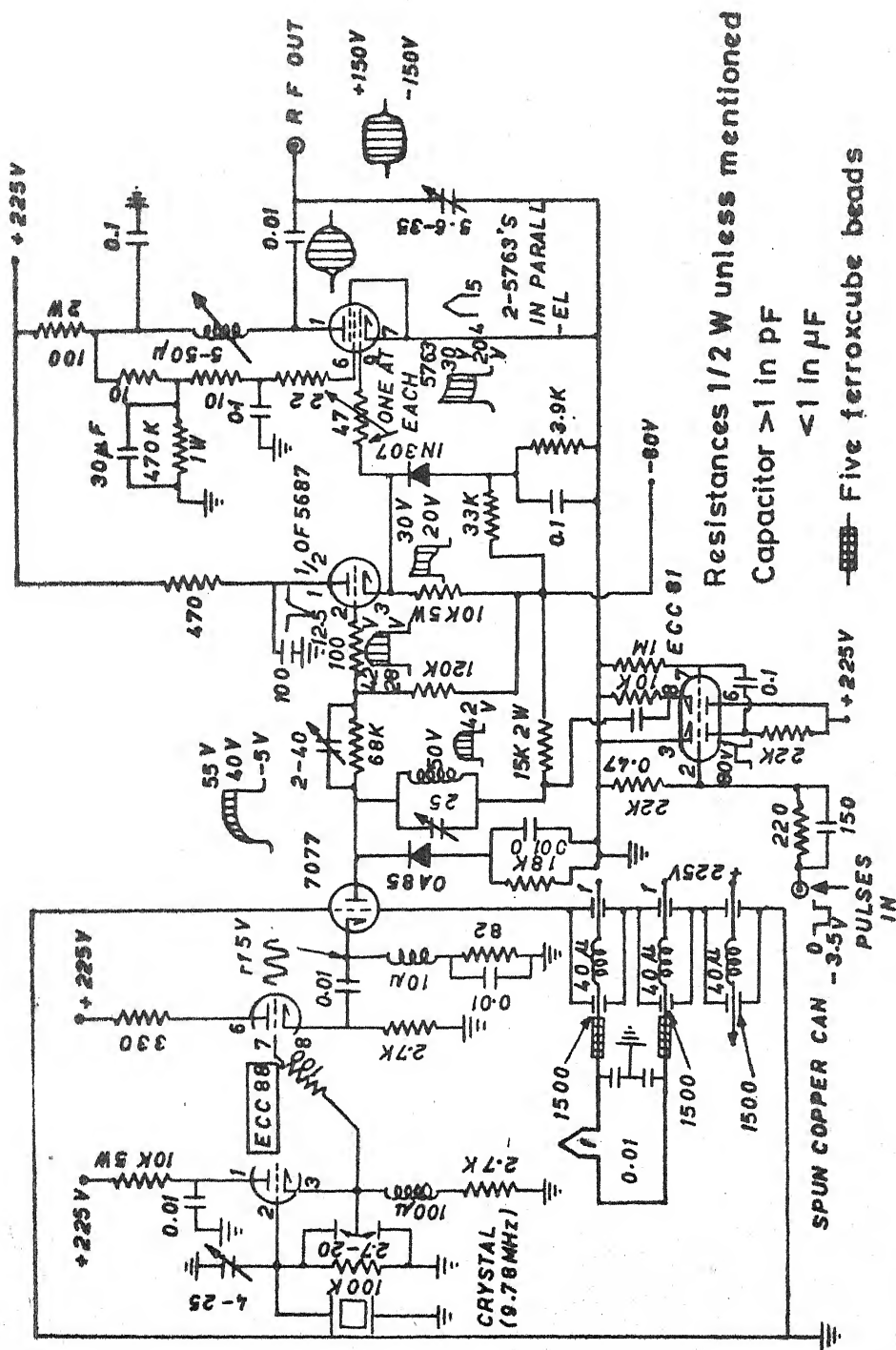
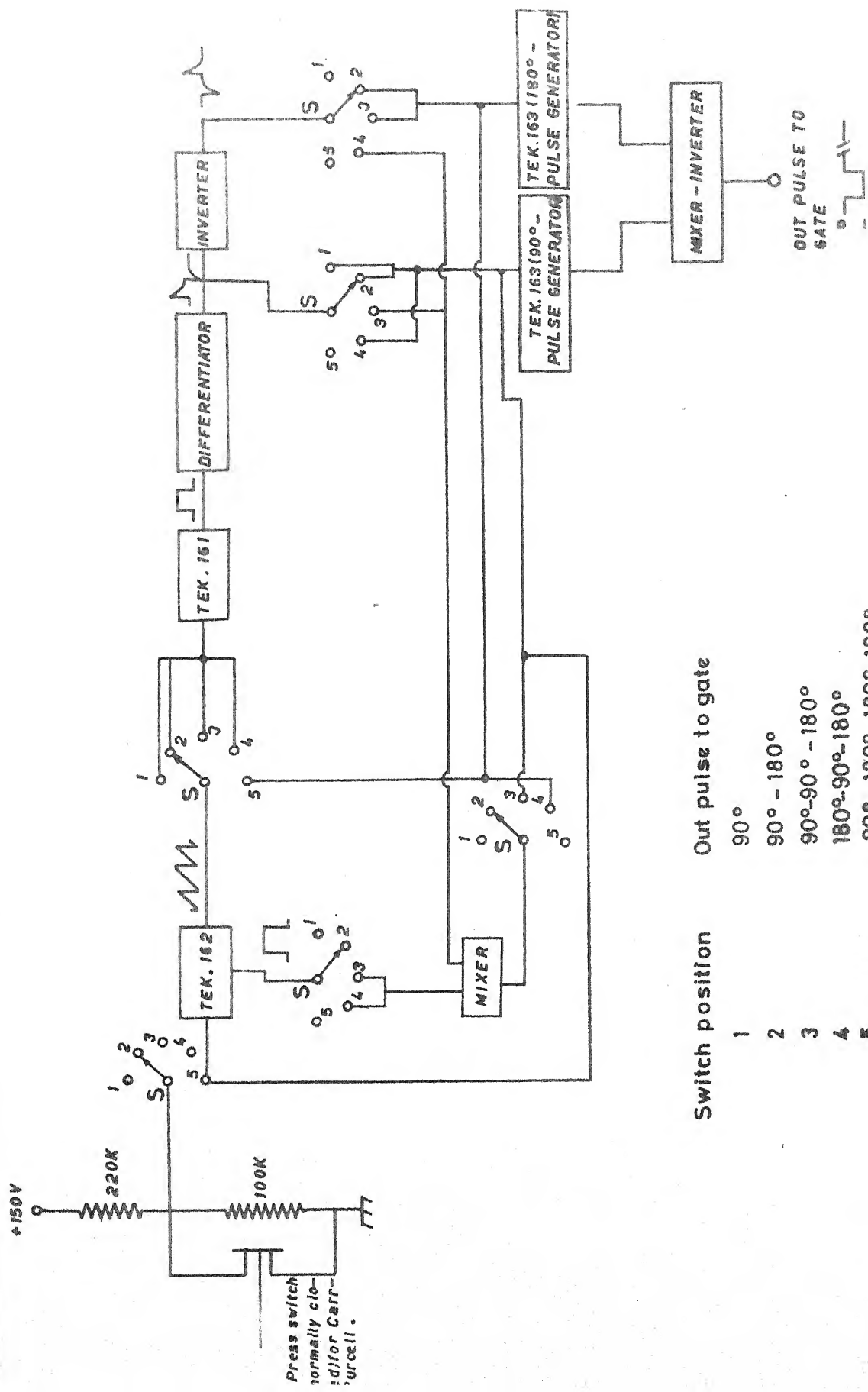


FIGURE 3. GATED OSCILLATOR



Switch position	Out pulse to gate
1	90°
2	90° - 180°
3	90°-90° - 180°
4	180°-90°-180°
5	90° - 180° - 180°-180°

(CARR-PURCELL)

FIGURE 4. PULSE PROGRAMMER

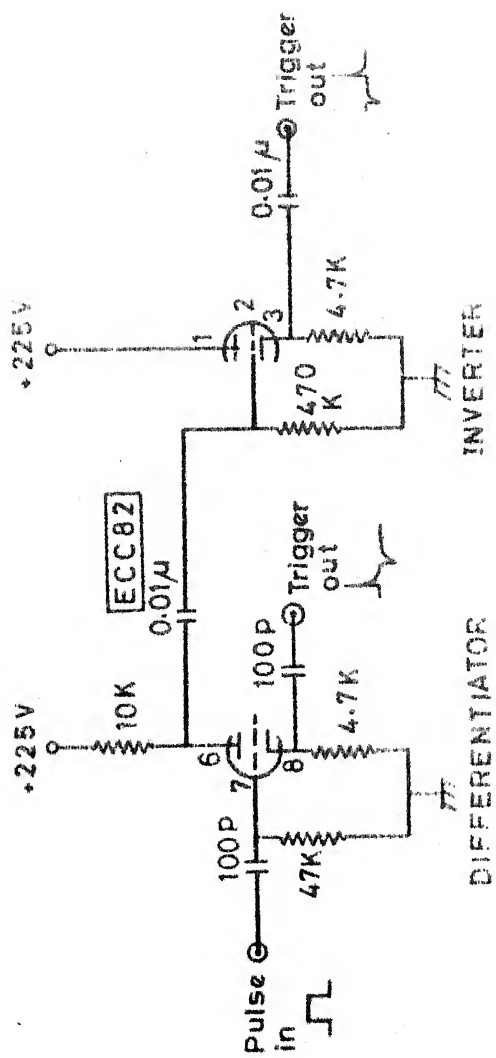


FIGURE 5. DIFFERENTIATOR-INVERTER

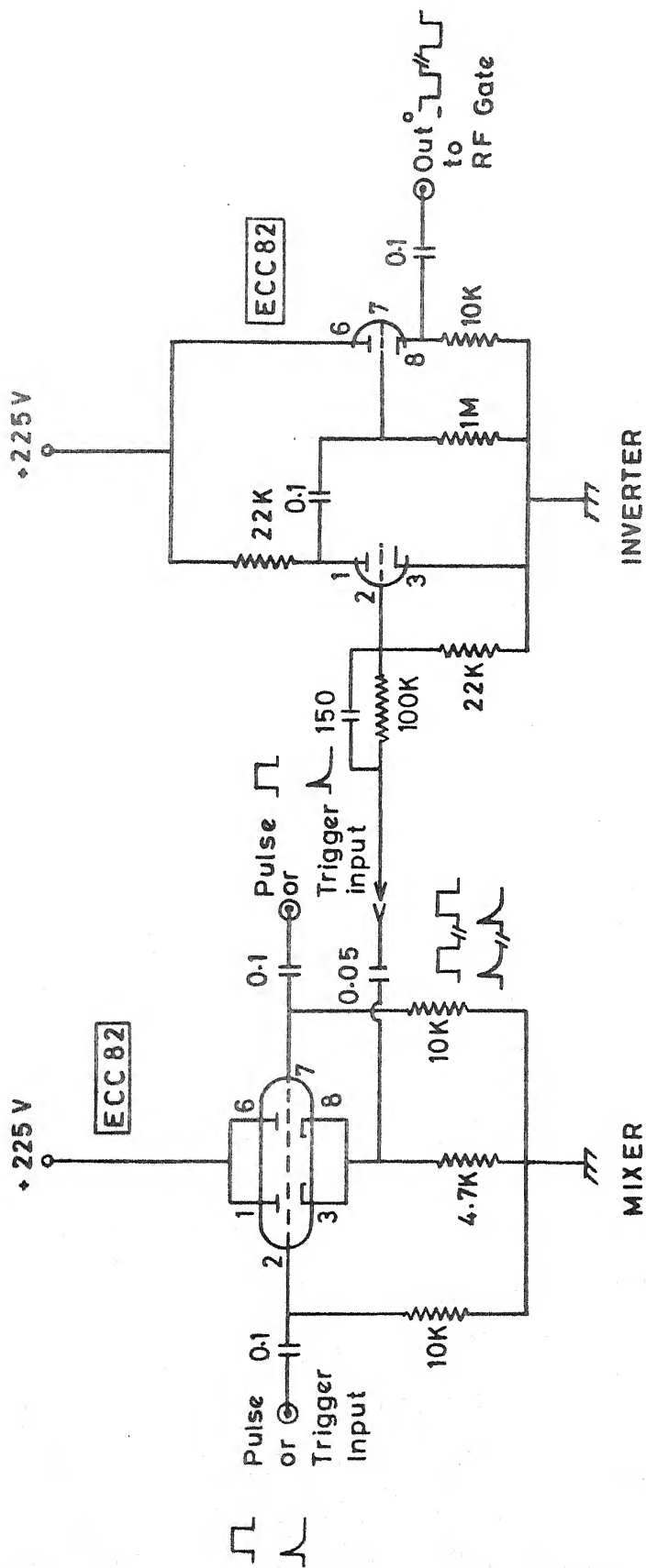


FIGURE 6. MIXER-INVERTER

only. (See for arrangement Figure 4.) The programmed pulse intervals are measured by an Hewlett-Packard counter (Model 521C) after passing through a pulse shaping unit (see Figure 7).

## 2.4 Receiver

The rf receiver has four stages of rf amplifier stagger-tuned to a centre frequency of nearly 9.78 MHz and a band width of 1 MHz. The circuitry (Figure 8) is of standard design. Mainly weather conditions, ageing of the active components and environmental vicissitudes, have from time to time necessitated tuning and tracking of the receiver for good signal-to-noise ratio and faithful reproduction of the signal. For signals which are too large or too small the diode can act nonlinearly and give faulty signal levels. The goodness of the receiver linearity for the range of signals of our interest is checked from time to time as follows. The pulse sequence is programmed to give an echo monitoring the strength of equilibrium magnetization. This echo amplitude is proportional to the number of resonating spins in the sample. Direct linear relationship between the signal strength and the number of spins in the coil which is in turn proportional to  $\rho n/M_h$ ; where  $\rho$  is the liquid sample density,  $n$  is the number of resonating spins per molecule and  $M_h$  is the molecular weight has been found for a variety of samples covering the entire range of our signal observation (see Figure 9). The receiver needs good rf-shielding and stout power and signal connections to avoid any untoward phase detection, noise, etc..

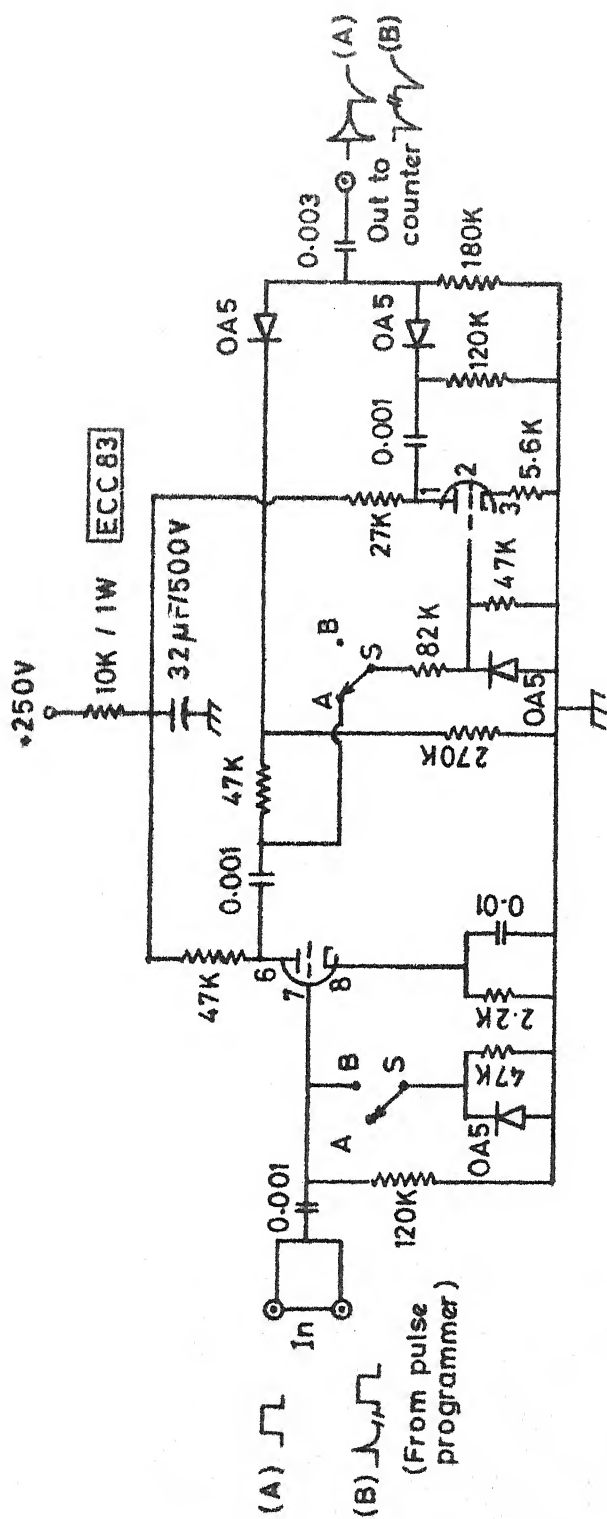


FIGURE 7. PULSE SHAPER



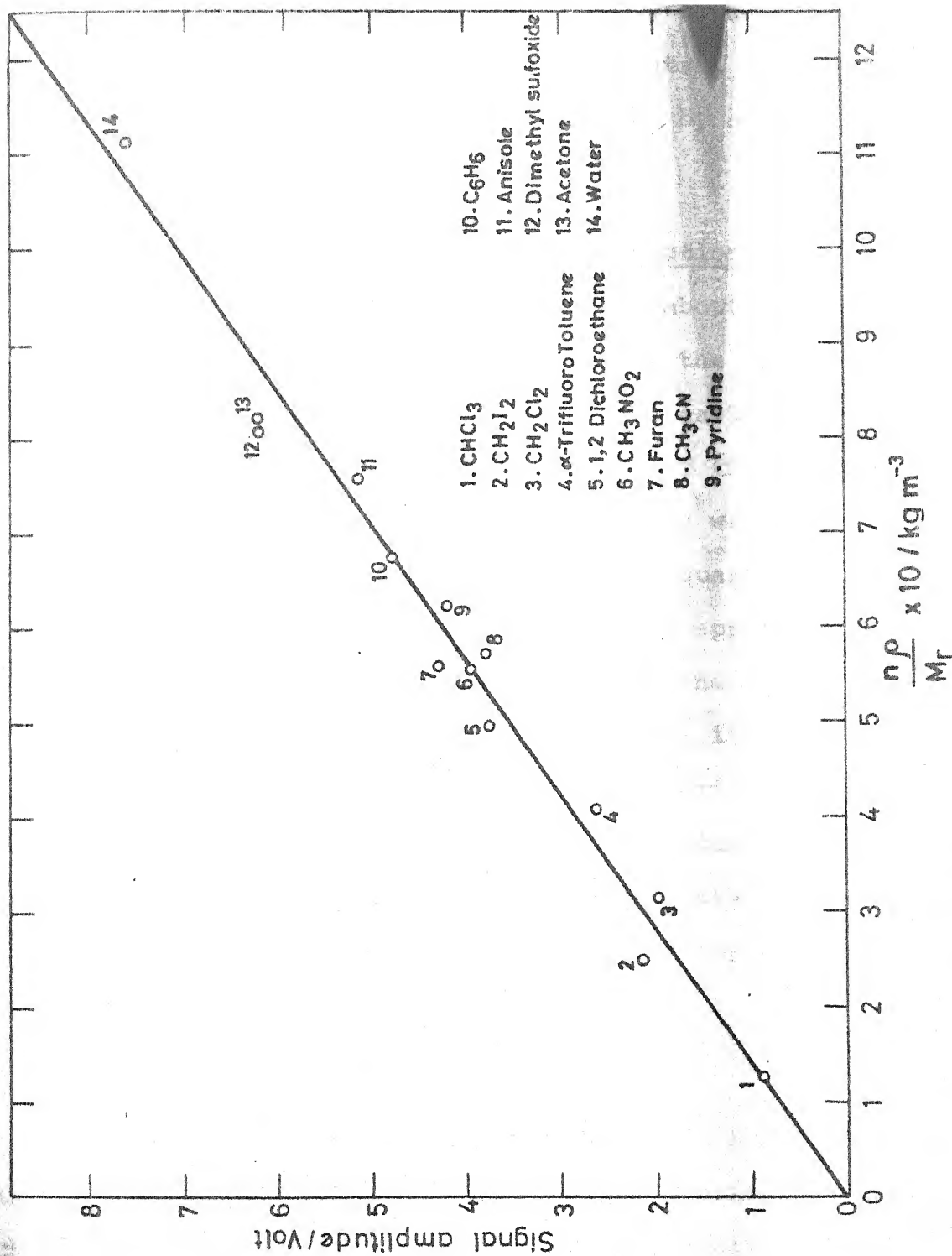


FIGURE 9. RECEIVER LINEARITY CHECK. SIGNAL AMPLITUDE VS. SPIN DENSITY PLOT.

## 2.5 Tank Coil

The tank coil consists of closely wound ten turns of SWG 18 copper wire. Positioned in the central region of the magnet, it is fixed to the thermostat lead by about 0.2 m of the same copper wire.

## 2.6 Transmitter-Tank Coil-Receiver Connection

A coaxial cable length (RG 59/U) about 2.2 m long spans the distance from the transmitter to the tank coil-head BNC T-connector. Another piece of similar cable about 1.0 m long joins the receiver to the other side of the tank coil-head of the BNC T-connector. These cable lengths were chosen by a cut-and-try-method as the use of the exact quarter wave lines (~7.5 m) has proved to be ideal rather than appropriate in real life. The copper wire length between the tank coil and the cryostat lid connector and the non-ideal impedances of the transmitter output and receiver input give rise to a quite complicated theoretical impedance matching problem. In view of this, with an aim to get maximum rf power delivery to the sample and maximum signal delivery to the receiver input the cut-and-try-method has been most practical.

## 2.7 Magnet

A 12" diameter Varian magnet Model VFR 2703 was used in the present work. Apart from the field variation due to changes in the mean level of the electric supply voltage

(depending on other loads on the electric supply line) and erratic fluctuations, the cooling of the magnet coils has been problematic when the water supply line pressure got low. The Hall probe sensing and regulating the magnetic field has a long cable to the magnet power supply. This long cable if not firmly connected can give field fluctuations due to the contact potential change at the connector head.

## 2.8 Field Gradient

A steady field gradient at the central region of the magnet is provided by a two coil system, with the coils placed close to the pole faces and having the common axis colinear with the magnet axis (Figure 10). Care must be taken that the sense of current in the coils gives rise to similar poles facing each other. Each of the pair of the coils consists of 50 turns of SWG 20 enamel coated copper wire wound on perspex formers ~7.0 cm in diameter separated from each other by 5.5 cm. A single 1.5 V dry cell is a good power source. A current of 50 mA gives rise to a field gradient of  $2.67 \text{ mT m}^{-1}$ . The change of magnetic field over the sample tube radius 5mm is  $\sim 13 \mu\text{T}$  which is much smaller than the rf-field amplitude  $H_1 \sim 600 \mu\text{T}$  thus satisfying the condition for good gradient field (Woessner (1960)).

## 2.9 Thermostat

The thermostat is a two-walled Dewar flask. The lid bears the BNC T-connector for the signal line with connections reaching from the tank coil at the bottom. The heater

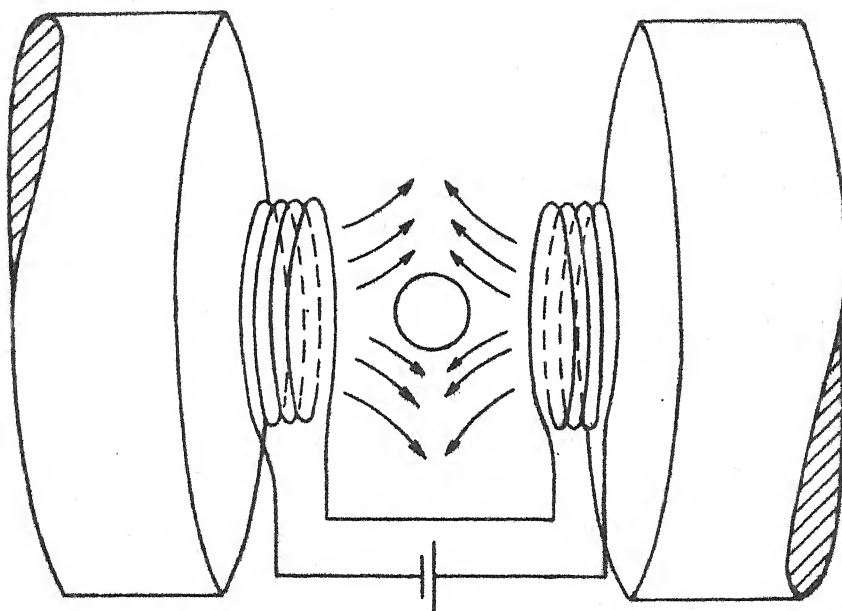


FIGURE 10. FIELD GRADIENT ARRANGEMENT

arrangement inside the thermostat for the sample heating is made up of nonmagnetic high resistance Eureka wires. Two identical heaters in series flank the sample tube symmetrically. Each of the heaters consists of two layers of the heater wire of equal number of turns. The sense of winding of one layer is opposite to that of the other so that the net magnetic field produced by each heater system is zero. Nonvanishing fields will greatly disturb the reckonable gradient field imposed for the self-diffusion coefficient measurement. The heater leads are taken out through the thermostat lid. A copper-constantan thermocouple is taken through the thermostat lid for the junction to sit on the sample and monitor the sample temperature. Good temperature stabilization of the sample is achieved within fortyfive minutes of maintaining a constant dc. The temperature gradient along the sample inside the thermostat sometimes gives violent convection currents in the liquid which is detrimental to the measurement. Such occurrences are scrupulously avoided by maintaining a constant temperature along the sample by means of proper thermal contacts. Onset of convection gives a lower  $D$ . (See Carr *et al* (1954), Kosfeld(1968)).

## 2.10 Sample Preparation

Good grade reagents (mostly of spectroscopic grade) obtained from commercial sources are doubly distilled to start with in order to get rid of dissolved and suspended impurities. Further processing is done in borosilicate glass sample tubes

which can withstand the internal vapour pressure at high temperature ( $\sim 60\text{atm}$  at the highest temperatures  $\sim 200^\circ\text{C}$ ) (see Figure 11). Above the bulb L containing the liquid there is sufficient free space (FS) to maintain liquid-vapour co-existence at the experimental temperatures. The free space volume (FS) at room temperature is so chosen that the sample volume at critical temperature fills the entire tube volume  $V(L + \text{FS})$ . The ratio of the sample liquid volume  $V(L)$  to the entire sample tube volume  $V(L + \text{FS})$  equals the ratio of critical density of the sample to the density at room temperature. There is a small well near the bottom of the tube into which is inserted the thermocouple junction for temperature reading. The distilled sample charged to the required level of the sample tube is frozen and the tube attached to the vacuum line capable of achieving a pressure of nearly  $10^{-3}$  Torr. The gas above the frozen liquid is evacuated. After a while the sample tube is isolated and the frozen liquid allowed to thaw. Because of the low pressure in the region FS dissolved gases in the liquid boil out. Subsequent re-freezing of the liquid in region L and evacuation removes these boiled out gases. Five or six such freeze-pump-thaw cycles proved adequate to divest the sample of any sizeable, highly disturbing paramagnetic oxygen gas impurity, after which the tube is sealed at  $S_1$ . Then the highly reactive barium getter G is fired to capture all the residual released gases. Finally the sample tube is sealed at  $S_2$  and separated. The pressure at the top of the frozen sample is now better than  $10^{-3}$  Torr.

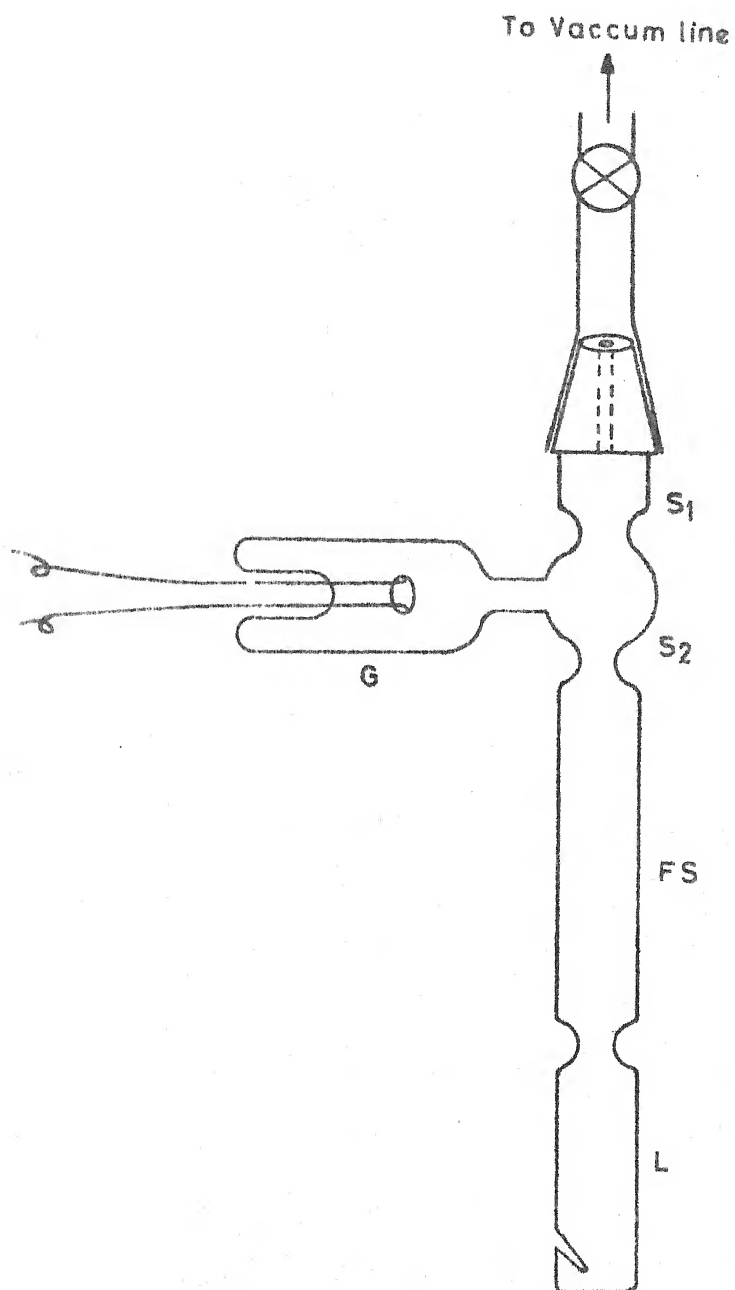


FIGURE 11. SAMPLE TUBE

## 2.11 Spectrometer Tuning

The magnet and the electronic system gets stabilized in half an hours time. Before observing the nmr signal the spectrometer is tuned as follows. The transmitter output level is set at about  $\sim 300V$  rf. The receiver band width and centre frequency are also checked by using a cw rf generator. This makes the transmitter-receiver system ready for the actual signal.

With the connections for signal flow made as shown in Figure 2 a vial of glycerine or tap water doped with a speck of a paramagnetic salt is placed inside the sample coil with the entire coil volume filled. A single pulse, a microsecond or two wide, is fed to the pass gate, repeating at an interval of one second. The magnetic field is now slowly increased with an eye on the oscilloscope screen. With the approach of the resonance frequency beat patterns appear on the screen. Exactly at resonance the beat frequency is zero with a long tail and hence the resonance is very easily discernible. The width of the pulse is now increased to a value which gives maximum tail height of the free induction decay. This would correspond to a  $90^\circ$  pulse. Several alternate pulse width and field settings are necessary to be at resonance and to get an exact  $90^\circ$  pulse. Next the  $90^\circ$  pulse is removed from the pass gate and the pulse channel which will give a  $180^\circ$  pulse is coupled in. The  $180^\circ$  pulse setting is made with the

visual monitor such that the tail height for a  $180^\circ$  pulse is zero. The receiver, going dead for a while after the large rf pulse, is unable to see the signal during the dead time. Hence it becomes difficult to monitor the exact tail height, and the  $180^\circ$  pulse setting is slightly arbitrary. However, the settings of the  $90^\circ$  and  $180^\circ$  pulses which are slightly off do not create any perceptible problem in subsequent measurements described below.

## 2.12 Signal Display and Measurement

Echoes are convenient to display and measure, and are free of receiver dead time. They are therefore better suited than free induction decays. The echo is stored on a Tektronix Model 549 storage oscilloscope screen. The height of the echo from the average base line is measured by a divider and scale. In the two-pulse  $90^\circ$ - $t$ - $180^\circ$  setting, if the interval  $t$  is short enough to give any reckonable relaxation, the echo height is a monitor of the equilibrium magnetization and is proportional to the number of resonating spins.

## 2.13 $T_1$ Measurement

A  $90^\circ$ - $t$ - $90^\circ$ - $\tau$ - $180^\circ$  pulse sequence where  $\tau \ll T_1$  and  $t$  can be programmed is used to give an echo at a time  $\tau$  after the last  $180^\circ$  pulse. The advantages of an echo measurement are cited in the previous section. If the resonating nuclei

are symmetrically placed in the molecule they are expected to have a single relaxation time given by the formula

$$S_z(t) = S(0) (1 - e^{-t/T_1}),$$

where  $S(0)$  and  $S_z(t)$  are the voltage amplitudes of the echo corresponding to the equilibrium magnetization and the growth of the longitudinal magnetization at time  $t$  respectively. The method of monitoring the equilibrium magnetization is described earlier.  $S_z(t)$  was measured for at least eight settings of  $t$ .  $S(0)$  is measured intermittently. Between successive measurements of  $S_z(t)$  a sufficient time ( $\sim 5T_1$ ) is allowed so that the spins relax back to their equilibrium value. A plot of  $\log \{S(0)/[S(0) - S_z]\}$  versus  $t$  gives a straight line of slope  $(\log e)/T_1$ . The accuracy of the relaxation times thus determined is found to be within 5%.

## 2.14 D Measurement

A steady field gradient of known value is essential here whereas the sole purpose of a gradient field in  $T_1$  measurement was for forming manageable echoes. In a two-pulse  $90^\circ - t - 180^\circ$  sequence the echo signal amplitude is related to the equilibrium value through the relation

$$S_z(t) = S(0) \exp (-\gamma^2 G^2 t^3 / 12D - t/T_2),$$

where  $G$  is the field gradient and others have their usual meanings. The gradient chosen must be such as to give a

more rapidly varying term than the second term but not so large as to forbid sufficient  $t$  range observations. A current of 50 mA through the gradient coils giving rise to a field gradient of magnitude  $2.67 \text{ mT m}^{-1}$  has been found to be suitable as well as convenient. In view of such a choice of the gradient the foregoing equation may be written as

$$S_z(t) = S(0) \exp (-\gamma^2 G^2 t^3 / 12D).$$

Hence a plot of  $\log (S(0)/S_z)$  versus  $t^3$  should give a straight line of slope  $\gamma^2 G^2 / 12D$  which will yield  $D$  if  $G$  is known. Mathematical formulae have been in vogue to estimate  $G$ . They are derivations for idealized cases bearing little resemblance to real life situations. On the other hand, the procedure used here is to take  $D$  of several test samples as stated below (§2.15) and to calculate  $G$  from the slope of the  $\log (S(0)/S_z)$  versus  $t^3$  straight line and the known value of  $D$ . The  $G$  thus found for the gradient current setting of 50 mA is used for calculating the  $D$ s of samples under test from the observed slopes. The accuracy of such  $D$  measurement is 5%. The observed slopes of the straight lines  $\log (S(0)/S_z)$  versus  $t^3$  at the various working temperatures are multiplied by the ratio of test sample  $D$  to its  $\log (S(0)/S_z)$  versus  $t^3$  straight line slope, to give the sample  $D$  at that temperature.

## 2.15 Test Sample Runs

Two test samples, one of water and the other of benzene, are used from time to time to check on the spectrometer functioning and the data credibility. Before and after each experimental sample run the  $T_1$  and  $D$  of the test samples at room temperature are measured to ascertain that the spectrometer behaved well during the experimental sample run. Test sample  $T_1$  and  $D$  measured in the way cited above (§ 2.13 and 2.14) are given in Figures 12 and 13. The errors in  $T_1$  and  $D$  thus measured are about  $\pm 5\%$ . Mills (1971, 1973) lists the various  $D$  measurements in these test samples. In water,  $T_1$  measured as a function of temperature is available in Simpson and Carr (1958). In benzene,  $T_1$  measured as a function of temperature are available in Green and Powles (1965), and Powles and Figgins (1965).

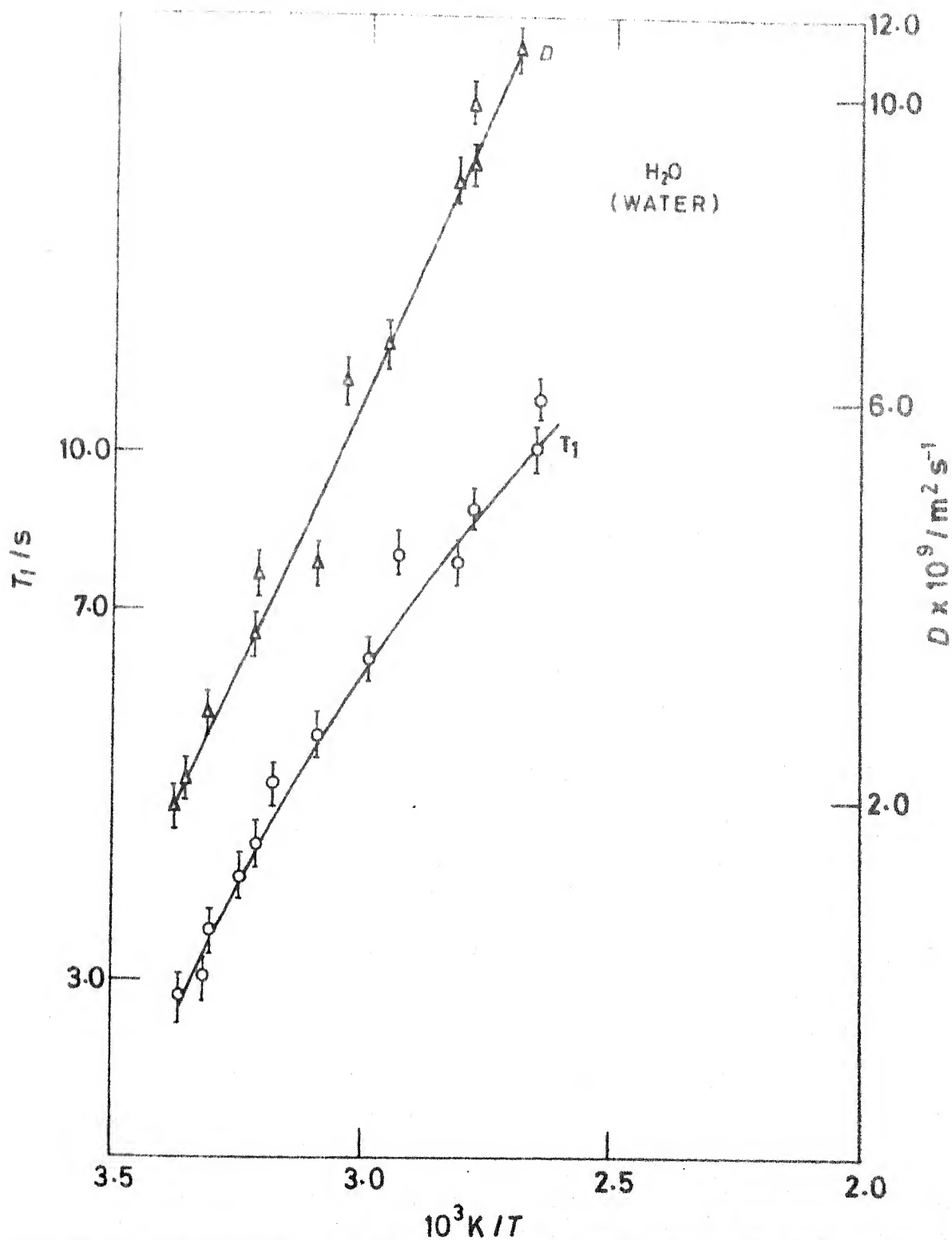


FIGURE 12. TEMPERATURE DEPENDENCE OF PROTON SPIN-LATTICE RELAXATION TIME ( $T_1$ ) AND SELF-DIFFUSION COEFFICIENT ( $D$ ) IN DISTILLED WATER.

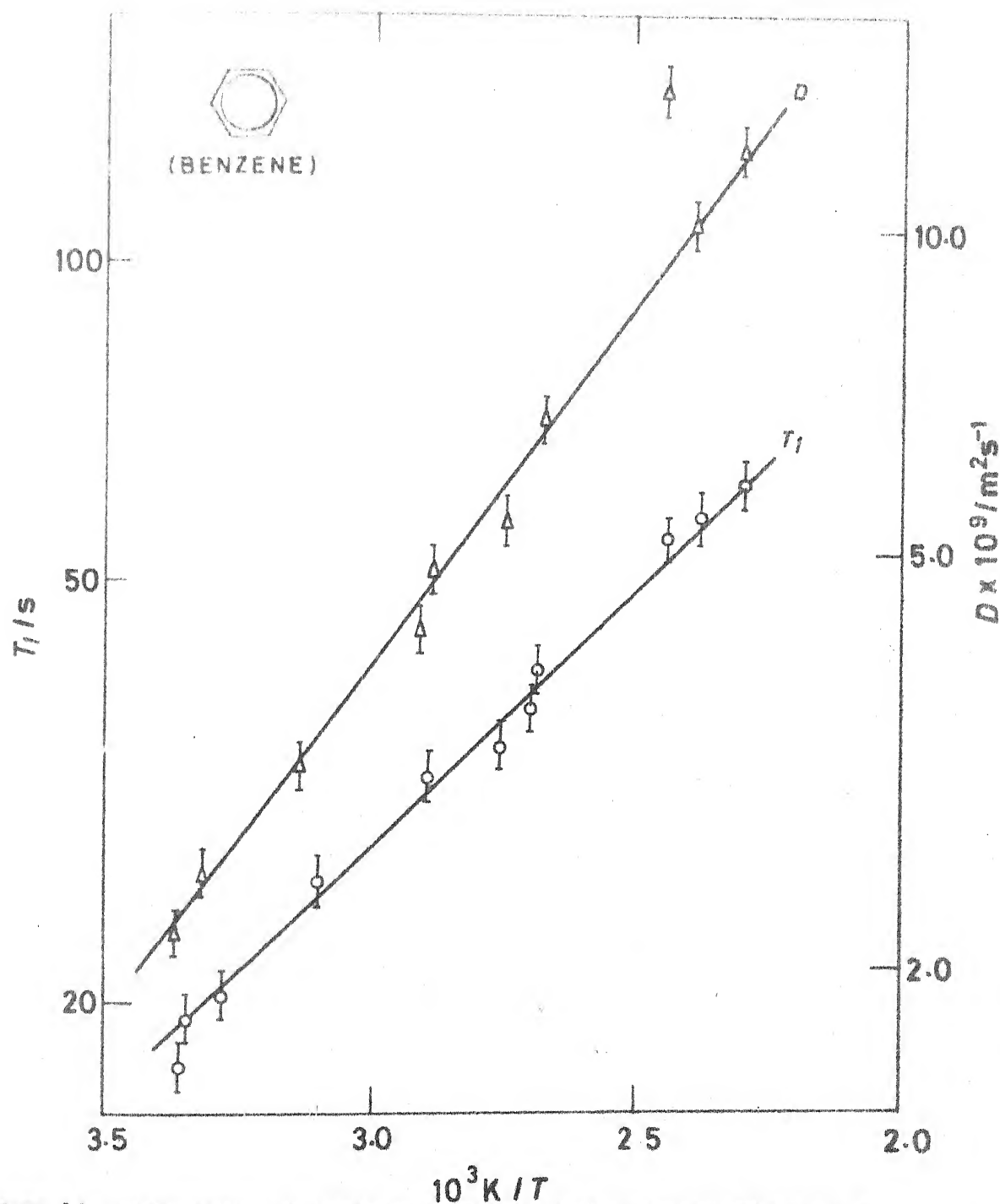


FIGURE 13. TEMPERATURE DEPENDENCE OF PROTON SPIN-LATTICE RELAXATION TIME ( $T_1$ ) AND SELF-DIFFUSION COEFFICIENT ( $D$ ) IN BENZENE.

*Coherence is all.*

### CHAPTER 3

#### SPIN-ROTATION RELAXATION IN LIQUIDS FOR DYNAMICALLY COHERENT REORIENTATION\*

Molecular dynamics, mainly the rotational motion in liquid, is much more intractable than that in gases and solids. In dilute gases the rotational motion is analyzed in analogy with quantum mechanical free rotors. In solids the molecules having been locked to the lattice sites the possible rotational motions are about the well defined molecular axes through well defined angular steps. In liquids the molecular rotational motion can take place about many an axis through unrestricted angular steps where the molecular symmetry axis is itself undergoing orientational changes. To add to the complication, non-spherical molecules too have greater facility for rotating preferentially about the molecular symmetry axis and the rotational anisotropy must be carefully taken into consideration.

As the molecules are energized (say, by increasing the temperature) the orientational changes are much more frequent but the molecule stays in its higher rotational states longer. In other words, the orientational correlation time decreases and the rotational correlation time increases with temperature rise (Gutowsky, Lawrenson and Shimomura (1961). Brown, Gutowsky

---

\*The work presented in this chapter appears in Chem. Phys. Lett. (1974) 27 592.

and Shimomura (1963), Hubbard (1963 Green and Powles (1965)). The orientational change affects the laboratory frame dipole-dipole interaction strength through the second order spherical harmonics  $Y_2^m(\theta, \phi)$ . Spin-rotation interaction takes place in the molecular frame, as the molecular rotation involves the motion of the associated charges and therefore gives rise to a sizeable magnetic field to couple to the nuclear spin under observation in the molecule. Since observations are made in the laboratory frame and the nuclear spins are polarized by the laboratory magnetic field the molecular rotations must be transformed to the laboratory frame and in so doing molecular orientational angles relative to the laboratory frame are involved. Therefore, the spin-rotation interaction seems to be both orientation- and rotation-dependent, whereas the intramolecular dipole-dipole interaction depends on the orientation of the dipole-dipole vector in the laboratory frame marked by the polarizing magnetic field.

At low temperatures and particularly in liquids it is usually taken for granted that many a molecular collisions go into randomly changing the molecular orientation through one radian. Since it has been shown (Huntress (1970), Chandler (1975)) that the collision time approximates the angular momentum correlation time the present situation is the diffusion case where  $\tau_J \ll \tau_\theta$ . In this diffusion limit the fluctuation in the magnitude of the angular velocity of the molecule has

the predominant contribution to the spin-rotation relaxation rate. As the temperature of the liquid is raised to the neighbourhood of the liquid-vapour critical temperature molecular collisions are less frequent and therefore the persistence of molecular rotation is much longer and in fact  $\tau_J \sim \tau_\theta$ . But at a temperature much below the critical temperature coherent rotational motions for periods longer than expected are observed (Moniz, Steele and Dixon (1963), Atkins, Loewenstein and Margalit (1969), Miller and Gordon (1970), Kitchlew and Nageswara Rao (1973b), Krishna and Gordon (1974), Mishra and Nageswara Rao (1974)). Such coherent motion will therefore give rise to stronger spin-rotation interaction than that expected in dipolar liquids. It is therefore worthwhile to derive the relation between the spin-rotation relaxation rate and temperature in the case of dynamically coherent motion.

The spin-rotation interaction can be given by a bilinear coupling, i.e. a coupling of the rotational angular momentum of the molecule with the angular momentum of the electrons and then the coupling of the angular momentum of the electrons with the nuclear spins. If  $\underline{I}$  is the nuclear spin  $\underline{J}(t)$  the angular momentum whose time-dependence arises due to collisions bringing about changes in it, and  $C_{ij}$  are the components of the spin-rotation coupling tensor, the interaction hamiltonian can be given by

$$H' = \underline{I} \cdot \underline{C} \cdot \underline{J}, \quad (3.1)$$

in the laboratory frame set up by the polarizing static magnetic field  $H_0$ .

In general the coupling tensor is not symmetric and therefore cannot be diagonalized. For the convenience of handling, the coupling tensor  $C$  is taken as the sum of a scalar tensor  $C^{(0)}$  whose elements are  $1/3 \text{Tr}(C)$ , an anti-symmetric tensor of rank one:  $C^{(1)}$ , whose elements are  $C_{ij}^{(1)} = 1/2 (C_{ij} - C_{ji})$  and a symmetric tensor of rank two:  $C^{(2)}$ , whose elements are  $C_{ij}^{(2)} = 1/2 \{C_{ij} + C_{ji} - 2/3 \text{Tr}(C)\}$  where  $C_{ij}$  is the  $(ij)^{\text{th}}$  element of  $C$ . Using the index  $\ell (=0, 1, 2)$  one can write

$$H' = \sum_{\ell} \underline{I} \cdot \underline{C}^{(\ell)} \cdot \underline{J}(t), \quad (3.2)$$

in the molecular frame. In general each component of the hamiltonian in the laboratory frame is given by

$$H'_{\ell} = \sum_{q=-\ell}^{\ell} (-1)^q F_{\ell}^q(t) A_{\ell}^{-q}, \quad (3.3)$$

where  $F^{-q}(t)$  is the time-dependent lattice operator responsible to bring about relaxation of the spin system and  $A^{-q}$  are the spin operators. As observations are made in the laboratory frame the foregoing form of the hamiltonian is most suitable in describing the relaxation of the spin system. The rate equation for the spins is given by

$$\frac{d\langle I_z \rangle^I}{dt} = -J(0) \sum_q (-1)^q \text{Tr}[A^q, [A^{-q}, I_z]] (\sigma_z^I - \sigma_0^I), \quad (3.4)$$

where  $\langle I_z \rangle^I$  is the expectation value of the spin magnetization

in the field direction,  $\sigma_0^I$  is the equilibrium value of the density matrix  $\sigma^I$ , (the superscript  $I$  denoting the use of the interaction picture) and  $J(0)$  is the usual spectral density under the extreme narrowing condition, i.e.  $\omega\tau \ll 1$ , having the form

$$J(0) = J^q(q\omega_0) = \int_0^\infty d\tau \langle F^*(t) F(t - \tau) \rangle, \quad (3.5)$$

is independent of both  $q$  and  $\omega_0$ . The important thing to note here is that under the extreme narrowing condition the integral of any lattice operator's time correlation function predominantly determines the rate of change of spin magnetization and that the knowledge of detailed nature of the lattice operator is not required.

As the molecular frame equation must be changed over to the laboratory frame in order to put Eq. 3.2 in a form like Eq. 3.3 the help of Wigner rotation matrices must be taken. Both  $I$  and  $J$  are operators of rank one and therefore the rotation matrices  $D^{(1)}$  are of use (Rose (1957)). One then writes

$$A_{\text{molecule-fixed}}^q = \sum_{q', q} D^{(1)}_{q'q}(\Omega) \Lambda_{\text{space-fixed}}^{q'}, \quad (3.6)$$

and a similar relation for  $F^q(t)$  operators. Inserting these into Eq. 3.4 one then finally gets

$$\begin{aligned}
-\frac{d}{dt} \langle I_z \rangle &= \sum_{\substack{\ell, q, \\ k, m, \\ q', m'}} (-1)^{m+k} C(1, 1, \ell, m-q, q, m) \\
&\quad C(1, 1, \ell, m'-q', q', m') C^{\ell m'} C^{\ell m} \\
\int_0^\infty d\tau \langle J^{(m-q)}(0) D_{kq}^{(1)*}(0) J^{(-m'+q')}( \tau ) D_{k-q'}^{(1)}( \tau ) \rangle_{av} \\
&\quad \text{Tr} \{ [A^{-k}, [A^k, I_z]] (\sigma - \sigma_0) \}, \quad (3.7)
\end{aligned}$$

where  $C(1, 1, \ell, m-q, q, m)$  etc. are the Clebsch-Gordon coefficients  $C_{\ell}^{m'}$  s are the components of the  $C_{\ell}^i$  tensor in the molecular frame with the rotational angular momentum operator connected to the lattice operator in the molecular frame by

$$F_{\ell}^{iq} = \sum_m (-1)^q C(1, 1, \ell, m-q, q, m) C_{\ell}^{m'} J^{m'+q}(t). \quad (3.8)$$

In Eq. 3.7 two types of correlation functions are involved. In the first kind the molecular rotation leads to the modulation of the components of  $C$  and hence the correlation arising because of  $C$  modulation must be noted. In the second kind of the correlation function within the angular brackets of Eq. 3.7 are fairly involved as they simultaneously contain operators pertaining to the angular momentum (i.e. rotational) persistence and the persistence of the orientation of the molecule relative to the laboratory frame. The exact evaluation of this correlation function in the most general case is very involved.

Although the use of  $\rho^{(1)}$  as a starting point comes naturally because of the rank of the operators  $\rho^{(1)}$  and  $\rho^{(2)}$  involved, transforming to use  $\rho^{(2)}$  as a starting point is most profitable as  $\rho^{(2)}$  happens to be arising most naturally in other relaxation mechanisms like the intramolecular dipolar interaction, chemical shift anisotropy, quadrupolar interaction where the second rank spherical harmonics are one to the fore. The consistent use of  $\rho^{(2)}$  for all relaxation mechanisms helps to compare the processes from the same platform. This has been successfully achieved by Hubbard (1963b). He connects  $\rho^{(1)}$  and  $\rho^{(2)}$  through the use of the spin operators. Having done so, for a spherical top molecule under the extreme narrowing limit, Hubbard's prescription (Hubbard 1963b), Huntress (1968), Maravott, Farrar and Malinovsky (1977), McCleung (1982) gives

$$\left(\frac{1}{T}\right)_{SR} = \frac{2\pi kT}{h^2} \left( \frac{1}{2} \left( \frac{1}{2} \right) \left( \frac{1}{2} \right) \right) + 2 \left( \frac{1}{2} \right) \left( \frac{1}{2} \right) \quad (3.9)$$

where  $I$  is the moment of inertia,  $k$  is the Boltzmann constant,  $T$  is the temperature and  $\rho$  has as an axis of symmetry such that

$$C_{xx} = (C_{xx} + 2C_{yy})/3, \quad C_{zz} = (C_{zz} - C_{xx})/3,$$

where  $C_{xx}, C_{yy}$  are the corresponding perpendicular and parallel components. The use of  $\rho^{(2)}$  gives as usual an explicitly angular momentum dependent correlation function related to the angular momentum correlation time

$$\tau_{J_1} = \int_0^{\infty} \frac{\langle J^{(1)}(0) \cdot J^{(1)}(t) \rangle}{\langle J^{(1)}(0) \rangle^2} dt, \quad (3.10)$$

and a complicated correlation function  $\langle J^{(2)*}(0) \rho_{qm}^{(2)*}(\phi, 0) J^{(2)}(t) \rho_{qm}^{(2)}(\phi', t) \rangle$  like the one in Eq. 3.7 related to a correlation time  $\tau_{J_2}$  involving integrals like

$$\int_0^{\infty} \langle J^{(2)*}(0) \rho_{qm}^{(2)*}(\phi, 0) J^{(2)}(t) \rho_{qm}^{(2)}(\phi', t) \rangle dt.$$

Like the correlation function in Eq. 3.7 handling the correlation function in the foregoing equation in the most general case is equally difficult. Separation of the angular momentum and orientation dependent parts is only achieved in extreme limits where such mutual dependence is greatly decoupled. The solution at such convenient limits is shown in the following.

For such limit consideration, a knowledge of the free molecular period is of great help. The inertia and thermal energy of the molecule determine the free period of rotation given by  $\tau_f = (I/kT)^{1/2}$ . Also of use is the correlation time  $\tau_J$ , a measure of fluctuation of the magnitude of the angular velocity  $|\omega|$ , given by a rotational diffusion equation  $\tau_J = I \rho_{\text{rot}}/kT$ . Two other correlation times of importance are  $\tau_{\theta_1}$  and  $\tau_{\theta_2}$ . Correlation time  $\tau_{\theta_1}$  is the one that arises in dielectric measurements giving us a measure of the orientational correlation of the dipolar axis through the integral of the correlation function of the spherical harmonic  $Y_1^m$ . The correlation time  $\tau_{\theta_2}$  arises in the strength of intramolecular dipolar interaction, quadrupolar interaction, chemical shift

anisotropy interaction etc. in nmr measurements giving us a measure of the orientational correlation of the appropriate vector pertaining to the interaction through the integral of the correlation function of the spherical harmonic  $Y_2^m$ .

In the diffusion limit many a molecular collisions are necessary finally to give a random orientational change by one radian. Therefore the collision time which is a measure of  $\tau_J$  is much shorter than  $\tau_{\theta_1}$  and  $\tau_{\theta_2}$  the orientational correlation times. During  $\tau_J$ , therefore, the orientation dependent  $\mathcal{D}^{(2)}(\theta, \tau)$  does not change appreciably. Two distinct simplifications arise thereof. First,  $J$  and  $\mathcal{D}^{(2)}$  in Eq. 3.11 are decoupled, and second, the constancy over the period leads to unit correlation, i.e.  $\mathcal{D}^{(2)}$ s are completely correlated over the interval. Hence the relation in Eq. 3.11 simplifies to that Eq. 3.10 giving  $\tau_{J_1} = \tau_{J_2} = \tau_J = 1/\mathcal{D}_{\text{rot}}/kT$ . Now insertion of the  $\tau_{J_1}$  and  $\tau_{J_2}$  values into Eq. 3.9 leads to the relation

$$(1/T_1)_{\text{SR}} \propto \mathcal{D}_{\text{rot}}. \quad (3.12)$$

It has further been shown (see for example Abragam (1961) p.299) that the diffusion equation leads to

$$\tau_{\theta_1} = 1/2 \mathcal{D}_{\text{rot}} \text{ and } \tau_{\theta_2} = 1/6 \mathcal{D}_{\text{rot}}.$$

As mentioned earlier, since  $\tau_{\theta_2}$  is directly proportional to intramolecular dipolar interaction and hence to the corresponding relaxation rate, one can write for the dipole-dipole

relaxation rate

$$1/T_{1d-d} \propto 1/\rho_{\text{rot}}. \quad (3.13)$$

The rotational processes being temperature-activated, Eqs. 3.12 and 3.13 show opposite temperature-dependence for the spin-rotation and intramolecular dipolar relaxation rates in the diffusion limit.

In the inertial limit, which is supposed to be achieved near the liquid-vapour critical temperature, the rotational motions are dynamically coherent (Steele (1963), Atkins (1969)), i.e. they occur for times comparable to orientational correlation time and molecular free rotation time, i.e.  $\tau_J \sim \tau_{\theta 1,2} \sim \tau_\theta$ . The separation of pure rotation and reorientation parts as in the diffusion limit is not possible as  $J$  and  $\rho^{(2)}$  have similar characteristic times and are thought to be very well coupled mutually. The free rotational motion is described as arising due to small rotational friction. A collision-governed diffusion equation fails to describe the rotational motion in this limit. To handle this problem Steele (1963) used a rotational Langevin equation which is nothing but Newton's second law with rotational friction effects properly considered. The diffusion limit definition of  $\tau_J = 10_{\text{rot}}/kT$  is discarded in favour of  $\tau_J = 1/\xi$ , where  $\xi$  is the rotational friction coefficient. Steele shows that in the region  $1/3 < \xi/(IkT)^{1/2} < 2$ ,  $\tau_{\theta l}$  approximates very well the integral of the free rotor

correlation functions which are gaussian. These results of Steele have also been arrived at by Hubbard (1972) independently. The Gaussian decays of the free rotor correlation function give

$$\begin{aligned} \tau_{\theta 1} &= \pi^{1/2}/2 \quad \tau_{\theta} = 1/2 \quad (\pi I/kT)^{1/2} \quad \text{and} \\ \tau_{\theta 2} &= 1/2 \quad (\pi/3)^{1/2} \quad \tau_{\theta} = 1/2 \quad \pi I/3kT)^{1/2}, \end{aligned} \quad (3.14)$$

i.e.  $\tau_{\theta 1}, \tau_{\theta 2} < \tau_{\theta}$ . Further the limit  $\xi/(IkT)^{1/2} < 1$  implies  $\tau_{\theta}/\tau_J < 1$  giving finally the relation  $\tau_{\theta 1}, \tau_{\theta 2} < \tau_{\theta} < \tau_J$ .  $\tau_{\theta 1}, \tau_{\theta 2}$  being now the smallest of all the correlation times, i.e. the orientational changes being quicker than the rotational changes, the orientational dependence (i.e. the nature of  $\tau_{\theta 1}, \tau_{\theta 2}$ ) predominantly governs  $\tau_{J1}$  and  $\tau_{J2}$ . We have, therefore, from Eq. 3.14 and as both  $\tau_{\theta 1}$  and  $\tau_{\theta 2}$  vary as  $T^{-1/2}$ ,  $\tau_{J1}$  and  $\tau_{J2}$  must both vary as  $T^{-1/2}$ . In Eq. 3.9 the spin-rotation relaxation rate is seen to be proportional to  $\tau_J T$ . Hence using the foregoing temperature-dependence of  $\tau_J$  the spin-rotation relaxation rate in the inertial limit will vary as  $T^{1/2}$ . The intramolecular dipolar relaxation being proportional to  $\tau_{\theta 2}$  will vary as  $T^{-1/2}$  (vide Eq. 3.14) in the inertial limit. In many dipolar liquids where both spin-rotation and intramolecular dipolar interactions are active relaxation mechanisms the slow increase of spin-rotation relaxation rate with temperature (as  $T^{-1/2}$ ) must give an essentially constant total dipolar relaxation rate over a large temperature range. The experimental observation of such a broad maximum

in total intramolecular relaxation rate would then hint at the presence of dynamically coherent reorientational motion.

Beyond the inertial limit one gets to the dilute gas region where the rotational coherence time is much longer than the free rotational time. As stated earlier this helps (Bloom, Bridges and Hardy (1971)) in considering the molecular system as a collection of quantum mechanical free rotors and in finding that  $\tau_{J_1}$  and  $\tau_{\theta_2}$  are linearly related. The present observation that  $\tau_{J_1}$  and  $\tau_{J_2}$  are proportional to  $\tau_{\theta_1}$  and  $\tau_{\theta_2}$  in the inertial limit is in the same ball park as the observations of Bloom, Bridges and Hardy (1971) and our results seem to be qualitatively correct (*vide* Chapters 4 and 5). The limited importance of such qualitative agreement must be borne in mind as the present discussion is based on the classical model of reorientation of the spherical rotors whereas the consideration of Bloom *et al* pertains to the quantum mechanical model of the free rotors. Other corroborating evidence to the  $\tau_{J_1}$  ,  $\tau_{\theta_2}$  inverse relationship in the Debye limit and direct relation in the inertial limit comes from McClung (1969, 1972).

*Thou shalt not methylate thy spirit.*

## CHAPTER 4

### STUDIES IN SOME METHYL GROUP CONTAINING MOLECULAR LIQUIDS

Investigations into the molecular motion in a group of compounds; methyl iodide ( $\text{CH}_3\text{I}$ ), acetonitrile ( $\text{CH}_3\text{CN}$ ), nitromethane ( $\text{CH}_3\text{NO}_2$ ), acetone ( $\text{CH}_3\text{COCH}_3$ ) and dimethyl sulfoxide ( $\text{CH}_3\text{SOCH}_3$ ) are reported in this chapter. Of these, methyl iodide and acetonitrile are symmetric top molecules. The barriers to the methyl group rotation in others are as follows:  $\text{CH}_3\text{NO}_2$  6.03 cal/mole and  $\text{CH}_3\text{COCH}_3$  0.778 kcal/mole (Wolrab (1967));  $\text{CH}_3\text{SOCH}_3$  2.2 kcal/mole (Lyerla and Levy (1974)). The working temperature range (300K to 450K) corresponds to a thermal energy range of nearly 0.6 to 1.0 kcal/mole as a result of which in all except the dimethyl sulfoxide the internal motion will be sufficiently activated. These molecules are fairly light ones with small moments of inertia, small root mean square angular momentum and are therefore possible candidates for a good deal of free rotation and consequent spin-rotation interaction (Herzberg (1950), Rugheimer and Hubbard (1963), Hackleman and Hubbard (1963)). Although none of these molecules are light enough to satisfy  $\sqrt{\langle J^2 \rangle}$  less than or equal to 5 (the condition for inertial motion), the possibility of fast motion about the methyl group symmetry axis makes the rotational coherence a possible governing factor for the

relaxation. The moments of inertia ( $I_A$ ,  $I_B$ ,  $I_C$ ) about the principal molecular axes are as follows:

Compound	$I_A \times 10^{47}$ $\text{kg}^{-1}\text{m}^{-2}$	$I_B \times 10^{47}$ $\text{kg}^{-1}\text{m}^{-2}$	$I_C \times 10^{47}$ $\text{kg}^{-1}\text{m}^{-2}$	Source of data
$\text{CH}_3\text{I}$	5.5	5.5	111.9	Lyerla <i>et al</i> (1971)
$\text{CH}_3\text{CN}$	5.5	5.5	91.1	Lyerla <i>et al</i> (1971)
$\text{CH}_3\text{NO}_2$	62.9	79.6	142.8	Cox and Waring (1972)
$\text{CH}_3\text{COCH}_3$	49.8	59.4	103.0	Koga <i>et al</i> (1973)
$\text{CH}_3\text{SOCH}_3$	119.0	119.3	121.5	Feder <i>et al</i> (1969)

At the out set remarkable asymmetry in the moments of inertia of  $\text{CH}_3\text{I}$  and  $\text{CH}_3\text{CN}$  are prominent from the preceding table and hence some large rotational asymmetry in molecular motion is envisaged. Also expected is the large preponderant intramolecular relaxation over the intermolecular relaxation. Zens and Ellis (1975) establish an empirical relation between the spin-rotation relaxation rate and the internal rotation barriers. The molecules of present interest are expected to give sizeable spin-rotation interaction contribution.

Apart from the general interest in investigating into the translational, reorientational and rotational motions, the added complication due to the superposition of the internal rotation on the overall molecular rotation is noticed.

The  $T_1$  and  $D$  measured over suitable temperature ranges for the present series of compounds are shown in Figures 14 to 21. Some of the general observations regarding molecular dynamics which can be made from the look of these curves are as follows. The slow decrease of  $T_1$  with temperature rise in  $\text{CH}_3\text{I}$  and  $\text{CH}_3\text{CN}$  (Figures 14 and 15), suggests surrounding independent free motion and the presence of large spin rotation interaction. The relaxation time of nitromethane increases very slowly with temperature (Fig. 16) and inertial motions are envisaged. The  $T_1$  variation with temperature in acetone (Fig. 18) is moderate and is in keeping with the asymmetric molecular shape with consequent collision limited temperature sensitive process. The bold  $T_1$  variation with temperature in dimethyl sulfoxide (Fig. 20) could be an outcome of a collision limited process. Self-diffusion coefficients in all these compounds seemingly obey the Arrhenius relation

$$D = D(0) \exp(-E/RT) , \quad (4.1)$$

where  $D(0)$  is a constant, and  $E$  is the activation energy over their respective temperature ranges of study. The limited temperature range of observation and the errors in  $D$  measurement makes it particularly hazardous to vouch for the  $D(0)$  and  $E$  parameters. Nevertheless, as some authors quote the self-diffusion activation energies for some of the presently discussed compounds, the calculated activation energies from our data are presented in Table 4.1 for the purpose of comparison.

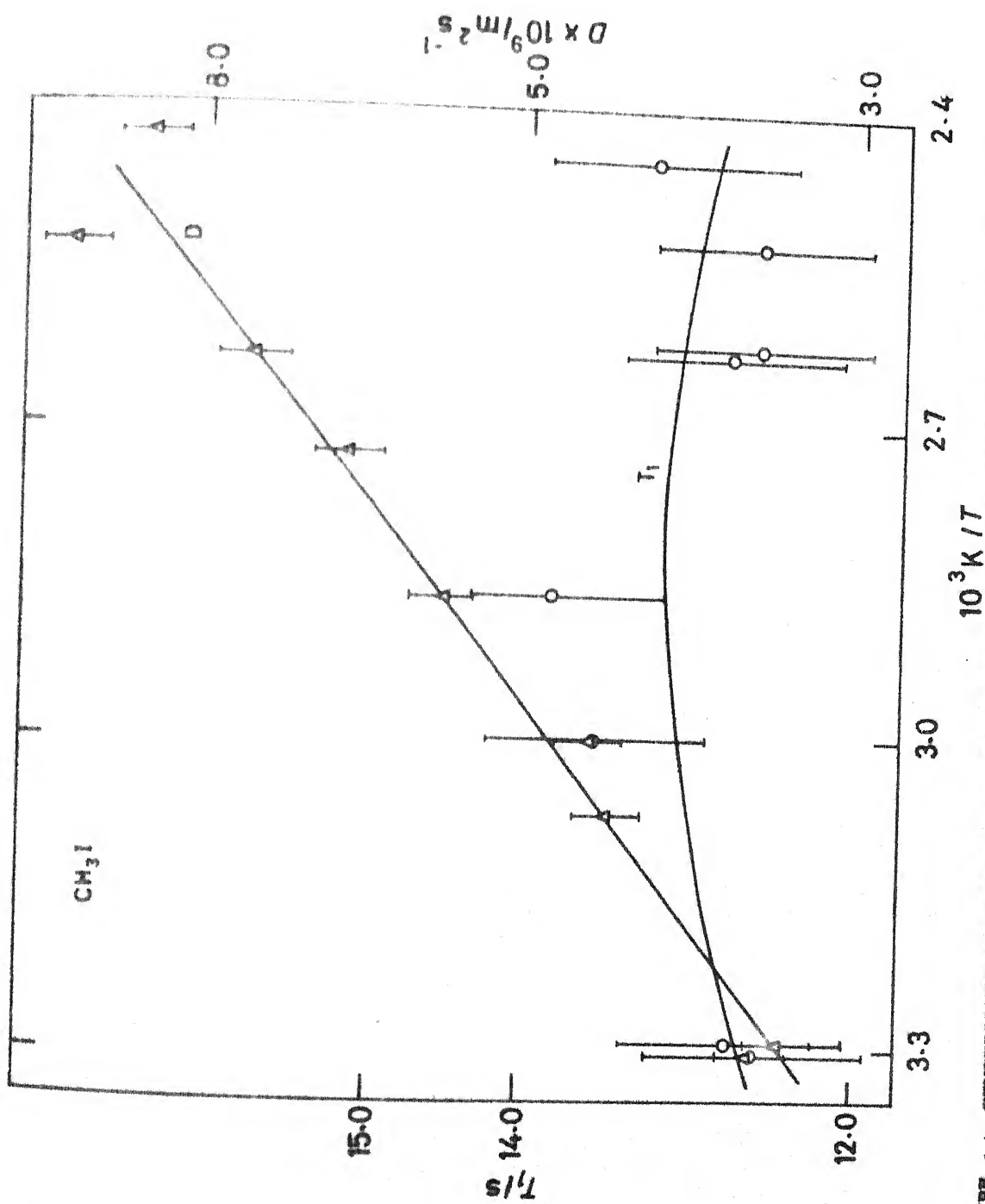


FIGURE 14. TEMPERATURE DEPENDENCE OF PROTON SPIN-LATTICE RELAXATION TIME ( $T_1$ ) AND SELF-DIFFUSION COEFFICIENT ( $D$ ) IN METHYL IODIDE.

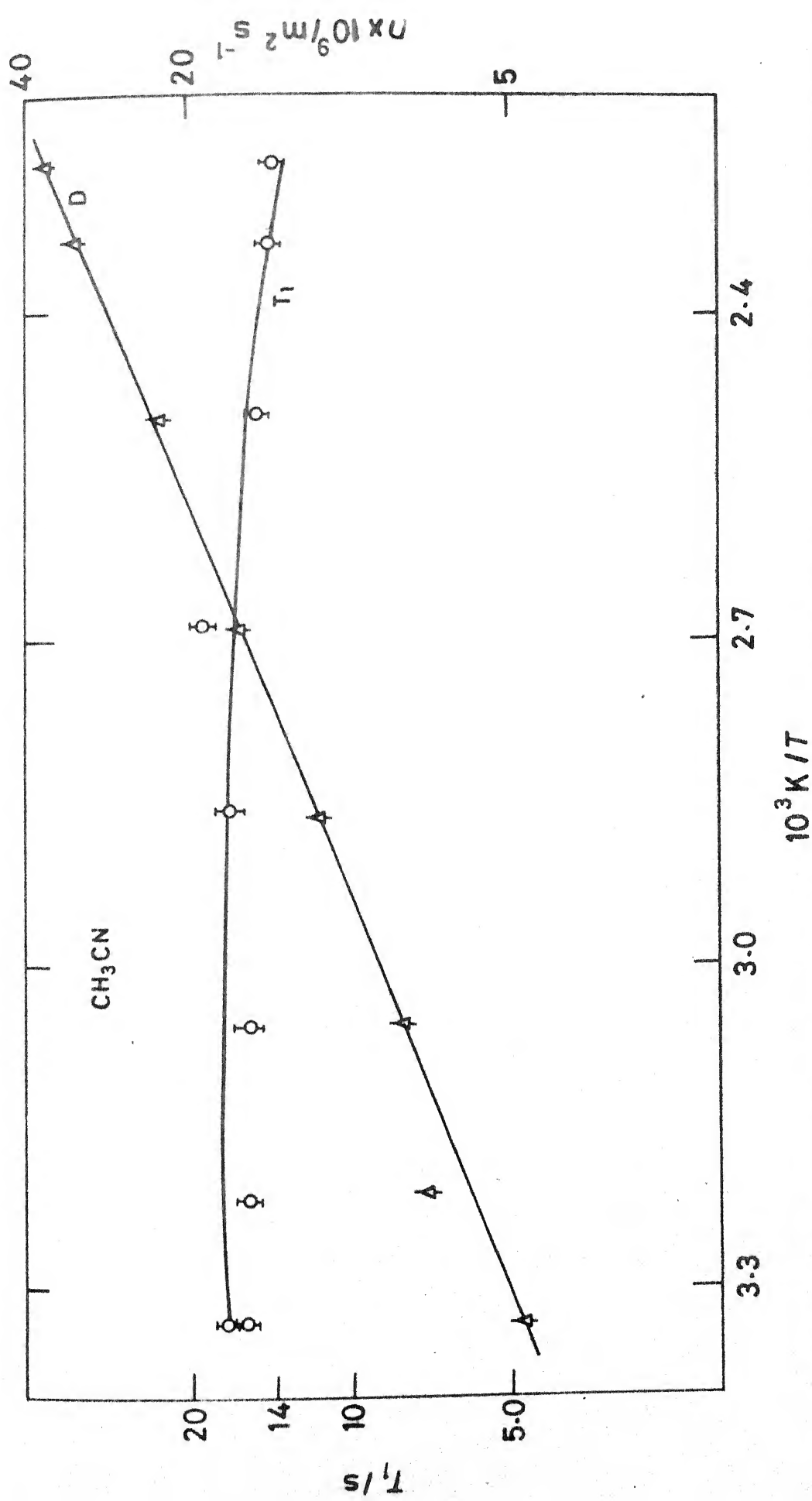


FIGURE 15. TEMPERATURE DEPENDENCE OF PROTON SPIN-LATTICE RELAXATION TIME ( $T_1$ ) AND SELF-DIFFUSION COEFFICIENT ( $D$ ) IN ACETONITRILE.

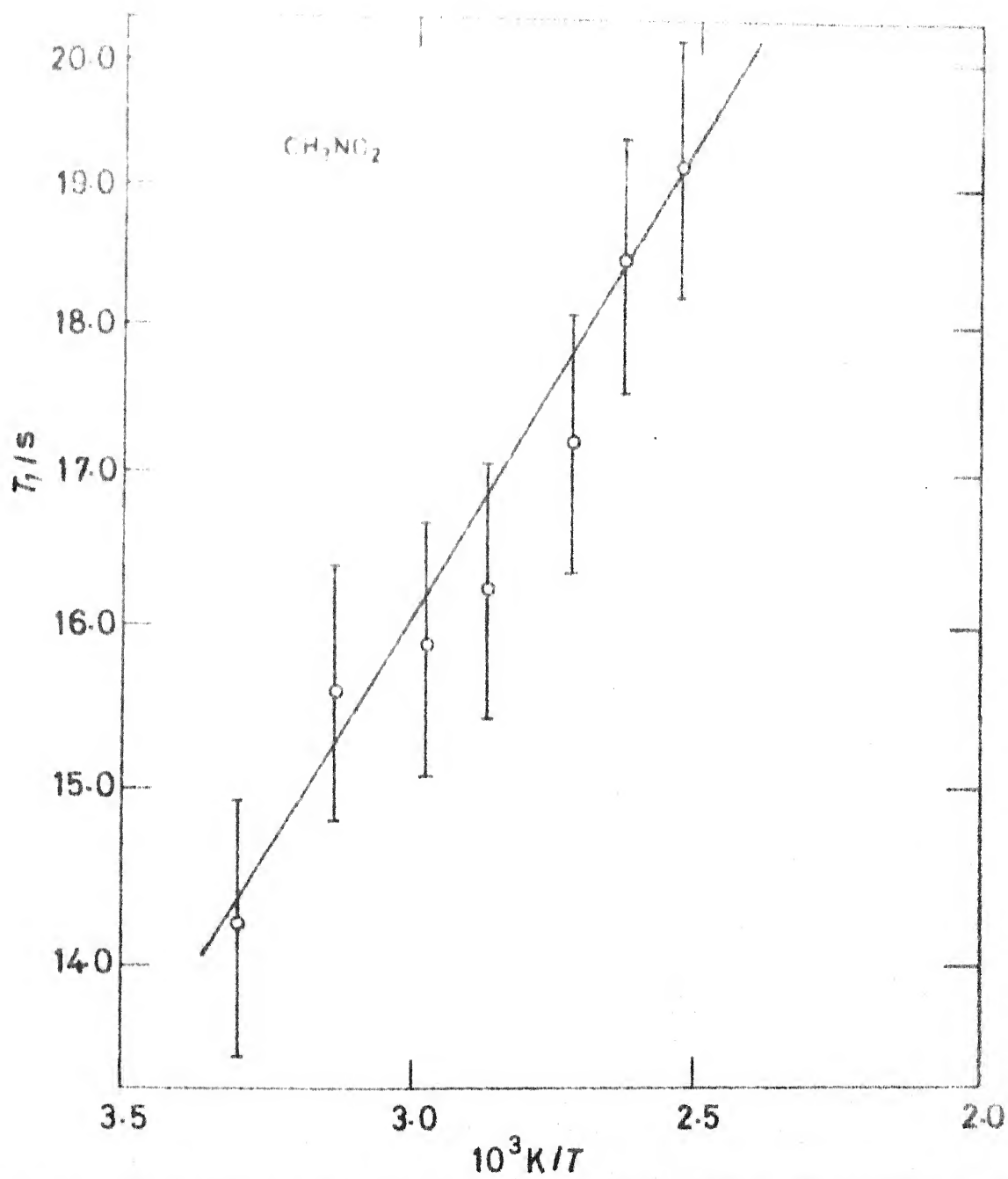


FIGURE 16. TEMPERATURE DEPENDENCE OF PROTON SPIN-LATTICE RELAXATION TIME ( $T_1$ ) IN NITROMETHANE.

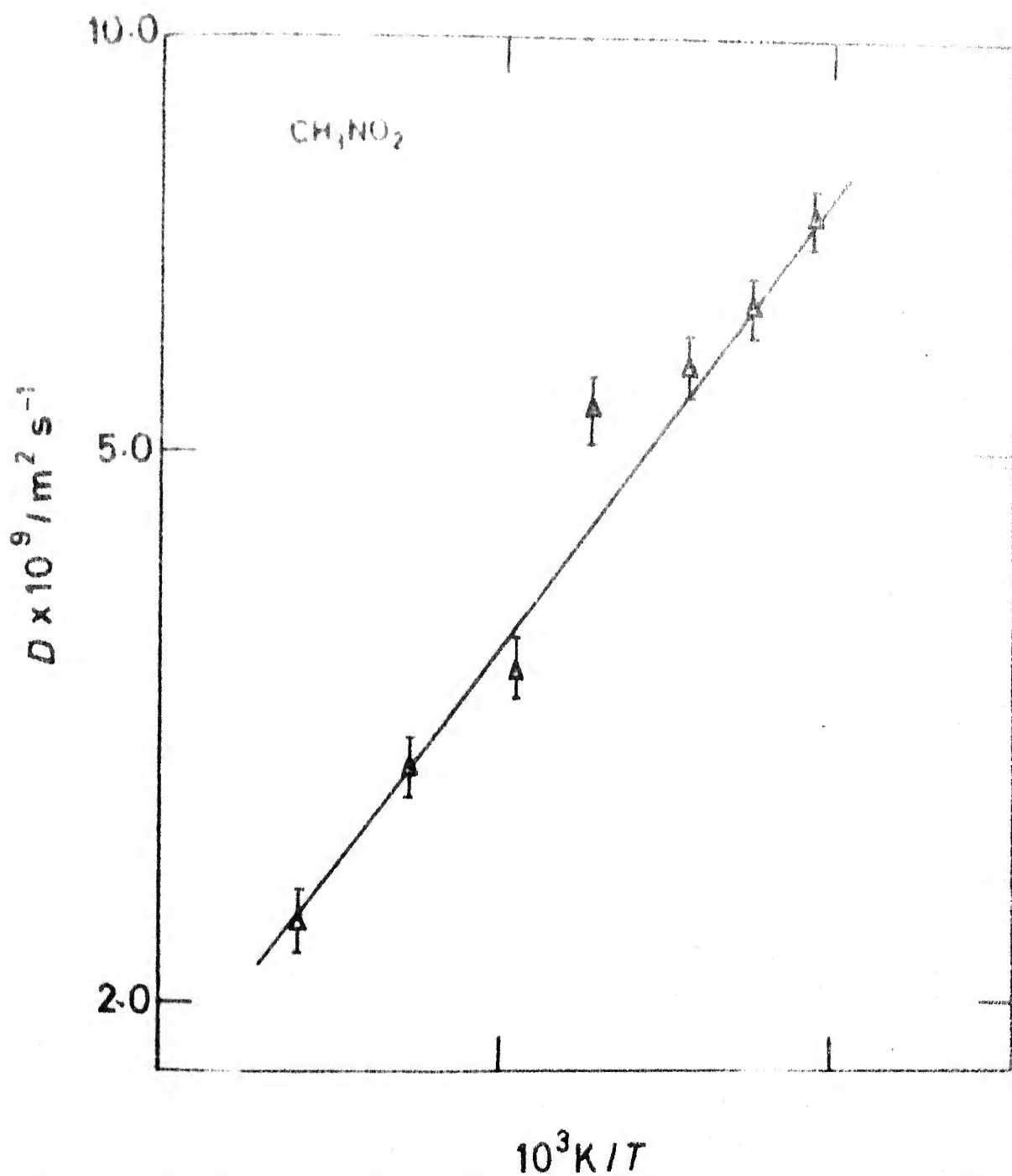


FIGURE 17. TEMPERATURE DEPENDENCE OF SELF-DIFFUSION COEFFICIENT ( $D$ ) IN NITROMETHANE.

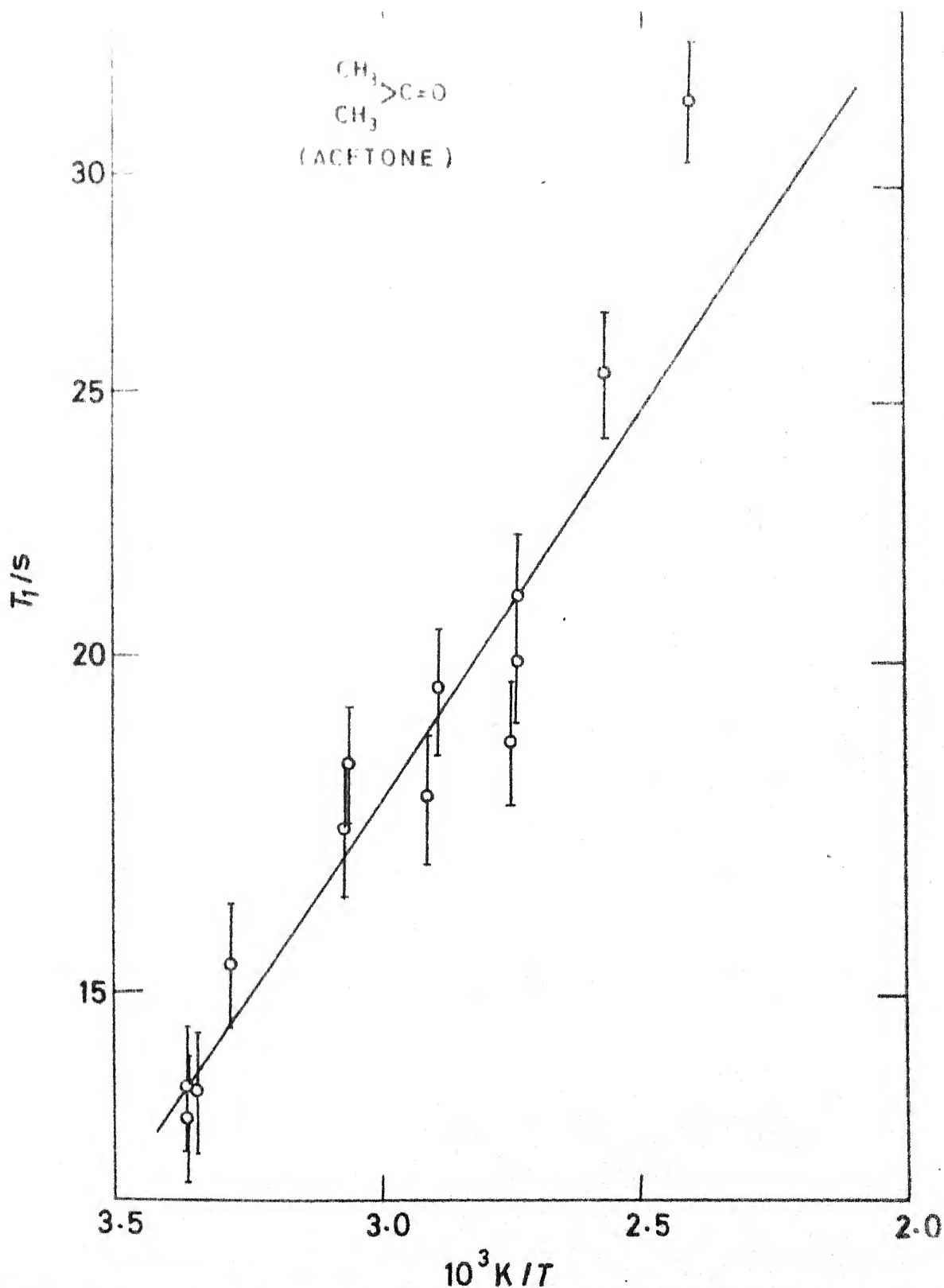


FIGURE 18. TEMPERATURE DEPENDENCE OF PROTON SPIN-LATTICE RELAXATION TIME ( $T_1$ ) IN ACETONE.

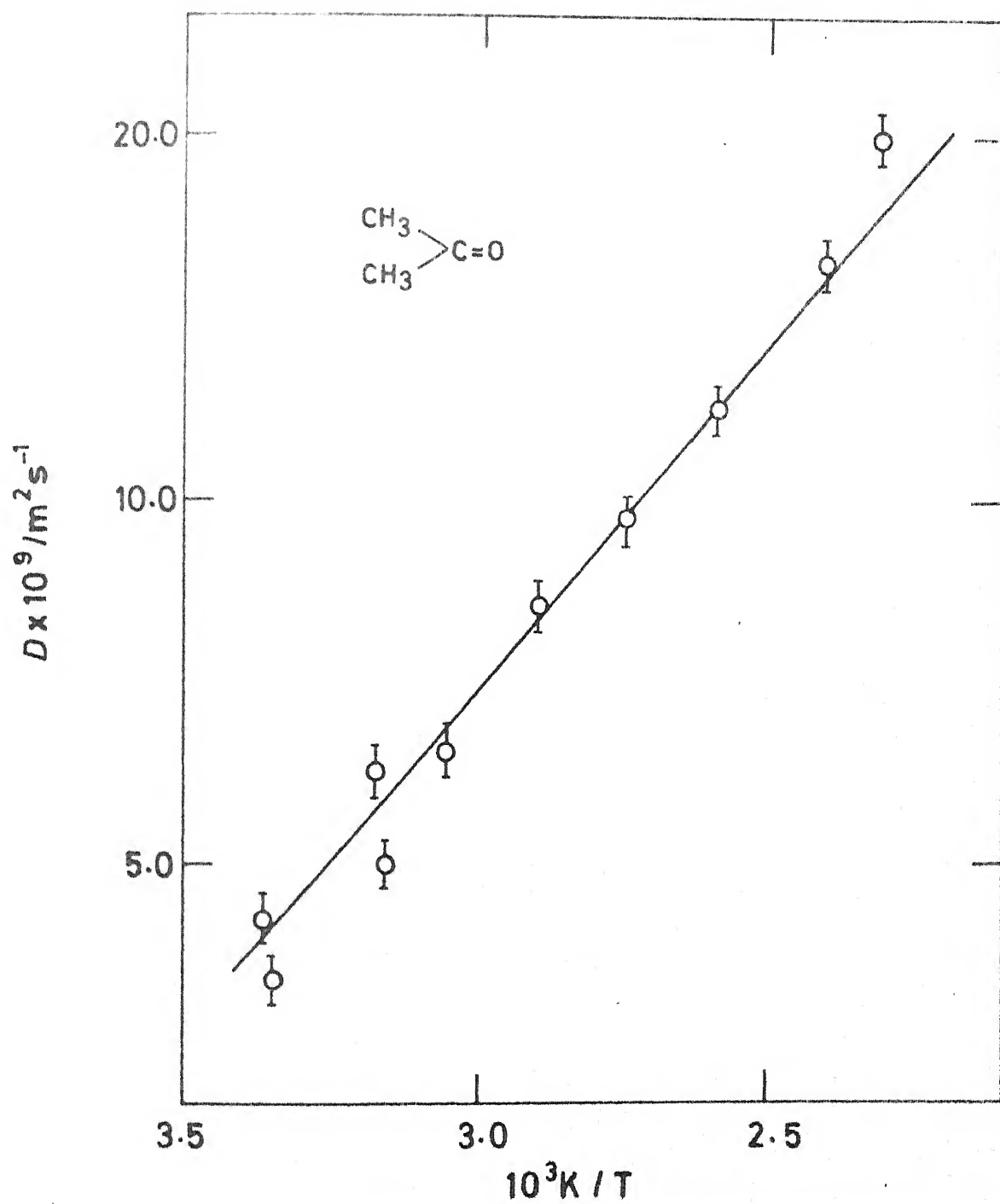


FIGURE 19. TEMPERATURE DEPENDENCE OF SELF-DIFFUSION COEFFICIENT ( $D$ ) IN ACETONE.

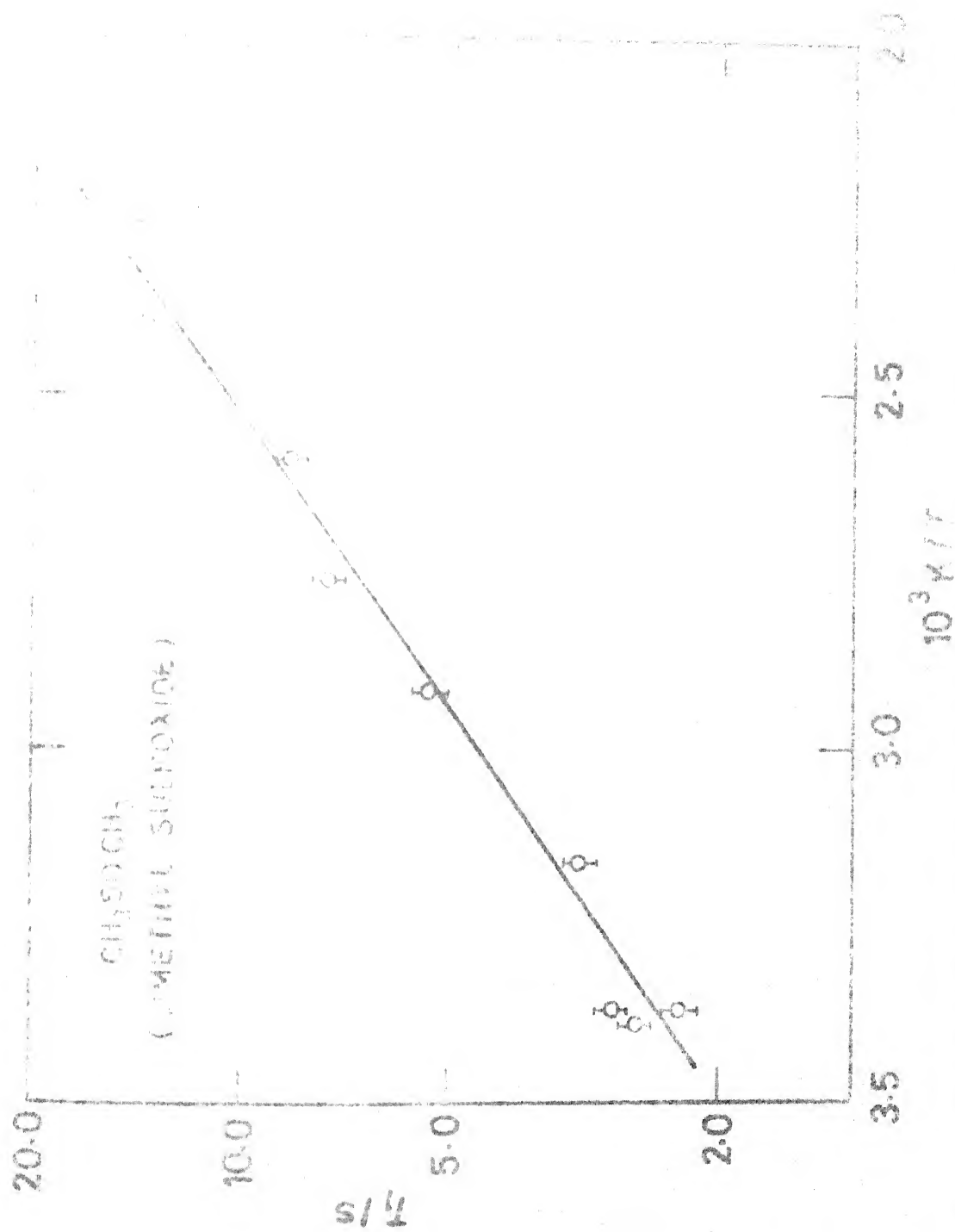


FIGURE 20. TEMPERATURE DEPENDENCE OF POLYMERIZATION RATES WITH LATTICE POLYMERIZATION OF (M<sub>1</sub>) IN DIMETHYL SULFOXIDE.

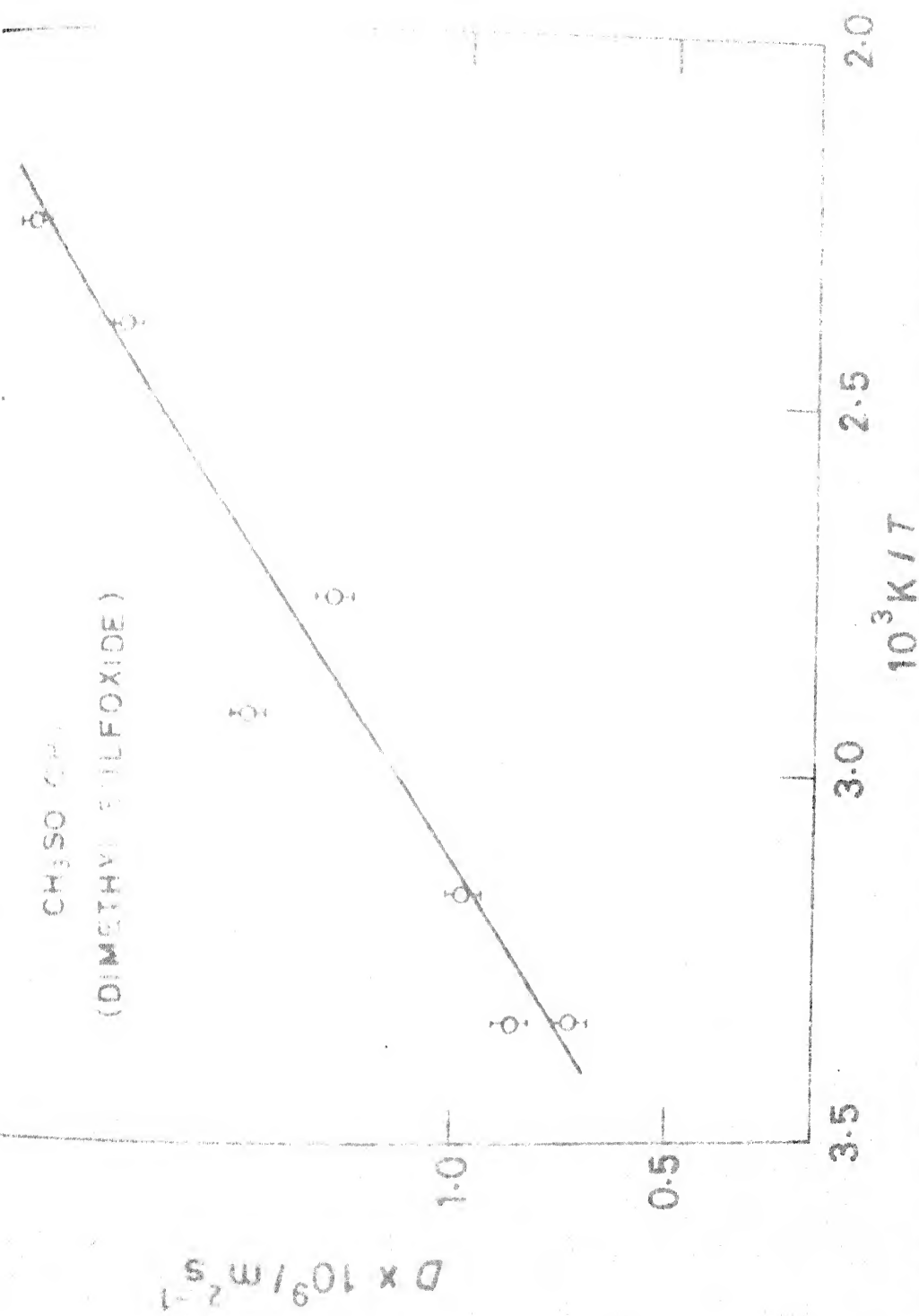


FIGURE 21. TEMPERATURE DEPENDENCE OF SELF-DIFFUSION COEFFICIENT ( $D$ ) IN DIMETHYL SULFOXIDE.

TABLE 4.1

THE ACTIVATION ENERGIES OF THE VARIOUS PARAMETERS IN THE METHYL GROUP CONTAINING COMPOUNDS

Compound	$E(D)$ (kcal) <sup>-1</sup> . mole	$E(\eta)$ (kcal) <sup>-1</sup> . mole	$E(\rho/D)$ (kcal) <sup>-1</sup> . mole	$E(\eta\rho/T)$ (kcal) <sup>-1</sup> . mole	$E(T/\eta)$ (kcal) <sup>-1</sup> . mole	$E(\eta/T\rho)$ (kcal) <sup>-1</sup> . mole	$E(R_{1intra})$ (kcal) <sup>-1</sup> . mole	$E(R_{1tot})$ (kcal) <sup>-1</sup> . mole
CH <sub>3</sub> I	2.42	1.51	2.75	2.62	2.28	2.05	-	-
CH <sub>3</sub> CN	3.65	1.83	4.26	3.10	2.28	2.19	-	-
CH <sub>3</sub> NO <sub>2</sub>	3.02	2.12	3.34	3.26	2.83	2.48	-	0.85
CH <sub>3</sub> COCH <sub>3</sub>	2.58	1.82	3.03	3.08	2.61	2.18	0.80	1.35
CH <sub>3</sub> SOCH <sub>3</sub>	2.86	3.18	2.56	-	-	-	3.70	3.37

$E(D)$  and  $E(T/\eta)$  are obtained from the corresponding linear plots obeying  $E(X) = -R \frac{\partial \ln X}{\partial 1/T}$  where  $X$  stands for  $D$  and  $T/\eta$ , and  $E(\eta)$ ,  $E(\rho/D)$ ,  $E(\eta\rho/T)$ ,  $E(\eta/T\rho)$ ,  $E(R_{1intra})$ , and  $E(R_{1total})$  are obtained from the corresponding linear plots obeying  $E(Y) = -R \frac{\partial \ln Y}{\partial 1/T}$ , where  $Y$  stands for  $\eta$ ,  $\rho/D$ ,  $\eta\rho/T$ ,  $\eta/T\rho$ ,  $R_{1intra}$  and  $R_{1total}$ .

The error in the activation energy calculation is about 5%.

As the various relaxation rates, comprising the total observed relaxation rate, are harbingers of different correlation times and motional processes it is imperative that they are first separated. As argued in Chapter 1 (p.31), Torrey's relation (Eq.1.10) gives good estimate of the intermolecular dipolar interaction contribution to the relaxation. With the help of  $\bar{V}$  observed *in situ* the molecular radius is first estimated using the Stokes-Einstein relation (see the Appendix) and then used in  $(1/T_1)_{\text{inter}}$  estimation. The density and viscosity data necessary for such calculations are culled out from the following sources:

Compound	Density data available in the temperature range	Source of the data
$\text{CH}_3\text{I}$	0 °C to 40 °C	<i>Int. Crit. Tables</i> (1928a)
$\text{CH}_3\text{CN}$	-45 °C to 60 °C	<i>ibid.</i> (1928b)
$\text{CH}_3\text{NO}_2$	0 °C to 100 °C	<i>ibid.</i> (1928b)
$\text{CH}_3\text{COCH}_3$	0 °C to 50 °C	<i>ibid.</i> (1928b)
$\text{CH}_3\text{SOCH}_3$	20 °C to 80 °C	Schläfer et al (1960)
Viscosity data available in the temperature range		
$\text{CH}_3\text{I}$	0 °C to 40 °C	<i>Int. Crit. Tables</i> (1930a)
$\text{CH}_3\text{CN}$	16.6 °C to 81.5 °C	<i>Landolt-Börnstein</i> (1969a)
$\text{CH}_3\text{NO}_2$	0 °C to 85 °C	<i>Int. Crit. Tables</i> (1930a)
$\text{CH}_3\text{COCH}_3$	0 °C to 54 °C	<i>ibid.</i> (1930b)
$\text{CH}_3\text{SOCH}_3$	20 °C to 80 °C	Schläfer et al (1960)

Since  $\eta$  and  $\rho$  are not available over the entire working temperature range, they are suitably extrapolated to be of use in the calculation.

The intermolecular relaxation rates of all these compounds thus calculated seemingly obey an Arrhenius relation (see Figs. 22 to 26). The activation energies for the intermolecular relaxation rates are given in Table 4.1. The difference between the total and intermolecular rates give the total intramolecular relaxation rate (plots in Figs. 22 to 26). It is seen that the intramolecular relaxation rates of  $\text{CH}_3\text{I}$ ,  $\text{CH}_3\text{CN}$  and  $\text{CH}_3\text{NO}_2$  increase with temperature as would be expected in the event of dominant spin-rotation interaction. It is rather unfortunate that even though intramolecular dipolar and spin-rotation interactions are the contributing factors to the total intramolecular relaxation rate, the experiment does not show the distinct trough in the relaxation rate *versus* temperature plot which would facilitate the separation of the two constituent relaxation rates as they would be equal at the trough of the plot. Even in the absence of such a situation the trend of variation of the various parameters as described below also hint at the molecular dynamics.

As the rotational and reorientational parts of the total intramolecular relaxation could not be separated, an effective reorientational correlation time is defined to give a handle on the general rotational situation. The intramolecular dipolar



FIGURE 22. PLOTS OF THE VARIATION OF THE VARIOUS RELAXATION RATES WITH TEMPERATURE IN METHYL IODIDE. ○, TOTAL RELAXATION RATE (OBSERVED). ○, INTERMOLECULAR RELAXATION RATE (CALCULATED). ●, INTRAMOLECULAR RELAXATION RATE.

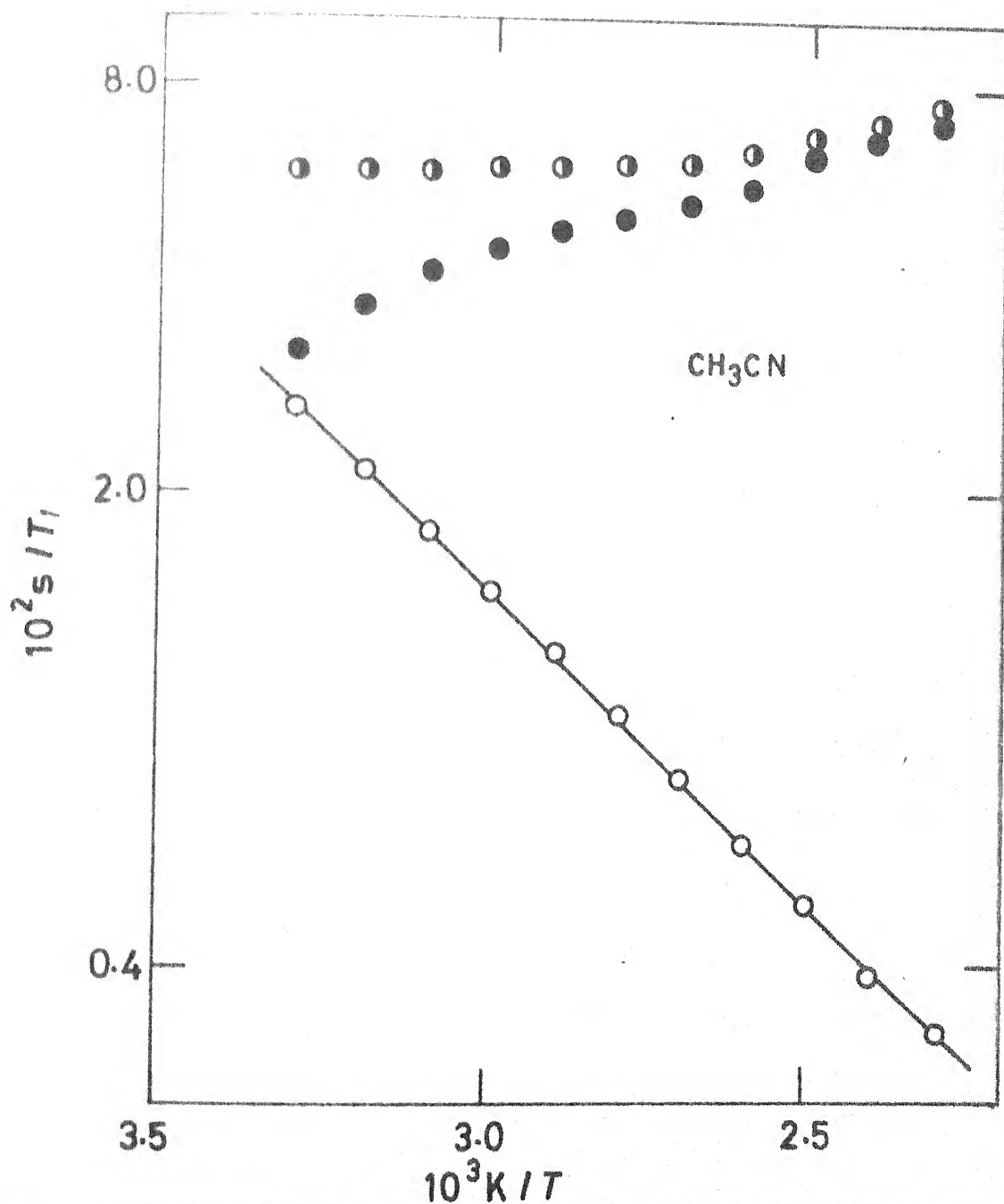


FIGURE 23. PLOTS OF THE VARIATION OF THE VARIOUS RELAXATION RATES WITH TEMPERATURE IN ACETONITRILE. ○, TOTAL RELAXATION RATE (OBSERVED). ○·, INTERMOLECULAR RELAXATION RATE (CALCULATED). ●, INTRAMOLECULAR RELAXATION RATE.

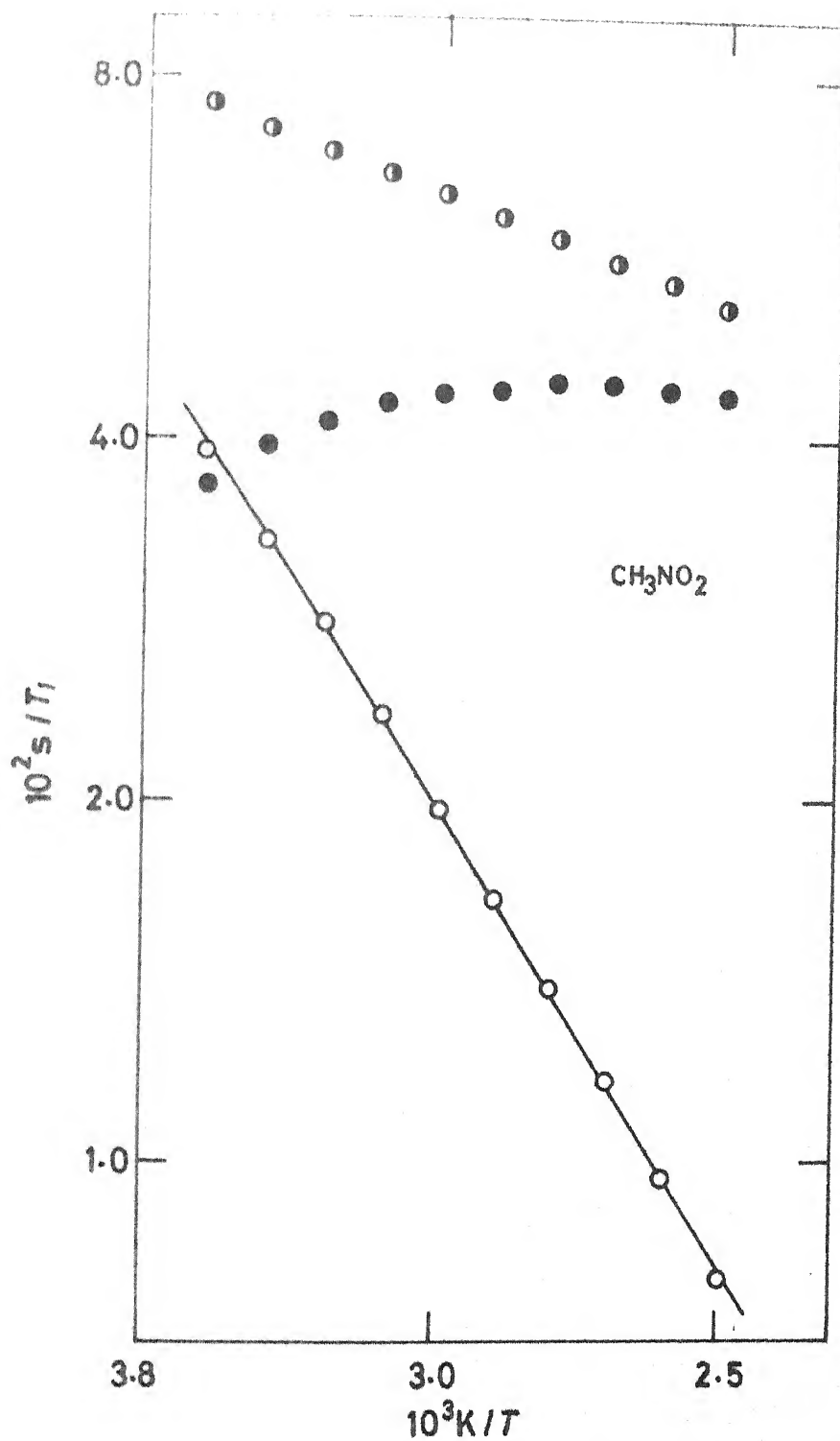


FIGURE 24. PLOTS OF THE VARIATION OF THE VARIOUS RELAXATION RATES WITH TEMPERATURE IN NITROMETHANE.  $\circ$ , TOTAL RELAXATION RATE (OBSERVED).  $\circ \cdot$ , INTERMOLECULAR RELAXATION RATE (CALCULATED).  $\bullet$ , INTRAMOLECULAR RELAXATION RATE.

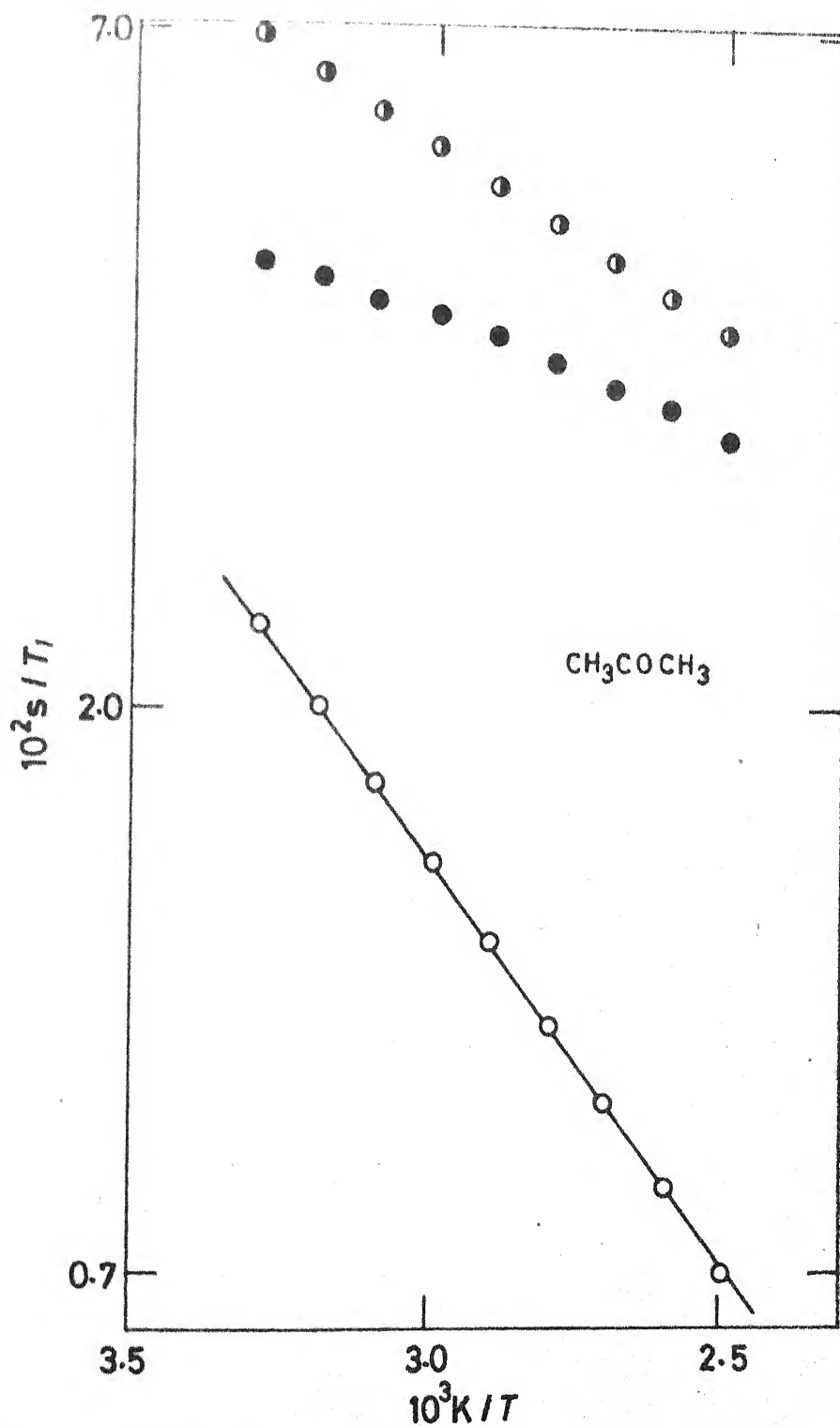


FIGURE 25. PLOTS OF THE VARIATION OF THE VARIOUS RELAXATION RATES WITH TEMPERATURE IN ACETONE.  $\circ$ , TOTAL RELAXATION RATE (OBSERVED).  $\odot$ , INTERMOLECULAR RELAXATION RATE (CALCULATED).  $\bullet$ , INTRAMOLECULAR RELAXATION RATE.

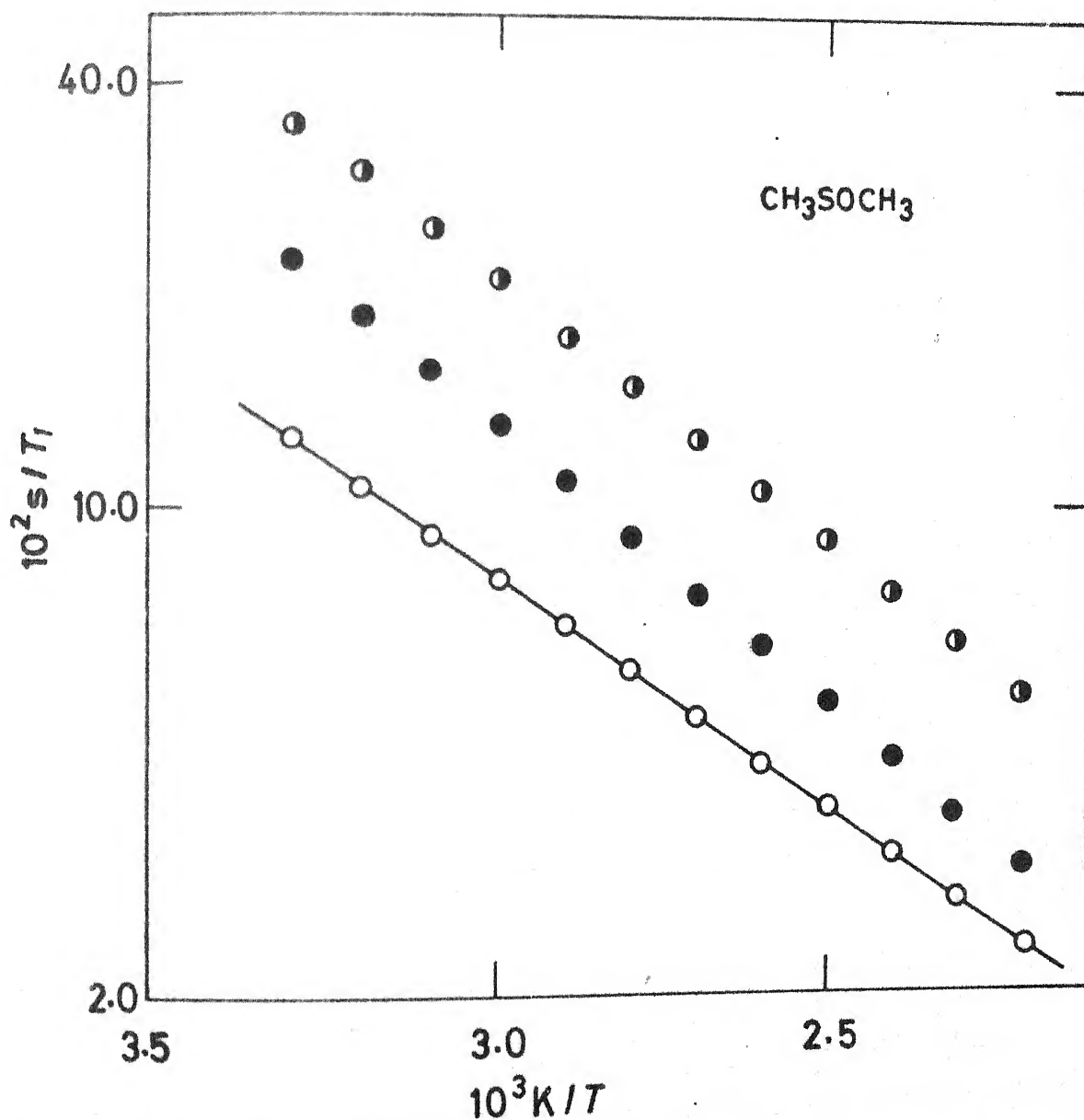


FIGURE 26. PLOTS OF THE VARIATION OF THE VARIOUS RELAXATION RATES WITH TEMPERATURE IN DIMETHYL SULFOXIDE.  $\odot$ , TOTAL RELAXATION RATE (OBSERVED).  $\odot$ , INTERMOLECULAR RELAXATION RATE (CALCULATED).  $\bullet$ , INTRAMOLECULAR RELAXATION RATE.

interaction is very steeply dependent on the spin separation (Eqs. 1.13 and 4.2) and as the distance between two spins belonging to the different methyl groups in acetone and dimethyl sulfoxide are quite far apart compared to the proton-proton separation within a group ( $1.78\text{\AA}$ ), intramolecular interaction is mainly confined to the interaction within a methyl group. Thus, all the compounds presently under study behave like 3-spin systems and the relation connecting the total intramolecular relaxation rate to the effective correlation time  $\tau_{\theta 2 \text{ eff}}$  is (Abragam (1961)),

$$(1/T_1)_{\text{intra}} = 3\gamma^4 \hbar^2 / \kappa^6 \tau_{\theta 2 \text{ eff}} \quad (4.2)$$

The plots of the effective correlation times against temperature are given in Fig. 27. The plot for dimethyl sulfoxide is reminiscent of the outcome of a collision limited process (see p. 41). The slow variation of acetone  $\tau_{\theta 2 \text{ eff}}$  with temperature is akin to the inertial reorientational motion discussed in Chapter 3 (p. 95).

Before embarking on the discussion about the individual compounds, it is worthwhile checking on the temperature variation of some parameters obtained combining  $T_1$ ,  $D$ ,  $\eta$  and  $\rho$  which could also project a rough picture of the molecular dynamics in the liquid state in the following manner.

$\eta$ : The viscosity coefficient is an outcome of the linear momentum transfer and hence, like the velocity dependent self-diffusion coefficient, is an attribute of the linear motion

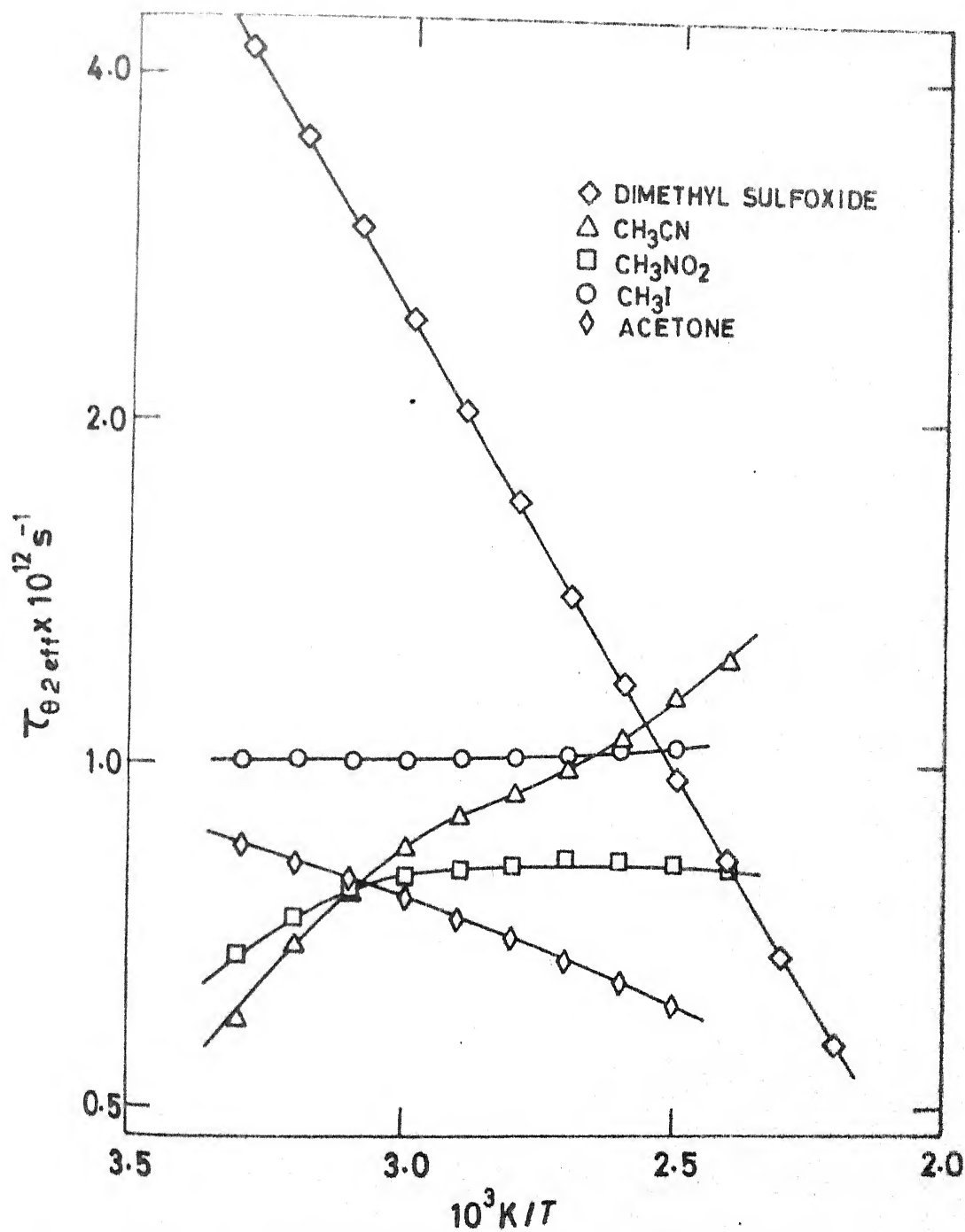


FIGURE 27. PLOTS OF THE VARIATION OF  $\tau_{02\text{eff}}$ , THE EFFECTIVE REORIENTATIONAL CORRELATION TIMES, WITH TEMPERATURE OF THE VARIOUS COMPOUNDS STUDIED.

of the molecules. Therefore the comparison of the corresponding activation energies (Table 4.1) will be revealing.

$\rho/D$ : In Torrey's relation (Eq. 1.10) the intermolecular relaxation rate is proportional to  $\rho/D$ . The variation of  $\rho/D$  with temperature is expected to be similar to the intermolecular relaxation rate and in experiments where the intermolecular relaxation rate is determined from the dilution studies in their isotopic analogues such a comparison will be illuminating. All these compounds under study have an Arrheniuslike  $\rho/D$  variation and the activation energies are given in Table 4.1.

$\eta\rho/T$ : When the Stokes-Einstein relation is valid  $(1/T_1)_{\text{inter}}$ ,  $\rho/D$  and  $\eta\rho/T$  are all proportional to each other (Eqs. 11 and 12). This premise can also be tested by independent observation of the variation of  $\eta\rho/T$  and  $\rho/D$  with temperature. So far as the trustworthiness of the two relations is concerned the Torrey's relation (comprising  $\rho/D$ ) seems to be direct, accurate and involves  $D$  which is measured quite accurately *in situ*. The activation energies for  $\eta\rho/T$  variation with temperature are given in Table 4.1.

$T/\eta$ : When the Brownian diffusion is valid for the reorientational motion the rotational diffusion coefficient ( $D_{\text{rot}}$ ) will be proportional to  $T/\eta$  (Eqs. 1.14, 1.17 and 1.19). It is also realized that the reorientational motion about an axis perpendicular to the molecular symmetry axis is diffusive, and hence  $D_{\perp}$  the corresponding rotational diffusion

coefficient is determined by  $T/\eta$  (Bopp (1967), Woessner, Snowden and Strom (1968), Gillen, Schwartz and Noggle (1971), Lyster, Grant and Wang (1971), and Heatley (1974)). The corresponding activation energies are given in Table 4.1.

$\eta/T_p$ : In the event of rotational Brownian motion and absence of spin-rotation interaction of any consequence the intramolecular dipolar relaxation rate which is proportional to the reorientational correlation time gets directly related to  $\eta/T_p$  through the Debye relation (Eq. 1.11). All except dimethyl sulfoxide (where the activation energy is found to be temperature dependent), have well defined activation energies as presented in Table 4.1.

There are some other derived parameters which are also of interest:

$T_{1\rho}/T$ : The initial suggestion by Blicharski that a decreasing  $T_{1\rho}/T$  with temperature increase suggests the presence of sizeable spin-rotation interaction was later shown to be due to convection currents in the experimental sample (Kosfeld (1968)). The observation in the present series of compounds does not show any appreciable decrease of  $T_{1\rho}/T$  with temperature rise - except in  $\text{CH}_3\text{CN}$  where it is fairly big.

$\eta T_1/T$ : Hydrogen bondings seem to sharply decrease  $\eta T_1/T$  with temperature rise (Hennel and Waluga (1962)).

increases from  $3.55 \times 10^9 \text{m}^{-2}\text{s}$  to  $4.71 \times 10^9 \text{m}^{-2}\text{s}$ ) suggesting distinctive diffusive process governing the relaxation.

The Table 4.2 carries the following informations at the upper and lower temperature limits of the experiments. It has the effective correlation time  $\tau_{\theta 2 \text{ eff}}$  defined by the Eq. 4.2 and the Bloembergen-Purcell-Pound correlation time  $\tau_{\theta 2 \text{ BPP}}$  as determined by Eq. 1.11 and the Stokes-Einstein radius from the Table App. 2. The maximum value of the reorientational correlation time in the Gaussian or inertial limit (Inertial  $\tau_{\theta 2 \text{ av}}$ ) as given by Eq. 1.20 is also presented. The molecular free rotational time (Bartoli and Litovitz (1972), Bauer, Brauman and Pecora (1974), Fury and Jonas (1976))

$$\tau_{\text{free av}} = 2\pi/9 \sqrt{I_{\text{av}}/kT} \quad (4.5)$$

(where  $I_{\text{av}}$  is the average moment of inertia of the molecule defined by

$$I_{\text{av}} = 3(I_A^{-1} + I_B^{-1} + I_C^{-1})^{-1}$$

is also presented in Table 4.2. The reorientational correlation time (Mod. Hill  $\tau_{\theta 2 \text{ av}}$ ) obtained using the modified Hill relation (see, Hill (1954), Mitchell and Eisner (1960), Assink and Jonas (1969), and Pajak *et al* (1970))

$$\tau_{\theta 2} = 2\sigma I_{\text{av}}\eta/mkT, \quad (4.6)$$

where  $\sigma$  the average of the semi axes of the molecule in the

TABLE 4.2

THE CORRELATION TIMES IN THE METHYL GROUP CONTAINING COMPOUNDS

Compound	$10^3 K/T$	$\tau_{\theta 2} \text{ eff}$ $\times 10^{13} \text{ s}^{-1}$	$\tau_{\theta 2} \text{ BPP}$ $\times 10^{13} \text{ s}^{-1}$	$\tau_{\text{free av}}$ $\times 10^{13} \text{ s}^{-1}$	Inertial $\tau_{\theta 2} \text{ av}$ $\times 10^{13} \text{ s}^{-1}$	Mod. Hill $\tau_{\theta 2} \text{ av}$ $\times 10^{13} \text{ s}^{-1}$
$\text{CH}_3 \text{ I}$	3.3	10.60	12.17	1.32	0.97	0.19
	2.5	13.80	4.90	1.15	0.84	0.08
$\text{CH}_3 \text{ CN}$	3.3	5.99	2.56	1.31	0.96	0.32
	2.3	13.20	0.72	1.09	0.80	0.09
$\text{CH}_3 \text{ NO}_2$	3.4	6.81	26.03	3.19	2.34	4.22
	2.5	8.06	7.30	2.73	2.00	1.19
$\text{CH}_3 \text{ COCH}_3$	3.3	8.52	11.63	2.74	2.01	1.50
	2.5	6.16	4.07	2.38	1.75	0.53
$\text{CH}_3 \text{ SOCH}_3$	3.3	42.11	117.97	4.02	2.95	18.60
	2.2	5.70	17.97	3.28	2.41	2.83

present calculation is taken to be the Stokes-Einstein radius,  $m$  is the mass of the molecule and others have their usual meaning. The total intramolecular relaxation rate, the Bloembergen-Purcell-Pound intramolecular dipolar relaxation rate, and the maximum intramolecular relaxation rate expected in the event of a Gaussian (inertial) reorientation (Moniz, Steele and Dixon (1963)), bear the same ratio to one another as the corresponding correlation times. The effective  $\chi$  parameter defined by

$$\chi_{\text{eff}} = \tau_{\theta_2 \text{ eff}} / \tau_{\text{free}}$$

is presented in Table 4.3.

The parameter  $a_2^m(0)$  defined by Moniz, Steele and Dixon (1963) as

$$a_2^m(0) = \tau_{\theta_2 \text{ eff}} \sqrt{kT/I} \quad (4.7)$$

in the inertial limit becomes  $a_2^m(0) = 1/2 \sqrt{\pi/3} \approx 0.5$ , and in the diffusion limit yields

$$a_2^m(0) = \xi/6\sqrt{IkT} \quad (4.8)$$

$a_2^m(0) (= a_2^m(0)_{\text{eff}})$  determined using Eq. 4.7, and the other  $a_2^m(0) (= a_2^m(0)_{\text{av}})$  obtained using Eq. 4.8 are presented in the Table 4.3.  $a_2^m(0)_{\text{av}}$  bears the following relation to the  $\chi$  parameter in the Debye diffusion limit, and the ratio of the intramolecular dipolar relaxation rate (estimated by Bloembergen, Purcell and Pound relation) to the relaxation rate in the Gaussian (inertial)

TABLE 4.3

SOME MOLECULAR PARAMETERS IN THE METHYL GROUP CONTAINING COMPOUNDS

Compound	$10^3 K/T$	$\chi_{\text{eff}}$	$a_2^m(0)_{\text{eff}}$	$a_2^m(0)_{\text{av}}$	Dipole moment $D^{-1}$
$\text{CH}_3\text{I}$	3.3	8.0	5.59	6.4	1.48
	2.5	11.5	8.37	3.0	
$\text{CH}_3\text{CN}$	3.3	4.6	3.19	1.4	3.39
	2.3	12.1	8.43	0.5	
$\text{CH}_3\text{NO}_2$	3.4	2.1	1.49	5.7	4.39
	2.5	2.9	2.06	1.9	
$\text{CH}_3\text{COCH}_3$	3.3	3.1	2.17	3.0	2.93
	2.5	2.6	1.81	1.2	
$\text{CH}_3\text{SOCH}_3$	3.3	10.5	7.31	20.5	3.9
	2.2	1.7	1.21	3.8	

limits are

$$\chi_{\text{Debye}} = 9/2\pi a_2^m(0)_{\text{av}} ,$$

$$\text{and } R_{\text{1rot BPP}}/R_{\text{1rot Gaussian}} = 2\sqrt{3/\pi} a_2^m(0)_{\text{av}}.$$

The dipole moments of the investigated molecules (McClellan (1963)) are also given in Table 4.3.

#### 4.1 CH<sub>3</sub>I and CH<sub>3</sub>CN

These two symmetric top molecules have been subjected to a large number of rotational and vibrational spectroscopic studies (Favolukes *et al* (1968), Rothschild (1969, 1970a, 1970b), Constant (1973a, 1973b), Griffiths (1973, 1974), Wright, Schwartz and Wang (1973), Yarwood (1973)). In nmr work the symmetric tops, being of next higher degree of complication than the spherical tops have proved to be the testing ground for the models for anisotropic rotational motion (Moniz and Gutowsky (1963), Zeidler (1965), Bopp (1967), Woessner, Snowden and Strom (1968), Bull and Jonas (1970), Franck, Hertz and Rädle (1970), Gillen, Schwartz and Noggle (1971), Lyerla, Grant and Wang (1971), Heatley (1974), Leipert, Noggle and Gillen (1974)).

The CH<sub>3</sub>I  $E(0) = 2.41$  kcal/mole obtained in the present work (Table 4.1) compares favourably with the results of Krüger and Weiss (1970) 2.0 kcal/mole and that of Sandhu (1975a) 2.11 kcal/mole. The intermolecular relaxation rate estimated using the Torrey's relation (Eq. 1.10') compares well with the corresponding values obtained *via* dilution study (Gillen, Schwartz and Noggle (1971)) and the respective activation

energies (2.75 kcal/mole and 2.4 kcal/mole) are quite close. Even though the separation of the intramolecular dipolar and spin-rotation relaxation rates could not be done the slow variation of the intramolecular relaxation rate in  $\text{CH}_3\text{I}$  and  $\text{CH}_3\text{CN}$  (Figs. 22 & 23) are indicative of coherent reorientational motion (p. 95). The close agreement between the  $\tau_{\theta 2}$  BPP and  $\tau_{\theta 2}$  eff in Table 4.2 is misleading because of the following reasons.  $\tau_{\theta 2}$  BPP estimates are usually large because of not taking into account the inertial effects (Moniz, Steele and Dixon (1963)) and  $\tau_{\theta 2}$  eff estimated here is larger than the reorientational correlation time because of the inclusion of large spin-rotation interaction contribution. Hence the present close agreement in no way suggests the validity of the diffusional model. Also because of the large contribution of spin-rotation interaction to the value of the effective rotational correlation time, the  $\chi_{\text{eff}}$  presented in Table 4.3 is also large, and seems to increase with temperature.

In  $\text{CH}_3\text{CN}$  the variation of the self-diffusion coefficient with temperature seems to be very fast. The  $E(D) = 3.65$  kcal/mole (Table 4.1) obtained here is much larger than the value 2.63 kcal/mole reported by Zeidler (1971b). The variation of the coefficient of viscosity ( $\eta$ ) with temperature is comparatively much slower ( $E(\eta) = 1.83$  kcal/mole in Table 4.1) and therefore gives a  $D\eta/T$  increasing quite fast in the experimental temperature range (Table App. 1). This leads to a higher average  $D\eta/T$  value and a consequent smaller Stokes-Einstein radius (see p.178). As a consequence of the large  $D$  variation, the  $\rho/D$  variation with

temperature is also quite fast, thus giving  $E(\rho/D) = 4.26$  kcal/mole (Table 4.1) which is much larger than the corresponding values, 2.0 kcal/mole reported by Woessner, Snowden and Strom (1968) and 2.2 kcal/mole reported by Gillen *et al* (1972). As mentioned in p.119 the rapid decrease of  $T_1\eta\rho/T$  with temperature rise probably suggests the presence of convection currents in the sample.

There is a growing feeling (Bopp (1967), Woessner, Snowden and Strom (1968), Gillen, Schwartz and Noggle (1971), Lyster, Grant and Wang (1971), and Heatley (1974)), that in the symmetric top molecules presently under consideration, the rotational diffusion about an axis parallel to the molecular symmetry axis is free inertial and that about an axis perpendicular to the symmetry axis is diffusional. We present in the following the corresponding estimated (Eqs. A.9, 1.11 and 4.5) rotational diffusion constants and those values presented by others. The values obtained with the assumption that the  $\text{CH}_3\text{CN}$  molecular radius is at least equal to the  $\text{CH}_3\text{I}$  Stokes-Einstein radius, are also presented.

Compound	$10^3\text{K}/T$	Calculated $D_1 \times 10^{-11}\text{s}$	Calculated $D_{\perp} \times 10^{-11}\text{s}$
$\text{CH}_3\text{I}$	3.3	1.37	20.8
	2.5	3.39	23.9
$\text{CH}_3\text{CN}$	3.3	6.5	20.8
	2.3	23.08	23.9
	3.3	1.80	20.8
	2.3	6.40	23.9

(In the preceding tabulation the third and fourth rows correspond to  $a_{SE} = 0.90 \text{ \AA}$  and the fifth and sixth rows correspond to  $a_{SE} = 1.38 \text{ \AA}$ .) The  $\nu_1$  and  $\nu_{11}$  values reported by others are as follows. In  $\text{CH}_3\text{I}$  :

Author(s)	$\nu_1 \times 10^{-11} \text{ s}$	$\nu_{11} \times 10^{-11} \text{ s}$
Gillen, Schwartz and Noggle (1971)	1.17	-
Griffiths (1973)	1.07	-
Heatley (1974)	1.1	13.2
Lyerla and Levy (1974)	1.4	20.0

In  $\text{CH}_3\text{CN}$ :

Author(s)	$\nu_1 \times 10^{-11} \text{ s}$	$\nu_{11} \times 10^{-11} \text{ s}$
Bopp (1967)	1.35	12.0
Zeidler (1971b)	1.4	12.0
Griffiths (1973)	1.51	-
Heatley (1974)	1.7	16.32
Lyerla and Levy (1974)	1.5	14.0

In  $\text{CH}_3\text{CN}$ , at  $10^3 \text{ K/T} = 3.3$ ,  $\chi$  is small (Table (4.2) and the reorientation is nearly inertial.  $a_2^m(0)$  seem also to be both theoretically and experimentally over-estimated although at  $10^3 \text{ K/T} = 2.3$   $a_2^m(0)_{av} = 0.5$  indicates Gaussian reorientational situation.

#### 4.2 CH<sub>3</sub>NO<sub>2</sub>

Nitromethane has a very small barrier to internal rotation (p. 97), a large dipole moment (Table 4.3), and a normal boiling point (100.8 °C) close to that of water. An early work by Anderson (1969) had shown that even in liquid nitromethane  $T_1 \neq T_2$ . Tyn and Calus (1975) find such olefinic derivatives as CH<sub>3</sub>NO<sub>2</sub> to be quite unpredictable whose molar volumes could not be easily ascertained. All these *prima facie* make liquid CH<sub>3</sub>NO<sub>2</sub> quite interesting to work on.

In the  $\mathcal{D}$  measurement instead of plotting  $\log S(0)/S_z$  vs  $t^3$  as stated in p. 81,  $1/t \log S(0)/S_z$  vs  $t^2$  are plotted to get  $\mathcal{D}$  from the slope and keep  $\mathcal{D}$  measurement immune from the 'effect of  $T_2$ '. Since  $T_2$  is of the order of a few seconds (but not very small where such  $T_2$  effects are hazardous) such a precautionary step seems to be in the conservative side. Our  $E(\mathcal{D}) = 3.02$  kcal/mole can be compared with the following results: 3.8 kcal/mole obtained by McCall *et al* (1959) and 2.53 kcal/mole obtained by O'Reilly *et al* (1971). As against Pendred, Pritchard and Richards (1966) reported value of  $T_1$  (12.7 s) the value obtained presently is 13.9 s. The small variation of  $T_1$  (Fig. 16) over the experimental temperature range suggests pre-eminence of the inertial motion which is further corroborated by the slow variation of the intramolecular relaxation rate with temperature (Fig. 24). The intramolecular relaxation rate which is of about the same magnitude as the intermolecular relaxation rate at the room

temperature becomes about five times larger at 127 °C indicating good deal of rotational coherence (Chap. 3). This is interesting as  $\text{CH}_3\text{NO}_2$  being highly polar would give a local structure which does not seem to affect the rotational motion. This also corroborates the earlier realization that molecular shape but not the dipole moment governs the reorientational motion (see p. 43).

In Table 4.3 the low  $\chi_{\text{eff}}$ , around 2.5 is suggestive of a good deal of inertial motion. Modified Hill method with accent on the reorientational motion seems to predict  $\tau_{02}$  well in  $\text{CH}_3\text{NO}_2$  at room temperature. The calculated overall rotational diffusion constant is given in the Appendix (Table App. 3).

#### 4.3 $\text{CH}_3\text{COCH}_3$ and $\text{CH}_3\text{SOCH}_3$

These two molecules although structurally similar, dimethyl sulfoxide has a higher barrier to internal rotation (2.2 kcal/mole) than acetone (0.778 kcal/mole as in p. 97, and 0.92 kcal/mole as obtained by Lyerla and Levy, (1974)), and as the methyl groups within each molecule are far apart these molecules essentially behave as three spin systems so far as the calculation of intramolecular interaction is concerned. Dimethyl sulfoxide is highly hygroscopic, acts as a good solvent, and seems to be of great physiological importance. The dimethyl sulfoxide molecule has a large dipole moment (3.9D) and interestingly enough has normal melting point (18.45 °C) close to the room temperature.

In acetone, the  $E(D) = 2.58$  kcal/mole (Table 4.1) can be compared with the following values obtained by others: 2.03 kcal/mole McCall *et al* (1959), 2.1 kcal/mole Krüger and Weiss (1970). In acetone the present finding  $E(R_1 \text{ total}) = 1.35$  kcal/mole compares well with 1.5 kcal/mole obtained by Bonera and Rigamonti (1965). As discussed in Chapter 3 the slow variation of the intramolecular relaxation rate in acetone (Fig. 25) might indicate dominant surrounding independent intramolecular rotational contribution to relaxation. This looks feasible as the acetone being fairly asymmetric in shape, the overall rotational coherence in the experimental temperature range looks improbable. The small  $\chi$  values for acetone in Table 4.3 also hints at possible inertial rotational motion. The  $\tau_{\theta_2 \text{ eff}}$  plot in Fig. 27 when fitted to an Arrhenius relation gives  $E(\tau_{\theta_2 \text{ eff}}) = 0.8$  kcal/mole which is fairly close to an approximate evaluation:  $E(T^{1/2}) = 0.37$  kcal/mole in  $10^3 K/T$  range 3.3 to 2.2. As discussed in Chap. 3 this is suggestive of a reorientational coherence in acetone over the present experimental temperature range which bears out the *prima facie* observation that the internal rotation barrier being low, the experimental temperature range will sufficiently activate the internal rotation.

The most significant observation in dimethyl sulfoxide is the fast and almost similar variation of the total, inter- and intramolecular relaxation rates with temperature (Fig. 26). (To be exact, the plots show the translational motion slightly more

facile than the overall rotational motion.) Since the fast decrease of intramolecular relaxation rate with temperature rules out any reckonable spin-rotation interaction contribution to relaxation the  $\tau_{02}$  eff is a measure of the dipolar correlation time. The Arrheniuslike variation of the reorientational correlation time could suggest a collision limited diffusive process governing the reorientational process. The similar variation of the intermolecular and intramolecular relaxation rates would then mean that the translational and reorientational process are well coupled. Since dimethyl sulfoxide looks structurally asymmetric and the internal rotational barrier is large such an observation looks quite tenable. However, with increase of temperature  $\chi$  seems to suggest a transition from the diffusion to an inertial limit.

## CHAPTER 5

### STUDIES IN A GROUP OF ASSORTED MOLECULAR LIQUIDS

Investigations into the molecular motion in a group of assorted compounds (methylene chloride ( $\text{CH}_2\text{Cl}_2$ ), methylene iodide ( $\text{CH}_2\text{I}_2$ ), anisole ( $\text{C}_6\text{H}_5\text{OCH}_3$ ), and  $\alpha$ -trifluoro toluene ( $\text{C}_6\text{H}_5\text{CF}_3$ )) are reported in the present chapter. In the temperature range of the experiment (300 to 450 K) the barrier to internal rotation of the  $\text{CF}_3$  group about the C- $\text{CF}_3$  bond is 0.2 to 0.4 kcal/mole (Bull, Barthell and Jonas (1971)), which is easily surmounted and a good amount of internal rotation is possible. As  $^{19}\text{F}$  has characteristically a large spin-rotation coupling constant, one expects large spin-rotation interaction contribution to  $^{19}\text{F}$  relaxation.

Some other general observations on these molecules are as in the following. Anisole is a bent molecule with the C-O- $\text{CH}_3$  angle  $\sim 108^\circ$ . The  $\text{C}_6\text{H}_5$  and  $\text{CH}_3$  protons in anisole are expected to be chemically shifted from one another to give cross-relaxation effects in the observation of the  $^1\text{H}$  overall relaxation. The overall molecular asymmetry is a common feature of the present group of compounds. The moments of inertia about the principal molecular axes available for all except anisole, are as follows.

Compound	$I_A \times 10^{47}$ $\text{kg}^{-1} \text{ m}^{-2}$	$I_B \times 10^{47}$ $\text{kg}^{-1} \text{ m}^{-2}$	$I_C \times 10^{47}$ $\text{kg}^{-1} \text{ m}^{-2}$	Source of data
$\text{CH}_2\text{Cl}_2$	26.3	253.0	278.0	Myers and Gwinn (1952)
$\text{CH}_2\text{I}_2$	37.4	1345.0	1377.0	Sandhu <i>et al</i> (1976)
$\text{C}_6\text{H}_5\text{CF}_3$	295	886.83	1035.26	Ogata and Cox (1976)

Apart from the large asymmetry in the moment of inertia about different axes in  $\text{CH}_2\text{Cl}_2$  and  $\text{CH}_2\text{I}_2$  it is also noticed that  $\text{CH}_2\text{Cl}_2$  ( $M_r = 84.94$ ) is much lighter than  $\text{CH}_2\text{I}_2$  ( $M_r = 267.87$ ), and therefore it is expected that in these two structurally similar molecules mass dependent dynamical properties might be discerned.

The molecular structural asymmetry of these compounds *a priori* suggests good translation-rotation coupling, which results in the similar variation of the intermolecular and intramolecular dipolar relaxation rates, and an overall diffusive reorientational motion.

$T_1$  and  $D$  measured over suitable temperature ranges in these compounds are shown in Figs. 28 to 35. At the outset the rapid variation of the proton  $T_1$  with temperature suggests that the relaxation is governed by surrounding dependent diffusive processes which are much more temperature sensitive than the inertial processes. The self-diffusion coefficients fit into an Arrhenius type relation whose activation energies are given in Table 5.1 (See also comments on p. 99.)

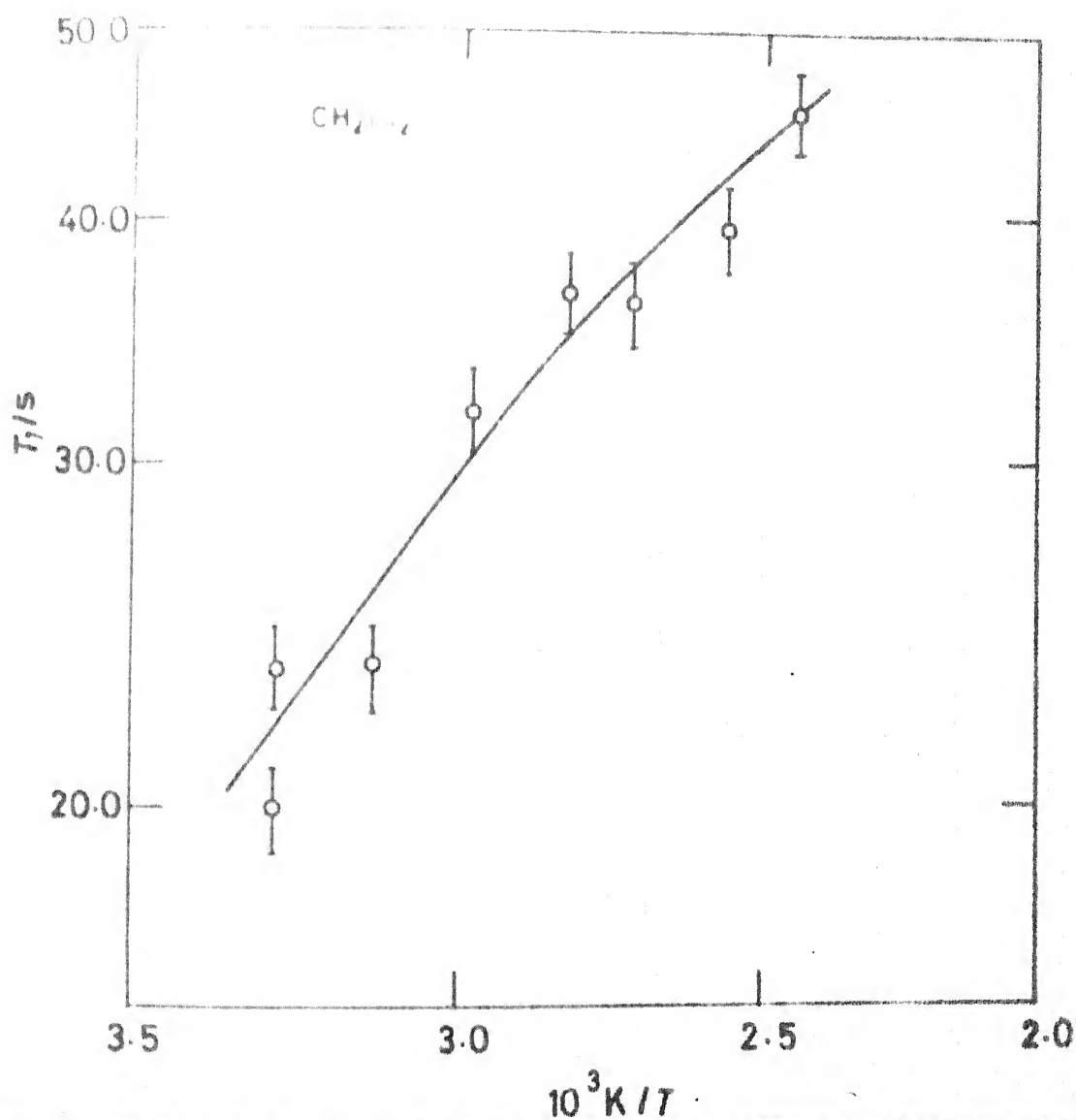


FIGURE 28. TEMPERATURE DEPENDENCE OF PROTON SPIN-LATTICE RELAXATION TIME ( $T_1$ ) IN METHYLENE CHLORIDE.

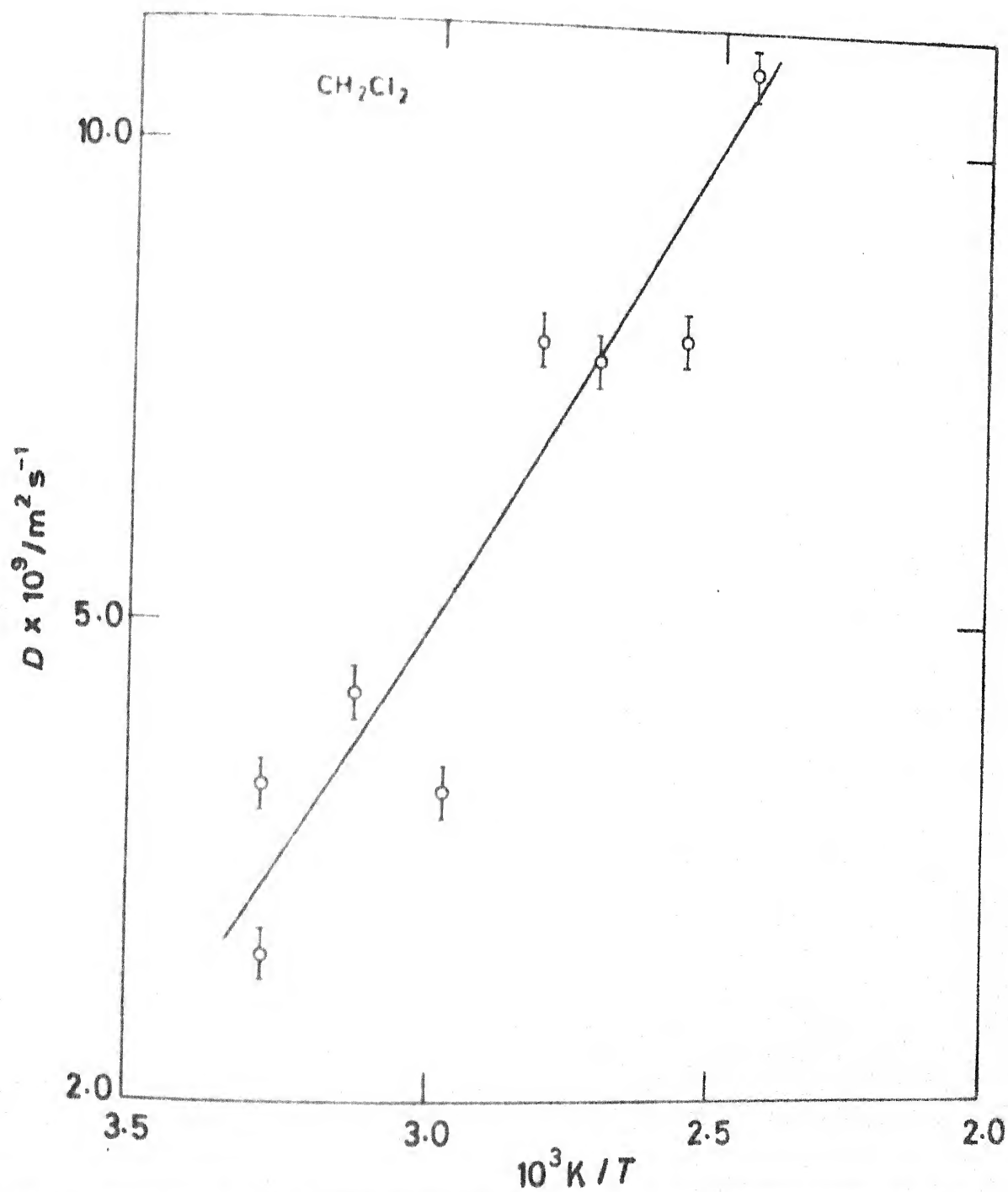


FIGURE 29. TEMPERATURE DEPENDENCE OF SELF-DIFFUSION COEFFICIENT ( $D$ ) IN METHYLENE CHLORIDE.

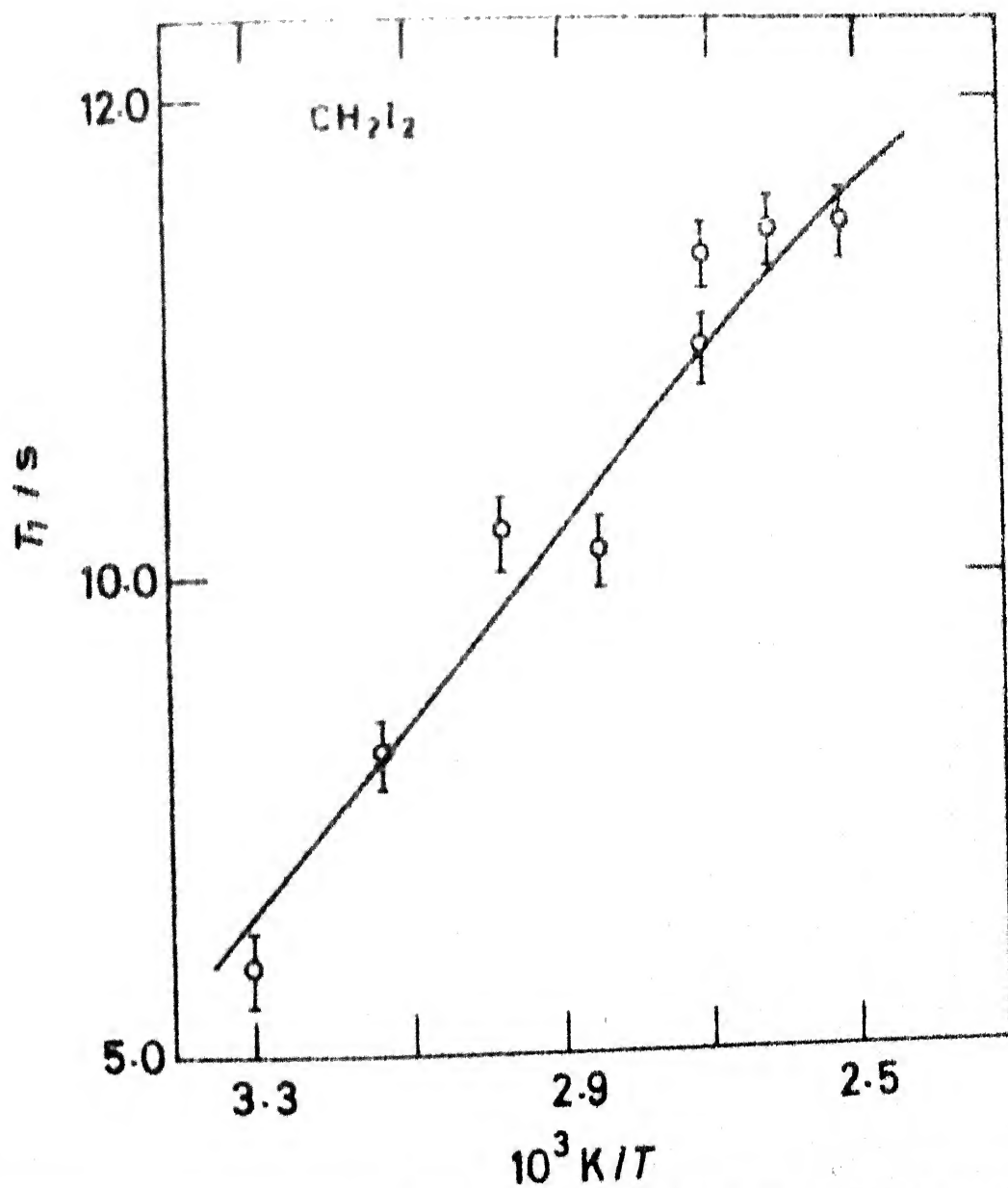


FIGURE 30. TEMPERATURE DEPENDENCE OF PROTON SPIN-LATTICE RELAXATION TIME ( $T_1$ ) IN METHYLENE IODIDE.

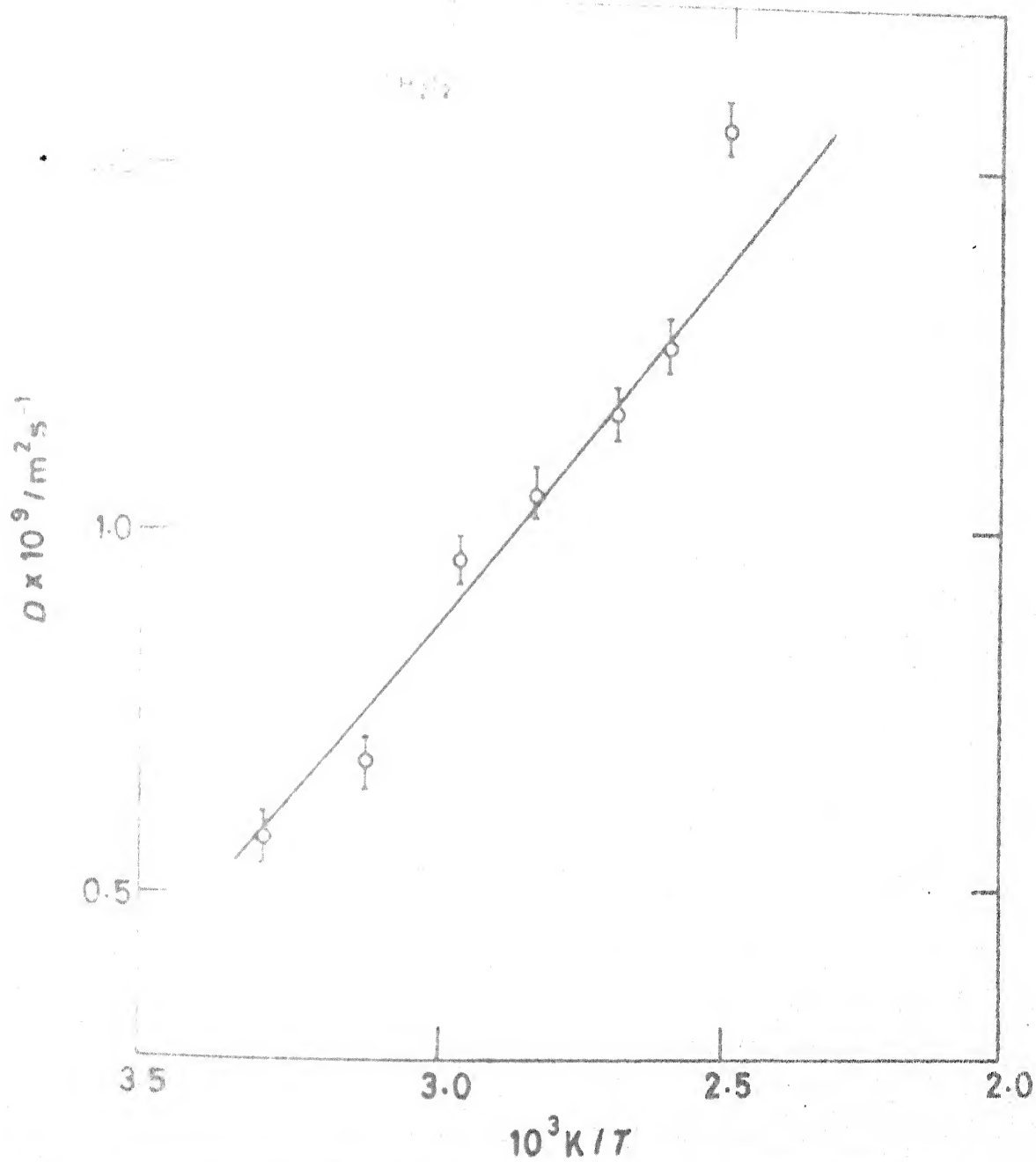


FIGURE 31. TEMPERATURE DEPENDENCE OF SELF-DIFFUSION COEFFICIENT ( $D$ ) IN METHYLENE IODIDE.

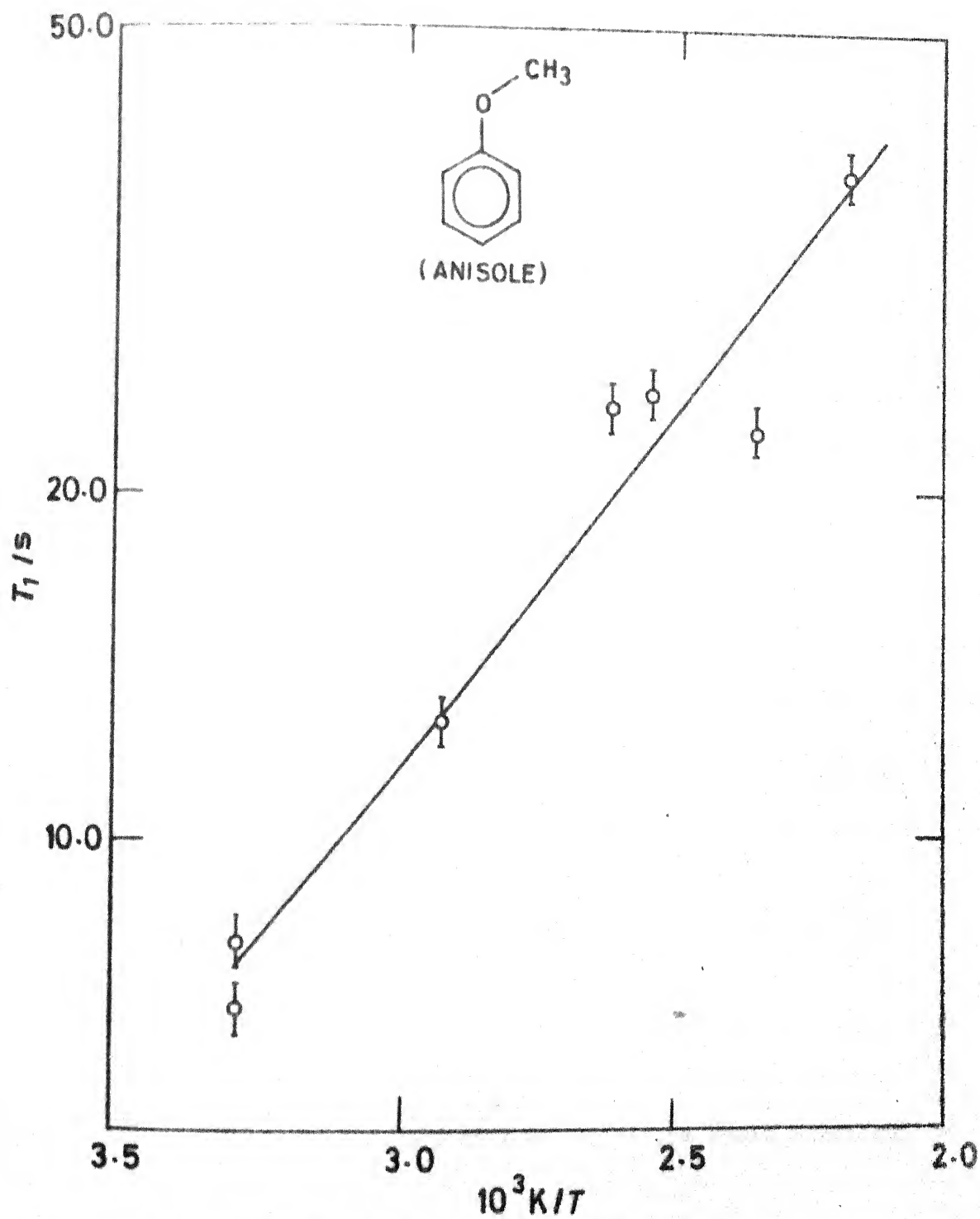


FIGURE 32. TEMPERATURE DEPENDENCE OF PROTON SPIN-LATTICE RELAXATION TIME ( $T_1$ ) IN ANISOLE.

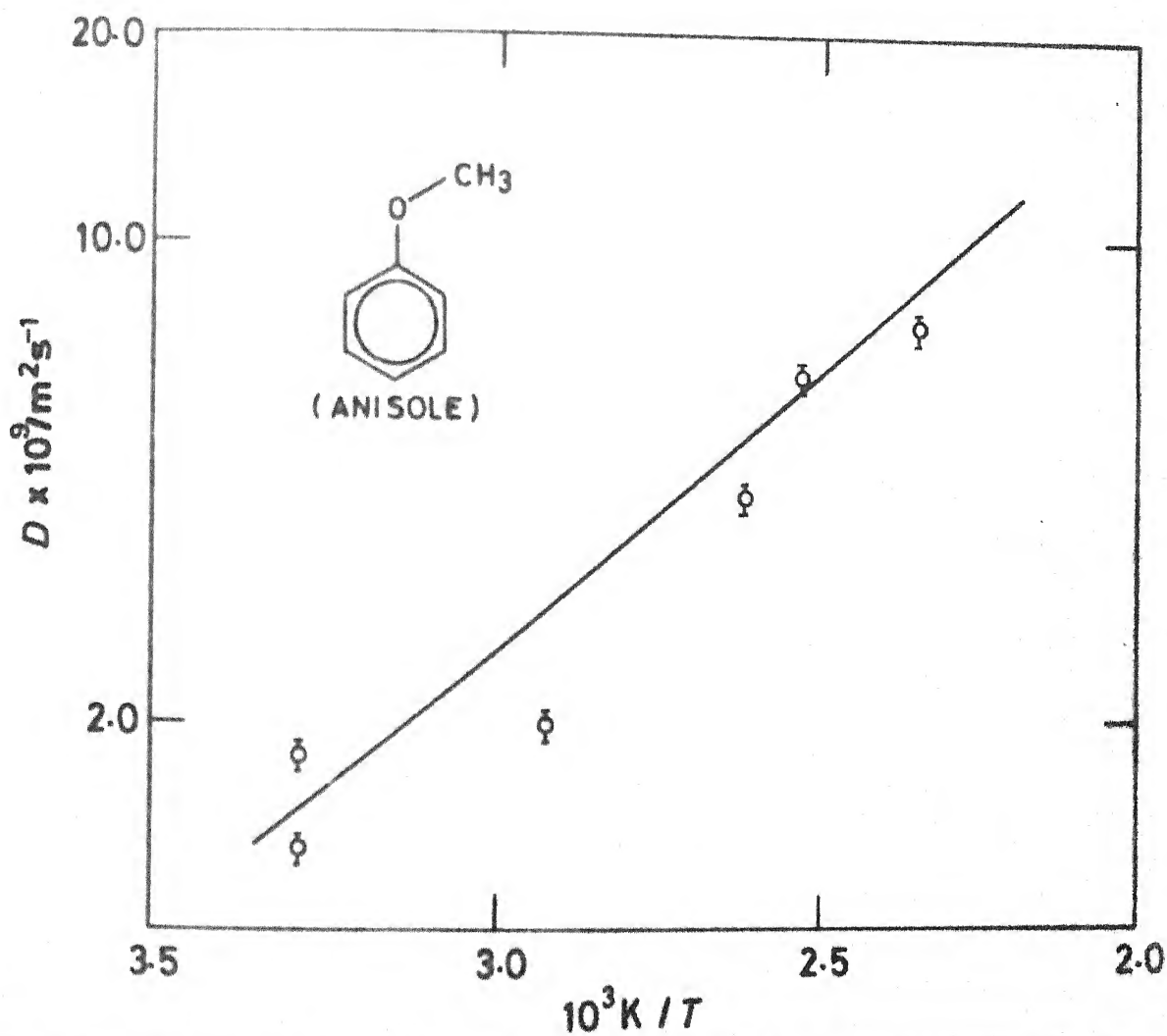


FIGURE 33. TEMPERATURE DEPENDENCE OF SELF-DIFFUSION COEFFICIENT ( $D$ ) IN ANISOLE.

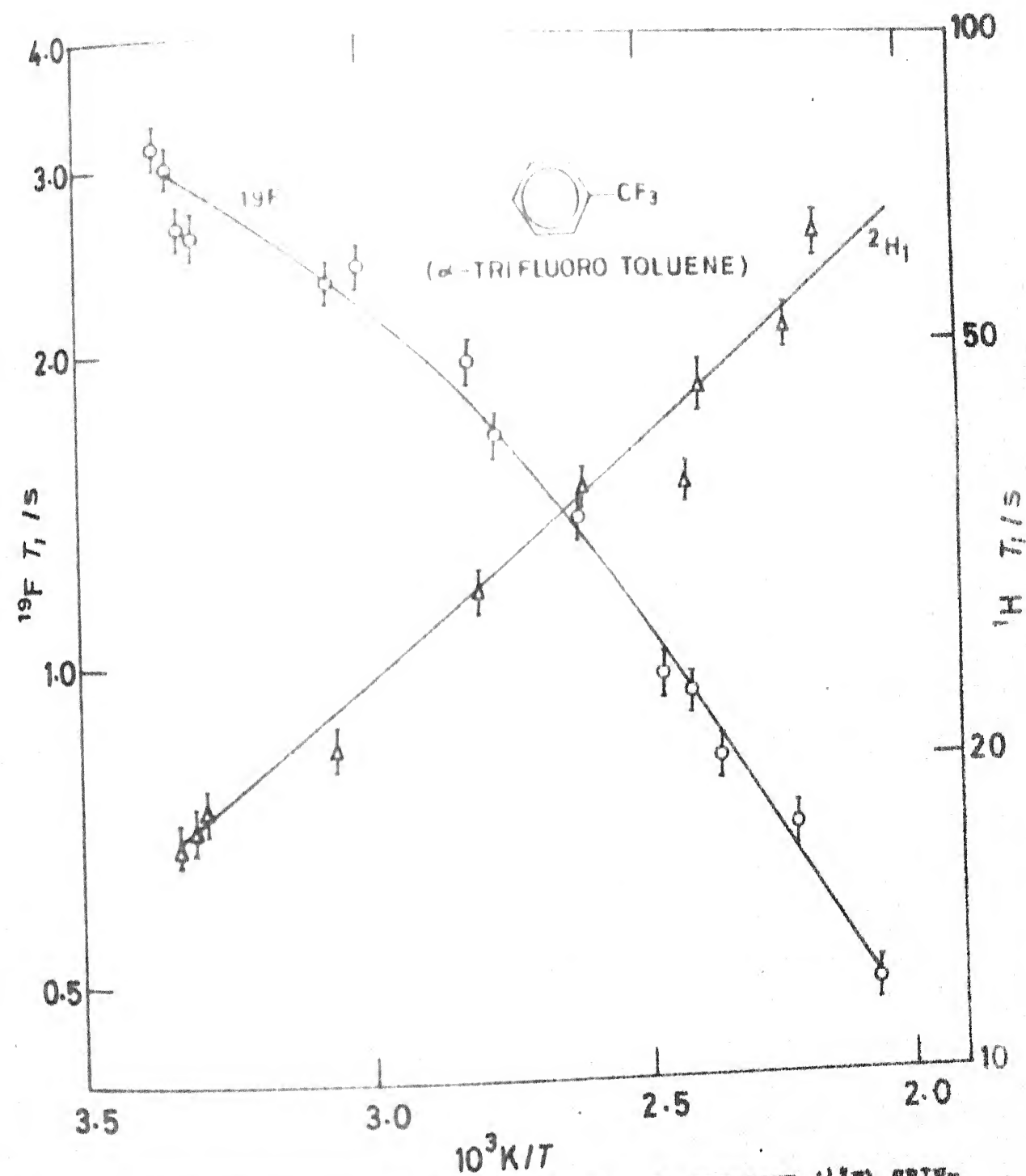


FIGURE 34. TEMPERATURE DEPENDENCE OF PROTON ( $^1\text{H}$ ) AND FLUORINE ( $^{19}\text{F}$ ) SPIN-LATTICE RELAXATION TIME ( $T_1$ ) IN  $\alpha$ -TRIFLUORO TOLUENE.

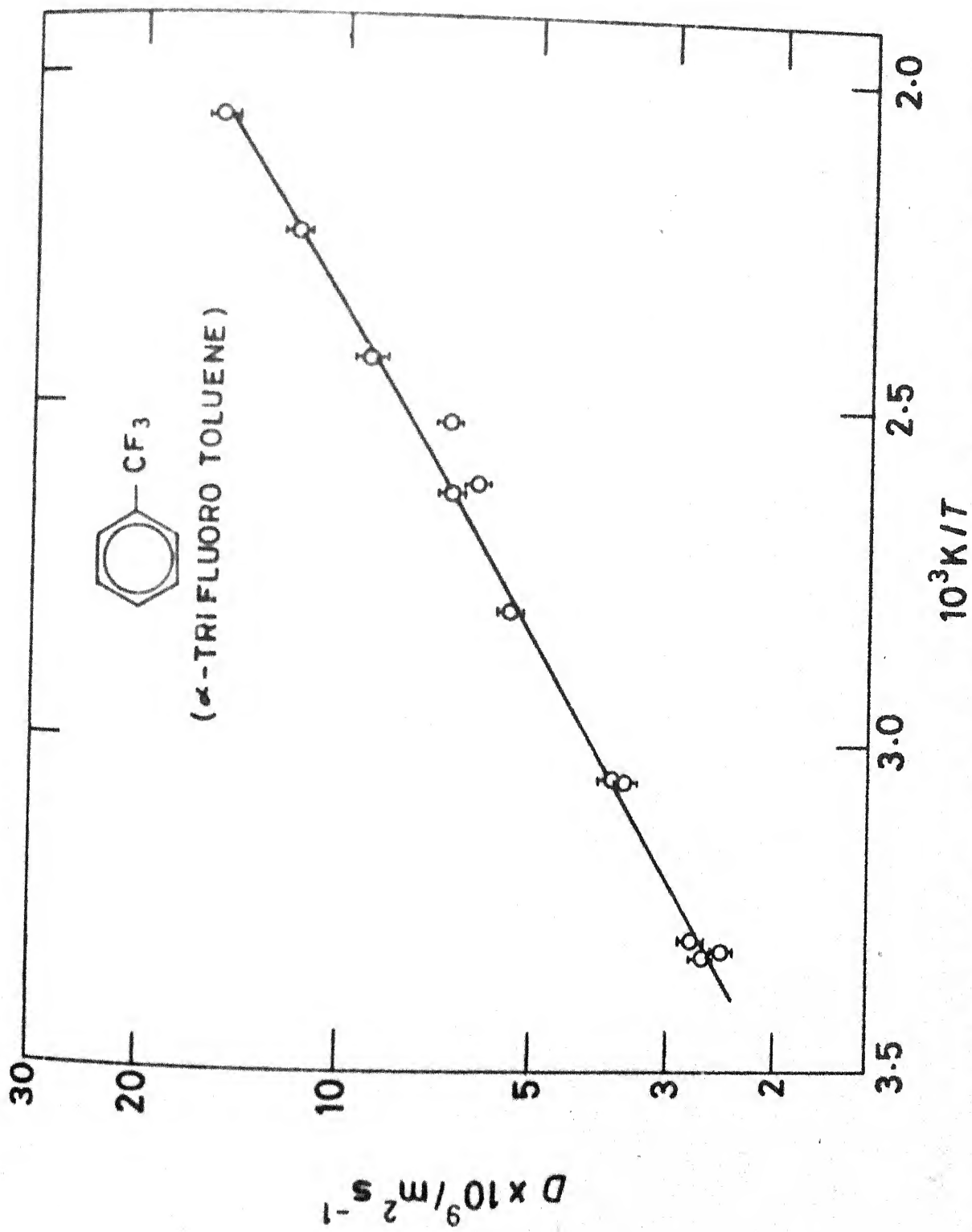


FIGURE 35. TEMPERATURE DEPENDENCE OF SELF-DIFFUSION COEFFICIENT ( $D$ ) IN p-TRIFLUORO TOLUENE.

TABLE 5.1

THE ACTIVATION ENERGIES OF THE VARIOUS PARAMETERS IN A GROUP OF ASSORTED COMPOUNDS

Compound	$E(D)$ (kcal) <sup>-1</sup> . mole	$E(\eta)$ (kcal) <sup>-1</sup> . mole	$E(\rho/D)$ (kcal) <sup>-1</sup> . mole	$E(\eta p/T)$ (kcal) <sup>-1</sup> . mole	$E(T/\eta)$ (kcal) <sup>-1</sup> . mole	$E(\eta/T\rho)$ (kcal) <sup>-1</sup> . mole	$E(R_{\text{intra}})$ (kcal) <sup>-1</sup> . mole	$E(R_{\text{total}})$ (kcal) <sup>-1</sup> . mole
CH <sub>2</sub> Cl <sub>2</sub>	3.37	1.58	3.73	2.69	2.34	1.84	-	-
CH <sub>2</sub> I <sub>2</sub>	2.73	2.3	2.92	3.21	3.01	3.03	-	-
C <sub>6</sub> H <sub>5</sub> OCH <sub>3</sub>	3.29	2.67	3.59	3.75	3.39	3.09	2.23	2.84
C <sub>6</sub> H <sub>5</sub> CF <sub>3</sub>	2.77	1.89	2.86	-	-	-	1.83	2.12

$E(D)$  and  $E(T/\eta)$  are obtained from the corresponding linear plots obeying  $E(X) = -R \frac{\partial \ln X}{\partial 1/T}$  where  $X$  stands for  $D$  and  $T/\eta$  and  $E(\eta)$ ,  $E(\rho/D)$ ,  $E(\eta p/T)$ ,  $E(\eta/T\rho)$ ,  $E(R_{\text{intra}})$ , and  $E(R_{\text{total}})$  are obtained from the corresponding linear plots obeying  $E(Y) = R \frac{\partial \ln Y}{\partial 1/T}$ , where  $Y$  stands for  $\eta$ ,  $\rho/D$ ,  $\eta p/T$ ,  $R_{\text{intra}}$  and  $R_{\text{total}}$ .

The error in the activation energy calculation is about 5%.

In order to estimate the molecular radius from Stokes-Einstein relation (Eq. 1.12) and the intramolecular relaxation rate from the Torrey's relation (Eq. 1.10) the viscosity and density data necessary in the experimental temperature range are the extrapolated values taken from the following sources:

---

Compound	Density data available in the temperature range	Source of data
$\text{CH}_2\text{Cl}_2$	-30 °C to 70 °C	Landolt-Börnstein (1971a)
$\text{CH}_2\text{I}_2$	10 °C to 90 °C	Griffing <i>et al</i> (1954)
$\text{C}_6\text{H}_5\text{OCH}_3$	0 °C to 15 °C	Landolt-Börnstein (1971b)
$\text{C}_6\text{H}_5\text{CF}_3$	Only at 14 °C	Handbook of Chemistry and Physics (1962)

---



---

Compound	Viscosity data available in the temperature range	Source of data
$\text{CH}_2\text{Cl}_2$	-32 °C to 70 °C	Landolt-Börnstein (1969b)
$\text{CH}_2\text{I}_2$	30 °C to 150 °C	<i>ibid.</i> (1969b)
$\text{C}_6\text{H}_5\text{OCH}_3$	14.55 °C to 152.2 °C	<i>ibid.</i> (1969c)
$\text{C}_6\text{H}_5\text{CF}_3$	20 °C to 60 °C	<i>ibid.</i> (1955)

---

In  $\text{C}_6\text{H}_5\text{OCH}_3$  and  $\text{C}_6\text{H}_5\text{CF}_3$ , the density data are available only in a very limited temperature range. Extrapolation over the

desired temperature range is carried out assuming that the density variation with temperature in  $C_6H_5OCH_3$ ,  $C_6H_5CF_3$  and  $C_6H_5CH_3$  (toluene) are similar. The similar variation of the coefficient of viscosity with temperature in  $C_6H_5CF_3$  and  $C_6H_5CH_3$  adds credence to this contention. The  $C_6H_5CH_3$  density data available in Vargaftik (1975) over the temperature range  $-100\text{ }^{\circ}\text{C}$  to  $110\text{ }^{\circ}\text{C}$  are made use of.

The  $D\eta/T$  values are given in Table App. 1 and the Stokes-Einstein molecular radii derived therefrom are given in Table App. 2. The total relaxation rates, the intermolecular relaxation rates obtained using the Torrey's relation (Eq. 1.10), and the total intramolecular relaxation rates as the difference between the two aforementioned relaxation rates for the compounds are plotted in Figs. 36 to 39. The corresponding activation energies, in cases wherever the stated parameters can be fitted to Arrheniuslike relation, are given in Table 5.1.

In the stated figures, attributes catching immediate attention are the following: Against our hope of fast variation of the relaxation rates in such asymmetric molecules, the slow variation of the intramolecular relaxation rate in  $CH_2Cl_2$  (Fig. 36) could be due to the facetious reorientational motion in this light molecule. Almost similar variation of the proton relaxation rates in  $CH_2I_2$  and  $C_6H_5CF_3$  implies good translation-rotation coupling quite becoming of such heavy asymmetric molecules. The  $^{19}\text{F}$  relaxation is almost totally determined by

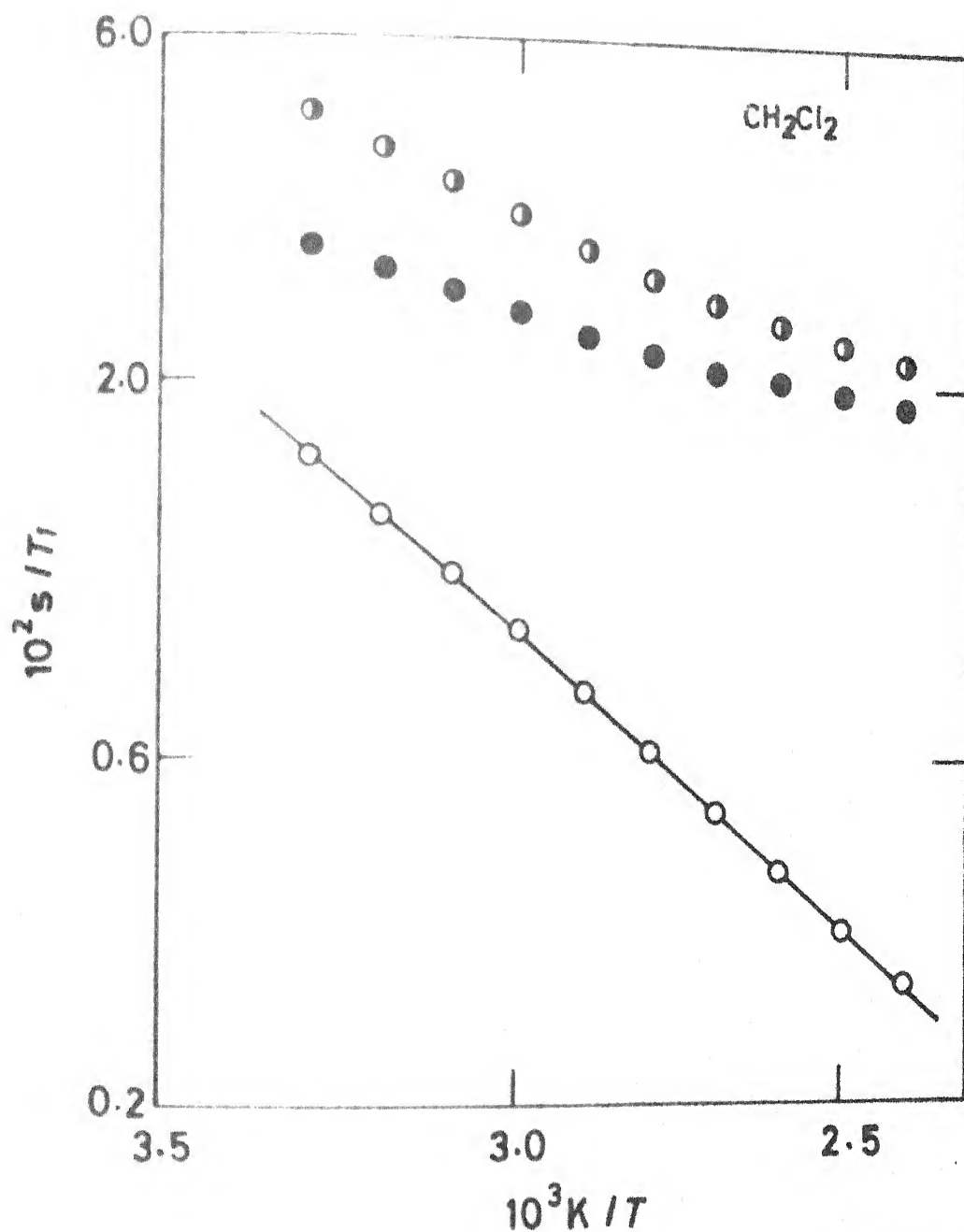


FIGURE 36 . PLOTS OF THE VARIATION OF THE VARIOUS RELAXATION RATES WITH TEMPERATURE IN METHYLENE CHLORIDE .  
 $\bullet$  , TOTAL RELAXATION RATE (OBSERVED).  $\circ$  , INTER-MOLECULAR RELAXATION RATE (CALCULATED).  $\bullet$  , INTRA-MOLECULAR RELAXATION RATE.

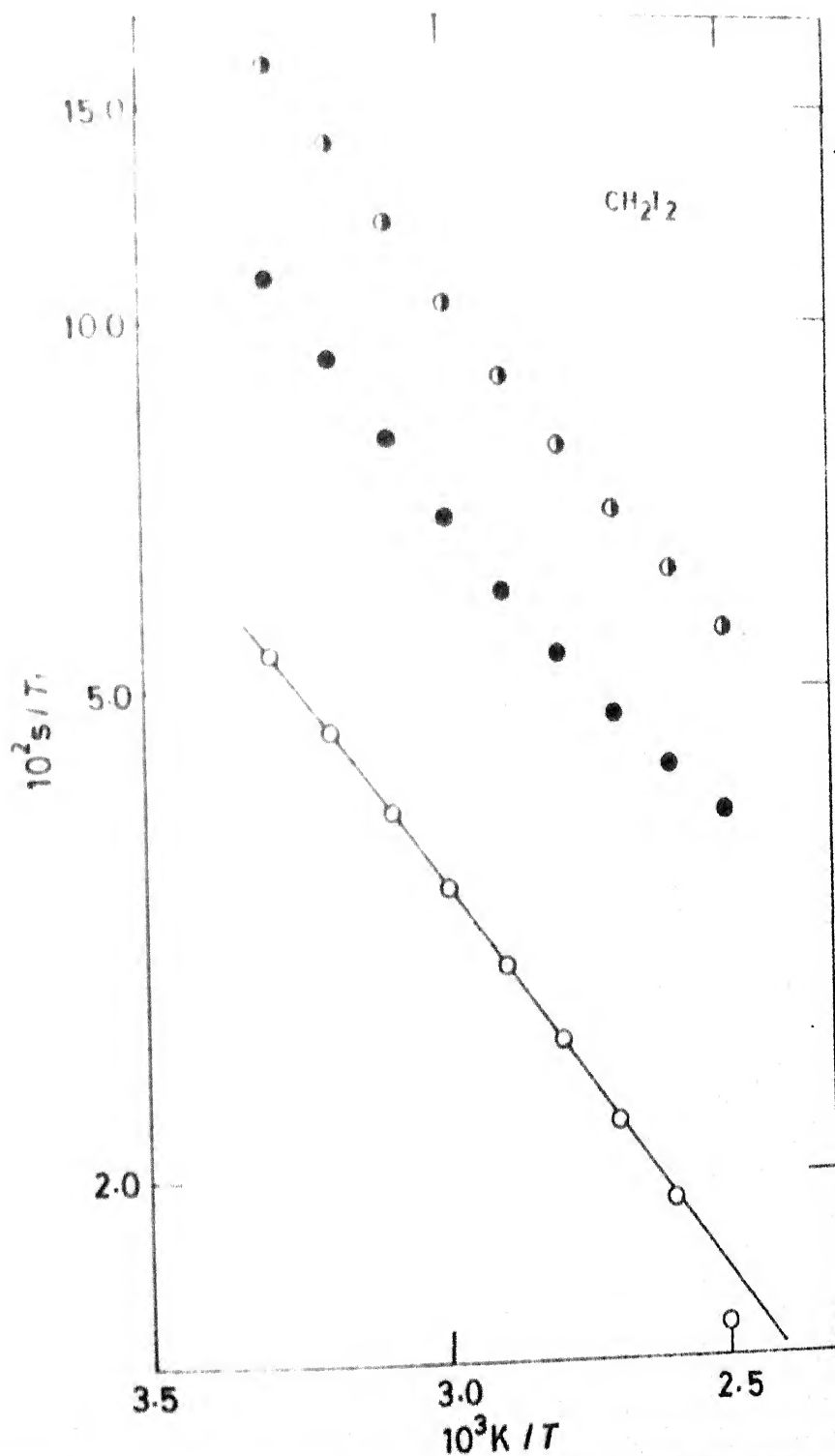


FIGURE 37. PLOTS OF THE VARIATION OF THE VARIOUS RELAXATION RATES WITH TEMPERATURE IN METHYLENE IODIDE.  $\odot$ , TOTAL RELAXATION RATE (OBSERVED).  $\circ$ , INTERMOLECULAR RELAXATION RATE (CALCULATED).  $\bullet$ , INTRAMOLECULAR RELAXATION RATE.

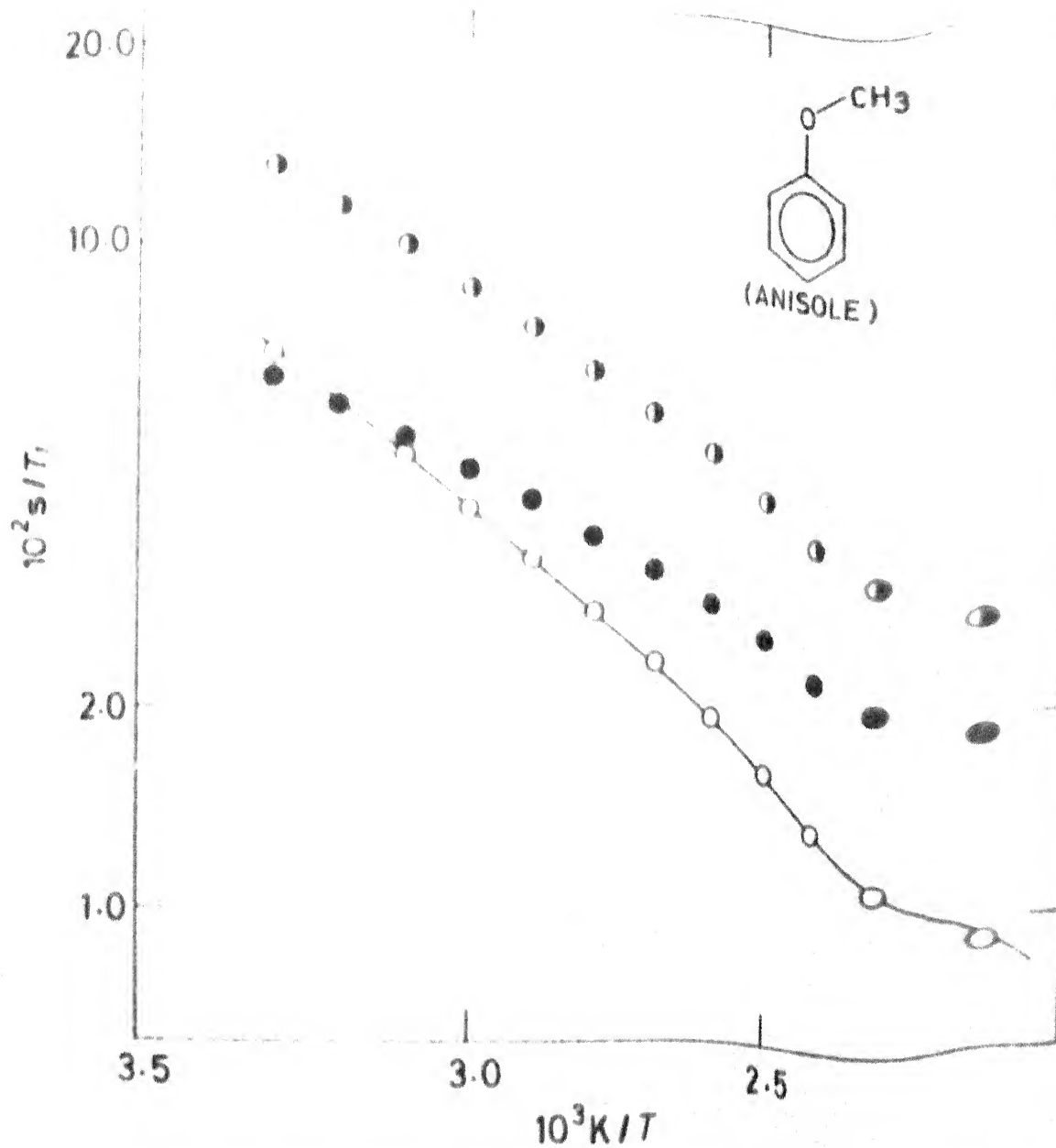


FIGURE 38. PLOTS OF THE VARIATION OF THE VARIOUS RELAXATION RATES WITH TEMPERATURE IN ANISOLE. ⊙, TOTAL RELAXATION RATE (OBSERVED). ○, INTERMOLECULAR RELAXATION RATE (CALCULATED). ●, INTRAMOLECULAR RELAXATION RATE.

the intramolecular spin-rotational interaction whose strength increases with temperature rise. In anisole (Fig. 38) although the inter- and intramolecular relaxation rates are close at room temperature, they widen out with temperature rise, with intramolecular relaxation rate dominating the relaxation more and more and decreasing more slowly than the intermolecular relaxation rate. The import of such an observation is that the intramolecular interaction is fairly strong and the reorientational motion is inertial in nature. Detailed discussions and analyses are relegated to the discussions on individual compounds.

Temperature variations of the derived parameters as described in pages 116 to 121 are also carried out in the present group of compounds. Wherever a fit to an Arrheniuslike relation is possible, the corresponding activation energy is given in Table 5.1.  $T_1\rho\eta/T$  and  $T_1\eta/T$  corresponding to the  $^{19}\text{F}$  relaxation decrease spectacularly with temperature, as would happen in case of strong spin-rotation interaction. Tables 5.2 and 5.3 give the parameters as described in Chap. 1 (see pp. 121 to 124).

### 5.1 $\text{CH}_2\text{Cl}_2$ and $\text{CH}_2\text{I}_2$

Each of these molecules is a two-spin system with possible H-Cl and H-I scalar coupling. Since the scalar coupling would not affect the relaxation rate (p. 38) the relaxation rate analysis is carried out ignoring it. The large asymmetry

TABLE 5.2

THE CORRELATION TIMES IN AN ASSORTED GROUP OF COMPOUNDS

Compound	$10^3 K/T$	$\tau_{\theta 2} \text{ eff}$ $\times 10^{13} \text{ s}^{-1}$	$\tau_{\theta 2} \text{ BPP}$ $\times 10^{13} \text{ s}^{-1}$	$\tau_{\text{free av}}$ $\times 10^{13} \text{ s}^{-1}$	Inertial $\tau_{\theta 2} \text{ av}$ $\times 10^{13} \text{ s}^{-1}$	Mod. Hill $\tau_{\theta 2} \text{ av}$ $\times 10^{13} \text{ s}^{-1}$
	3.3	11.42	7.37	2.77	2.03	1.12
$\text{CH}_2\text{Cl}_2$	2.4	6.96	2.72	2.36	1.73	0.40
	3.3	40.40	135.40	3.52	2.58	4.91
$\text{CH}_2\text{I}_2$	2.5	14.80	39.83	3.07	2.25	1.45
	3.3	10.42	36.83	-	-	-
$\text{C}_6\text{H}_5\text{OCH}_3$	2.2	3.08	5.60	-	-	-
	3.3	50.44	27.31	7.99	5.86	9.70
$\text{C}_6\text{H}_5\text{CF}_3$	2.3	20.40	5.55	6.67	4.89	1.97

TABLE 5.3

SOME MOLECULAR PARAMETERS IN A GROUP OF ASSORTED COMPOUNDS

Compound	$10^3 K/T$	$\chi_{\text{eff}}$	$a_2^m(0)_{\text{eff}}$	$a_2^m(0)_{\text{av}}$	Dipole moment D <sup>-1</sup>
<chem>CH2Cl2</chem>	3.3	4.1	2.88	1.9	1.85
	2.4	2.9	2.06	0.9	
<chem>CH2I2</chem>	3.3	11.5	8.0	26.8	1.1
	2.5	4.8	3.37	9.1	
<chem>C6H5OCH3</chem>	3.3	-	-	-	1.16
	2.2	-	-	-	
<chem>C6H5CF3</chem>	3.3	6.3	4.41	3.3	2.6
	2.3	3.1	2.14	1.5	

between the moment of inertia components (see p.135) of these molecules is interesting. Although  $I_A$  is much smaller than  $I_B$  and  $I_C$ ;  $I_B$  and  $I_C$  seem to be close. The farinfrared work of Evans and Myron (1976) shows  $\text{CH}_2\text{Cl}_2$  to behave as a symmetric top molecule. Recently the depolarized Rayleigh and Raman scattering studies in liquid  $\text{CH}_2\text{Br}_2$  by Wang, Jones and Christensen (1976) has shown the slip boundary condition to be tenable. These suggest *a priori* a good deal of rotational freedom at least in case of  $\text{CH}_2\text{Cl}_2$ , the lightest of the trio ( $\text{CH}_2\text{Cl}_2$ ,  $\text{CH}_2\text{Br}_2$  and  $\text{CH}_2\text{I}_2$ ).

The self-diffusion coefficients fitted to an Arrhenius relation gives for  $\text{CH}_2\text{Cl}_2$   $E(D) = 3.37$  kcal/mole which is large compared to 2.12 kcal/mole obtained by Sandhu (1971) and 2.40 kcal/mole obtained by O'Reilly *et al* (1972), and that for  $\text{CH}_2\text{I}_2$   $E(D) = 2.73$  kcal/mole which is less in comparison to 3.29 kcal/mole obtained by Sandhu (1971). Each molecule of  $\text{CH}_2\text{I}_2$  being much heavier than that of  $\text{CH}_2\text{Cl}_2$  naturally gives a smaller  $D$  at room temperature. But the expectation that the self-diffusion of a heavier molecule of similar shape will have greater surrounding dependence, higher temperature sensitivity and large  $E(D)$  as seen by Sandhu (1971) is not presently borne out in the studies of  $\text{CH}_2\text{Cl}_2$  and  $\text{CH}_2\text{I}_2$ . Just as observed in  $\text{CH}_3\text{CN}$  (Chap. 4) the  $\text{CH}_2\text{Cl}_2$  self-diffusion coefficient varies much faster with temperature than the corresponding  $\eta$ .

The observed relaxation rates, intermolecular relaxation rates obtained using Torrey's relation (Eq. 1.10) and the intramolecular relaxation rates as the difference between the preceding two are plotted in Figs 36 and 37. The effective reorientational correlation times obtained using Eq. 1.13 are plotted in Fig. 40. Whereas the slow variation of the intramolecular relaxation rate  $\text{CH}_2\text{Cl}_2$  might suggest the presence of some rotational coherence and consequent contribution to the relaxation the fast variation of the intramolecular relaxation rate with temperature in the heavier  $\text{CH}_2\text{I}_2$  involves spin-rotation contributing meaningfully to relaxation. The  $\tau_{\theta_2 \text{ eff}}$  for  $\text{CH}_2\text{I}_2$  is essentially the corresponding dipolar reorientational correlation time. It is seen from Fig. 40 that  $\text{CH}_2\text{Cl}_2$  reorientational correlation time is smaller and varies slower than that of  $\text{CH}_2\text{I}_2$ , reminiscent of an inertial reorientation process. The effective  $\chi$  for  $\text{CH}_2\text{Cl}_2$  in Table 5.3 is less than 3 at the highest working temperature and could also suggest inertial motion. The fast, and almost identical variation of the relaxation rates with temperature in  $\text{CH}_2\text{I}_2$  (Fig. 37) shows the reorientation and translation processes to be temperature dependent in a similar way, suggesting good translation-rotation coupling in the liquid phase of this heavy molecule.

The calculations of the overall rotational diffusion constants are presented in the Table App. 3. As against Heatley (1974)'s

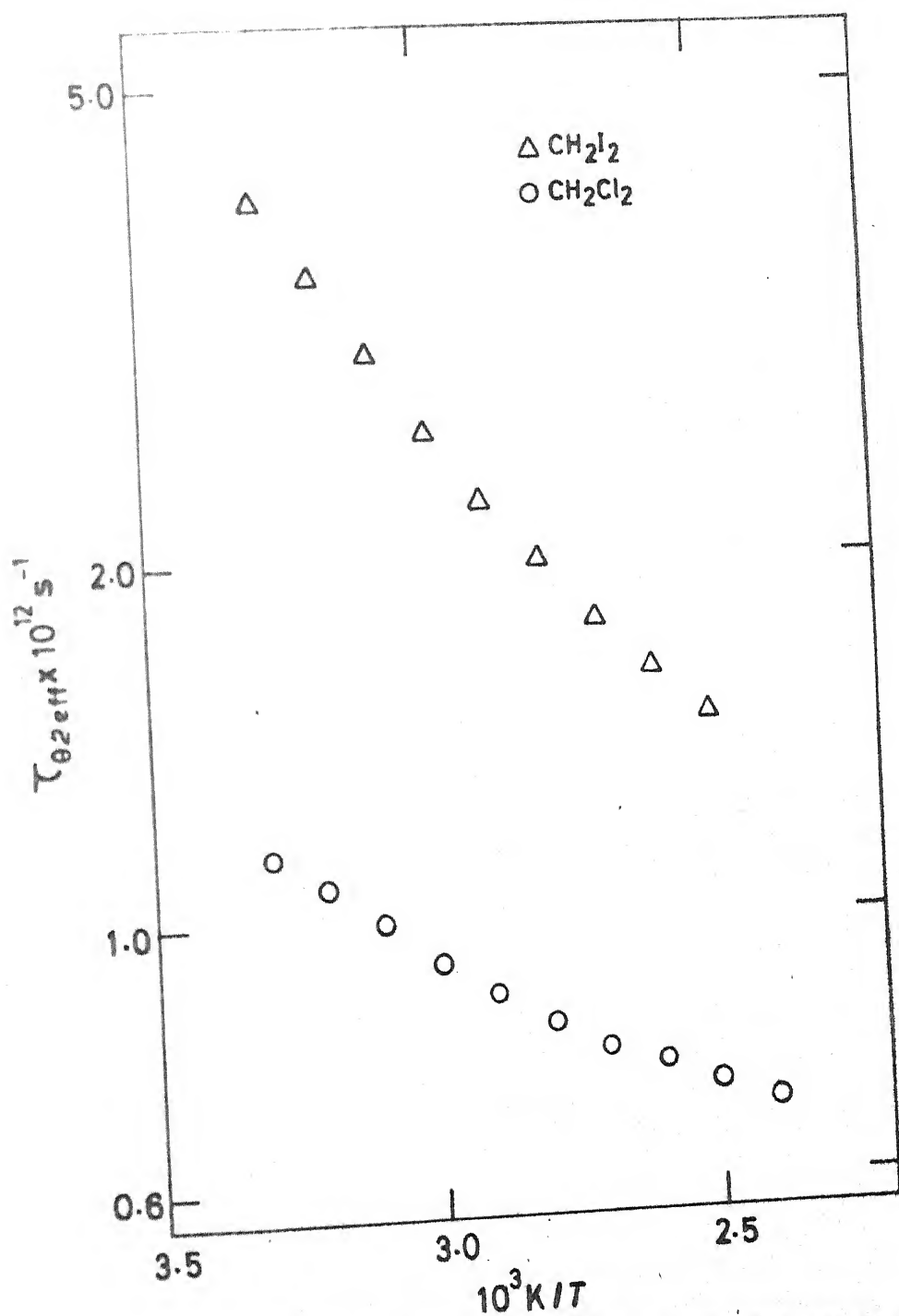


FIGURE 40 . PLOTS OF THE VARIATION OF THE EFFECTIVE REORIENTATIONAL CORRELATION TIMES ( $\tau_{02\text{eff}}$ ) WITH TEMPERATURE IN METHYLENE CHLORIDE ( $\circ$ ) AND METHYLENE IODIDE ( $\Delta$ ).

$\rho_1 = 2.2 \times 10^{11} \text{s}^{-1}$  at normal room temperature the present calculation at room temperature gives  $\rho_1 = 2.18 \times 10^{11} \text{s}^{-1}$  with an Arrheniuslike activation energy 2.34 kcal/mole over the experimental temperature range.  $\rho_{11}$  calculated under the assumption of free parallel motion (see p.127) is  $9.52 \times 10^{11} \text{s}^{-1}$  at room temperature which is much larger than the Heatley (1974)'s corresponding value of  $4.4 \times 10^{11} \text{s}^{-1}$ . The motion about the parallel symmetry axis in  $\text{CH}_2\text{Cl}_2$  is therefore somewhere between free and diffusive but nearer the diffusive end whereas the motion about the approximate perpendicular symmetry axis is diffusive. In the light of this, it is fair to expect both the rotational motions about the approximate perpendicular and parallel symmetric axis in the heavier  $\text{CH}_2\text{I}_2$  to be diffusive.

## 5.2 $\text{C}_6\text{H}_5\text{OCH}_3$

In anisole there are two distinct groups of proton containing species ( $\text{C}_6\text{H}_5$  and  $\text{CH}_3$ ). There could be intramolecular relative motion between the species and that  $\text{CH}_3$  could be quite mobile. (It is unfortunate that the rotational parameters on the molecule could not be gotten as yet.) The overall relaxation has contribution from the two distinct groups and from the cross-correlation between the two. Cutnell *et al* (1975) have shown that at  $10^3 \text{K}/T = 3.3$  the cross relaxation contribution to the total relaxation is 23.8% and decreases sharply with temperature reducing to 16% at  $10^3 \text{K}/T = 3.0$ . It can thus be assumed that at our highest working temperature ( $10^3 \text{K}/T = 2.2$ ) the cross relaxat:

contribution is negligibly small. It is also seen by Cutnell *et al* that the  $\text{CH}_3$  group relaxation rate is the more dominant one. The present work provides complementary  $\rho$  data and takes a look into the problem of analysis of the  $T_1$  and  $\rho$  data in a somewhat simplified way.

The measured self-diffusion coefficients could be fitted to an Arrheniuslike relation (Fig. 33) which gives an activation energy 3.29 kcal/mole (Table 5.1). The observed overall  $^1\text{H}$  relaxation seems to be exponential in time thus showing, if any, small effect due to cross relaxation. Also in the work of Cutnell *et al* (1975) an almost similar variation of the overall proton relaxation rates in  $\text{CH}_3$  and  $\text{C}_6\text{H}_5$  could help make such a contention. (Actually the slightly weaker variation of the  $-\text{CH}_3$  proton relaxation rate with temperature might be because of a lesser dependence on the surrounding which might suggest an internal motional freedom.) The activation energy of the observed total relaxation rate agrees well with the value 2.77 kcal/mole obtained by Cutnell *et al* (1975). The intermolecular relaxation rate over the experimental temperature range are estimated using Eq. 1.10. The total relaxation rate, intermolecular relaxation rate, and the intramolecular relaxation rate as the difference between the previous two rates are plotted in Fig. 38. The intramolecular relaxation rate although comparable to the intermolecular relaxation rate at room temperature decreases comparatively slowly with temperature increase. The activation

energies of the inter- and intramolecular relaxation rates are 3.59 and 2.23 kcal/mole respectively (Table 5.1). This suggests that the intramolecular relaxation to be a temperature activated process of lesser strength than the intermolecular relaxation rate. Further analysis of the intramolecular relaxation rate is based on Gutowsky and Woessner (1956)'s relation,

$$R_{\text{intra}} = 3/2 \gamma^4 \hbar^2 (N_{\text{C}_6\text{H}_5}^{-1} \sum r_{ij}^{-6} + N_{\text{CH}_3} \sum r_{kl}^{-6}) \tau_{\theta_2 \text{ eff}} \quad (5.1)$$

where N is the number of resonating spins in the corresponding species subscripted to N,  $r_{ij}$  and  $r_{kl}$  are the separation between the protons in  $\text{C}_6\text{H}_5$  and  $\text{CH}_3$  groups respectively. Since  $r_{ij}$ s for the ortho, meta and para protons are respectively 2.44, 4.23 and 4.88 Å and  $r_{kl} = 1.78$  Å, the first term within the bracket of the foregoing relation (Eq. 5.1) is about 11% of the total. It is, therefore, essentially the  $\text{CH}_3$  group motion which determines the  $^1\text{H}$  intramolecular relaxation. An effective correlation time defined by Eq. 5.1 is evaluated (Table 5.2). The  $\tau_{\theta_2 \text{ eff}}$  seems to be lesser than  $\tau_{\theta_2 \text{ BPP}}$  where the later is an underestimated value (because of the use of small Stokes-Einstein radius, see Appendix) which might suggest a freer reorientational motion arising because of the possible  $\text{CH}_3$  rotation.

### 5.3 $\text{C}_6\text{H}_5\text{CF}_3$

An early work on  $\alpha$ -trifluoro toluene was made by Green and Powles (1965). In the present work apart from measuring the  $^1\text{H}$  and  $^{19}\text{F}$  relaxation times the complementary

self-diffusion coefficients are measured from room temperature to about 180 °C. The relaxation times seem to agree well with those reported by Green and Powles (1965). A fit of the diffusion data to an Arrhenius relation (Fig. 34) gives an activation energy 2.77 kcal/mole. The observed relaxation seems to be exponential in time and it is assumed that all the protons relax identically. The intermolecular relaxation rates are as usual evaluated using the Torrey's relation (Eq. 1.10) for both  $^1\text{H}$  and  $^{19}\text{F}$ . The intramolecular relaxation rates are obtained as the difference between the total and intermolecular relaxation rates. All these relaxation rates are plotted in Fig. 39. For  $^{19}\text{F}$  relaxation the intramolecular interaction seems to almost completely determine the total relaxation rate. The large value and fast increase of the  $^{19}\text{F}$  intramolecular relaxation rates seem to be completely due to the spin-rotation interaction. The rotational coherence giving rise to such large  $^{19}\text{F}$  spin-rotational relaxation could not be because of overall rotational coherence and arises due to the persistence of the rotation of the facile  $\text{CF}_3$  group. Further, the strong temperature dependence of the  $^{19}\text{F}$  intramolecular relaxation rate suggests a temperature activated rotational process but not a free rotation which is weakly temperature sensitive.

The proton intramolecular relaxation rate steadily decreases with temperature increase suggesting to be arising due to intramolecular dipolar interaction. As in anisole (p.156) the

Gutowsky and Woessner relation (Eq.5.1) is used for the  $C_6H_5$  group to determine the proton effective reorientational correlation time. The correlation times and other parameters are usual presented in Table 5.2 and 5.3 where  $\chi_{eff}$  corresponds to  $^1H$ . The large reorientational correlation time is clearly suggestive of a diffusive process determining the  $^1H$  relaxation.

orientational changes would arise simultaneously. Molecular asymmetry, translation-rotation coupling and diffusive motions seem to go on hand in hand. Although the translational motion seems to be mostly diffusional, the orientational motions are often unexpectedly inertial in somewhat heavy but asymmetric molecules. In the case of inertial molecular dynamics the motion is mostly characterised by the moment of inertia and mass of the molecule and is less mindful of the surrounding molecules. Since, in the type of temperature variation work presented here, the molecular kinetic energy and packing are greatly affected and molecular surroundings have little effect on the inertial molecular dynamics, the analogous parameters have little temperature sensitivity and viscosity dependence.

The aim of this work has been to separate the translation, orientation and rotation dependent parameters as functions of temperature. In order to do this, a good estimation of the molecular dimension is necessary. In liquids the picture of the average molecular radius is particularly hazy. There seem to be many approaches for such estimations found suitable for a variety of cases (Appendix). The best course, from the point of view of the analysis of the nmr dynamical parameters, is felt to be through the estimation of the Stokes-Einstein radius. The molecular radius thus obtained is smaller than those obtained through molecular models but obviates the need for micro-viscosity correlations necessary for such molecular motion in

its own surrounding, and is also in agreement with some other work as stated in the Appendix. Using the  $D$  measured *in situ* and available viscosity data over the experimental temperature range, the average Stokes-Einstein molecular radius for the molecule is obtained. Although the best method to determine the intermolecular relaxation is through the measurement of  $T_1$  as a function of concentration in its isotopic analogue, Torrey's relation for the intermolecular relaxation rate in conjunction with the Stokes-Einstein radius gives good estimates of such relaxation rates. This method obviates the dubious procedure of the consideration of hexagonal close packing of molecules in liquids and the simultaneous use of microviscosity correction factors to make the relaxation rate estimates reasonable. The separated intramolecular relaxation rate has contributions from both orientational changes and rotational motion of the molecule. Although a constant density  $T_1$  and  $D$  measurement could have been more informative such temperature variation work as presented in this thesis nevertheless gives valuable information about the molecular dynamics.

The coherent pulsed nmr assembly for such temperature variation work as reported here gives good  $T_1$  and  $D$  data with an error  $\pm 5\%$ . With the help of the available density and the coefficient of viscosity data over the experimental temperature range, and moments of inertia, the various derived parameters and correlation times obtained give valuable information

about the molecular dynamics. The dipole moments of some of these molecules though quite large, have seemingly little effect on the dynamics. It is mainly the molecular shape which determines the dynamics.

The methyl group of compounds are particularly interesting because of the rotational freedom about the axis joining the  $\text{CH}_3$  group to the molecular skeleton. In the study of symmetric top  $\text{CH}_3\text{I}$  and  $\text{CH}_3\text{CN}$  molecular liquids over the experimental temperature range (room temperature to about  $140^\circ\text{C}$ ) large spin-rotational contributions to relaxation are observed. The possibility of rotational freedom about the molecular symmetry axes is responsible for this. The rotational motion about an axis perpendicular to the symmetry axis is, however, diffusional. The study in the highly polar  $\text{CH}_3\text{NO}_2$  (over the temperature range room temperature to about  $130^\circ\text{C}$ ) shows the intramolecular interaction relaxation contribution to total relaxation getting more and more important with temperature rise. As  $\text{CH}_3\text{NO}_2$  is highly polar and would in the liquid phase give rise to a local structure, such a local structure does not seem to affect the reorientational coherence. In acetone the study over the temperature range, room temperature to about  $130^\circ\text{C}$ , shows reorientational coherence which could be because of the intramolecular methyl group rotation. Dimethyl sulfoxide, although structurally close to acetone, seems to have a diffusive reorientational motion over the temperature range, room temperature to nearly  $180^\circ\text{C}$ . Also a good translation-rotation

coupling ensues. Although  $\text{CH}_2\text{Cl}_2$  is an asymmetric molecule, interestingly enough it exhibits a good amount of reorientational coherence over the experimental temperature range- room temperature to about  $140^\circ\text{C}$ . This, however, does not happen in the structurally similar but bulkier  $\text{CH}_2\text{I}_2$  over the same temperature range. In addition, in the molecular dynamics of methylene iodide a good amount of translation-rotation coupling is present. A noteworthy observation in  $\text{CH}_2\text{Cl}_2$  molecular dynamics is that although the rotational motion about the perpendicular symmetry axis is diffusive, such a motion about the parallel symmetry axis though not inertial is seemingly somewhat closer to the diffusive limit. The work in anisole over the temperature range room temperature to  $210^\circ\text{C}$  is analysed in a particularly simplified way. In view of the small cross-correlation effects in the overall  $^1\text{H}$  relaxation in this molecule and the earlier reported almost similar variation of the  $\text{C}_6\text{H}_5$  and  $\text{CH}_3$   $^1\text{H}$  spin-lattice relaxation times, the use of  $\rho$  measured *in situ* is particularly rewarding. The  $^1\text{H}$  relaxation is dominated by the intramethyl group interaction but the effect of somewhat more facile  $\text{CH}_3$  group motion is evident from the intramolecular relaxation rate.  $\alpha$ -trifluoro toluene has the facile intramolecular  $\text{CF}_3$  group rotation giving rise to the most dominant spin-rotation interaction contribution of the  $^{19}\text{F}$  relaxation. The temperature variation of the  $^{19}\text{F}$  intramolecular relaxation over the temperature range, room temperature to about  $160^\circ\text{C}$ , however, hints at a temperature activated  $\text{CF}_3$  group rotation.

The reorientation of the  $C_6H_5$  is diffusive which is shown to be so through the  $^1H$  relaxation.

In obtaining further detailed information about the molecular dynamics a more rewarding picture will be obtained on the following lines.  $T_1$ ,  $D$  data at constant density will be quite revealing and for that matter pressure variation work need be incorporated. Relaxation studies on more than one spin bearing different structural symmetries within the molecule will better reflect the molecular rotational asymmetric motions. The sister branches of studies such as light scattering, neutron scattering, dipole relaxation etc. need be combined to get a comprehensive picture of the molecular dynamics in the molecular liquids. Since the measurement of spin-rotational interaction seems to be a special feature of nmr a study over the largest possible liquid-vapour coexistence range will be rewarding. Although description of either of the limits of molecular dynamics could be easily made a successful attempt to encompass the entire range is lacking. Molecular dynamics in polar liquids as well as solution studies are gradually engaging more and more attention.

Be fruitful, and add

## APPENDIX

### ON THE ESTIMATION OF MOLECULAR RADIUS AND DIFFUSION COEFFICIENTS IN MOLECULAR LIQUIDS

The generalized Einstein diffusion coefficient relates the diffusion coefficient  $D$  to the coefficient of friction  $\zeta$  through the relation

$$D = kT/\zeta . \quad (A.1)$$

For spherical bodies the Stokes relations for the translational and rotational friction are respectively,

$$\zeta_{\text{trans}} = 6\pi\eta a^3, \quad (A.2)$$

$$\text{and } \zeta_{\text{rot}} = 8\pi\eta a^3 . \quad (A.3)$$

Einstein used these macrobody friction coefficients for microbody molecular motions. The consequent mathematical relationships between the diffusion coefficients, molecular radius, viscosity and temperature is known as the Stokes-Einstein relation. The questions are how far such an approximation is correct and what  $a$  is to be taken for the molecules. It is argued in the following that the hydrodynamical relationship is valid, provided not much physical significance is attached to the molecular radius values. The molecular radii of approximated hardspherical bodies are merely artifacts to get agreeable numerical values for dynamical parameters. It is also pointed out that such a course imbibes less number of approximations than the other methods for finding  $a$ .

The methods under discussion for finding  $a$  are :

- (1) the hexagonal close packing of molecules in liquid,
- (2) the van der Waals volume of the molecule, (3) the Lennard-Jones separation for minimum mutual potential energy, and (4) the Stokes-Einstein relation.

In the hexagonal close packing model of the liquid, spheres approximated for molecules are imagined to hexagonally close pack the lattice. The molecular radius  $a_{\text{HCP}}$  is then obtained using the relation

$$\frac{4}{3} \pi a_{\text{HCP}}^3 = 0.74 M_r / \rho N_A \quad (\text{A.4})$$

where  $M_r$  is the molecular weight of the compound,  $\rho$  is the density of the liquid, and  $N_A$  is the Avogadro constant. The validity of such a relation over the entire liquid phase and for all types of non-spherical molecules is suspect. To amend for the expected discrepancy between the theoretical and experimental diffusion coefficients microviscosity correction factors (Gierer and Wirtz (1953)) are used (p.40). Thus the diffusion coefficients are given by

$$D_{\text{trans}} = kT / 6\pi\eta a_{\text{HCP}} \mu_t, \quad (\text{A.5a})$$

$$D_{\text{rot}} = kT / 8\pi\eta a_{\text{HCP}}^3 \mu_r, \quad (\text{A.5b})$$

where, for neat liquids,  $\mu_t$  the translational microviscosity factor is 0.5 and  $\mu_r$  the rotational microviscosity factor is  $1/6.125$  ( $\approx 0.163$ ).

The van der Waals incremental volumes (Edwards (1970)) for the constituents of the molecules are also used to estimate the molecular volume and then the equivalent spherical molecular radius. Such a van der Waals molecular radius is given by

$$4/3 \pi a_W^3 = V_W . \quad (A.6)$$

Lennard-Jones parameters provide a rough picture of the liquid state as well. Svehla (1962) lists the low velocity collision diameters (which is the distance at which the intermolecular potential vs separation changes sign, attractive to repulsive and vice versa). Half of this collision diameter is taken to be the Lennard-Jones radius  $a_W$  in the present discussion.

The fourth and seemingly the least cumbersome way of finding the molecular radius is through the validity of the Stokes-Einstein relation. Experimental values of  $D$  and  $\eta$  are used to find  $D\eta/T$  at several sample temperatures. The Stokes-Einstein relation for the translational diffusion gives,

$$D\eta/T = k/6\pi a . \quad (A.7)$$

The constancy of  $D\eta/T$  over the working temperature range is a pointer towards the validity of the hydrodynamic relation for the translational motion. The values of  $D\eta/T$  at different temperatures for several compounds are listed

in Table App. 1. The near constancy of  $\eta/T$  over the working temperature range helps finding the Stokes-Einstein molecular radius  $a_{SE}$  using

$$a_{SE} = k/6\pi(\eta/T)_{av} \quad (A.8)$$

where  $(\eta/T)_{av}$  is the average value of  $\eta/T$  over the working temperature range.

The molecular radii obtained by the aforementioned four different ways are listed in Table App. 2. It is seen that for every molecule under consideration  $a_{HCP}$  gives the largest and  $a_{SE}$  the smallest molecular radius value. The ratio  $(a_{SE}/a_{HCP})$  and  $(a_{SE}/a_{HCP})^3$  are also listed in the Table App. 2.  $a_{SE}$  is found to be about half of  $a_{HCP}$  for each molecule. The average  $a_{SE}/a_{HCP}$  and  $(a_{SE}/a_{HCP})^3$  for the series of compounds are 0.539 and 0.165 respectively. It therefore appears that instead of using the hexagonal close packing and microviscosity factors to maintain the diffusion coefficient and  $a_{HCP}$  relation (Eqs. A.4, A.5a and A.5b) one can straight away use the Stokes-Einstein relations (Eqs. A.1, A.2 and A.3) to find  $a$ . The success of this procedure depends on the validity of the Stokes-Einstein relation whereas the hexagonal close packing method, in addition, assumes hexagonal close packing of molecules in the liquid phase and also a microviscosity model. Nevertheless the Stokes-Einstein relation is shown to be valid in the liquid phase quite well. (Flowers and Mendoza (1970)).



COMPARISON OF MOLECULAR RADII OF SEVERAL COMPOUNDS BY VARIOUS METHODS

Compound	$a_{\text{HCP}}/\text{\AA}$	$a_w/\text{\AA}$	$a_{\text{LJ}}/\text{\AA}$	$a_{\text{SE}}/\text{\AA}$	$(a_{\text{SE}}/a_{\text{HCP}})$	$(a_{\text{SE}}/a_{\text{HCP}})^3$
Water	1.74	1.70	1.32	0.95	0.546	0.163
Benzene	2.96	2.68	2.67	1.79	0.605	0.221
$\text{CH}_3\text{I}$	2.63	2.37	2.12	1.38	0.525	0.145
$\text{CH}_3\text{NO}_2$	2.51	2.11	-	1.52	0.625	0.244
$\text{CH}_3\text{CN}$	2.49	2.24	-	0.90	0.361	0.047
$\text{CH}_3\text{COCH}_3$	2.78	2.49	2.30	1.57	0.565	0.180
$\text{CH}_3\text{SOCH}_3$	2.80	-	-	1.80	0.643	0.266
$\text{CH}_2\text{Cl}_2$	2.65	2.38	2.45	1.24	0.468	0.102
$\text{CH}_2\text{I}_2$	2.87	2.70	2.58	1.77	0.617	0.235
Anisole	3.18	2.94	-	1.55	0.487	0.115
Thiophene	2.85 <sup>(1)</sup>	2.57	-	1.58	0.554	0.170
1,2 Dichloroethane	2.85 <sup>(1)</sup>	2.34	-	1.39	0.488	0.116
$\text{C}_6\text{H}_5\text{CF}_3$	3.30	2.99	-	1.74	0.529	0.148

<sup>(1)</sup> Kitchlew (1971)

One important thing to note here is that as the intermolecular relaxation rate due to Torrey (1953)  $R_{1inter}$  is proportional to  $aD$ ,

$$(R_1)_{inter} = \pi \gamma^4 \hbar^2 N_A n_p / 5 M_h a D$$

and as  $a$  bears an inverse relation to  $D$  (Eq.A.7), the error in estimating  $a$  through  $D$  measurement and the use of the Stokes-Einstein relation however does not affect the  $(R_1)_{inter}$  estimation. In spite of the small  $a_{SE}$  the validity of the hydrodynamic relation and the correct estimation of  $(R_1)_{inter}$  are quite heartening.

van Loef (1975) shows that for neat molecular liquids the packing fraction ranges from 0.465 to 0.52. Parkhurst and Jonas (1975) also show that for benzene the packing fraction is 0.493. The use of such a smaller than the hexagonally close packing fraction (0.74) will predict more agreeable diffusion coefficients. All these works advocate for an  $a$  shorter than  $a_{HCP}$ . The work of McCool, Collings and Woolf (1972) in benzene over a temperature range 15°C to 50°C at a pressure 1.01N/m gives an average  $a = 1.63\text{\AA}$  which compares favourably with the value 1.79Å obtained in the present work (Table App. 1). Although water, due to association, is fairly difficult to be understood, the contentions of Rahman and Stillinger (1971), and Walford, Clarke and Dore (197) that the water molecules can be approximated to spheres of 1Å

radius is also borne out by our Stokes-Einstein radius of 0.95 Å (see Table App. 2).

It is worthwhile chronicling two other approaches in reducing the Debye correlation time estimates or the molecular radius to explain the observations. The mutual viscosity model of Hill (1954) shows that the hydrodynamic estimates of reorientation correlation times need to be reduced to 1/5 the value, and 1/5 compares favourably to our average  $(a_{SE}/a_{HCP})^3 = 0.539$ . Longuet-Higgins and Pople (1956) show that the hard sphere radius is 9/5 times the Stokes-Einstein radius for consistency between the hard sphere thermodynamic model and the hydrodynamic result which also compares favourably with  $a_{HCP}/a_{SE} = 0.165$ .

As mentioned in Chapter 1 (p.42) the translation-rotation coupling parameters is large ( $\kappa \sim 1$ ), when the anisotropic part of the intermolecular potential is large and the translation-rotation coupling is small ( $\kappa \ll 1$ ) for very weakly anisotropic potentials.  $\kappa$  calculated using Eq. 1.25, at the highest and the lowest working temperatures in some of the presently investigated molecular liquids where the intramolecular dipolar interaction is strong enough to determine the total intramolecular relaxation are as follows:

Compound	$10^3 K/T$	$\kappa$	$10^3 K/T$	$\kappa$
$CH_3COCH_3$	3.3	0.753	2.5	1.511
$CH_3SOCH_3$	3.3	0.357	2.2	0.317
$CH_2Cl_2$	3.3	0.669	2.4	0.390
$CH_2I_2$	3.3	0.298	2.5	0.372
$C_6H_5OCH_3$	3.3	0.240	2.2	0.549
$C_6H_5CF_3$	3.3	1.846	2.3	3.679

Molecules with large spin-rotation interaction give rise to a  $\tau_{\theta 2}$  off larger than actual  $\tau_{\theta 2}$  corresponding to the intramolecular dipolar interaction. This yields a large  $\kappa$  which might mislead in suggesting a good translation-rotation coupling. The high temperature  $\kappa$  value in  $CH_3COCH_3$  is a case to the point. Although ample of translation-rotation coupling and large  $\kappa$  in  $C_6H_5CF_3$  motion is expected the  $\kappa$  values are found to be little too large (greater than 1) which is little disconcerting. The reason could lie in our  $^1H$  intramolecular dipolar relaxation rate estimation (and the consequent  $\tau_{\theta 2}$  value) being about two times larger than the values reported by others (Bull and Jonas (1970)).

The methods to theoretically estimate the translational and rotational diffusion coefficients in molecular liquids are described in the following. The Stokes-Einstein radius  $a_{SE}$  obtained from measurements (Table App. 2) can be directly

used in the Debye relation (Eq. 1.11) and

$$D_{\text{rot}} = 1/6\tau_{\theta} \quad (\text{A.9})$$

(see Abragam (1961)), to give the  $D_{\text{rot}}$  which are presented under  $D_{\text{rot}}$  SE in Table App. 3. Relations given by Eqs. A.5a and A.5b along with the translational and rotational microviscosity factors given in p.168 are used to calculate the translational and rotational diffusion constants listed under the legend HCP cum  $\mu$ visc in Table App. 3. Notwithstanding the limitation of the cubic cell model in treating the translation motion alone (Houghton (1964)) the self-diffusion coefficient predictions thereof are very good. The results presented in Table App. 3 are obtained using the relation

$$D = RT\rho v^{2/3}/6\eta M_r, \quad (\text{A.10})$$

where the cube volume  $v$  assigned to each molecule is

$$v = M_r/N_A\rho,$$

and other parameters have their usual meaning. The translational diffusion coefficients measured *in situ* are also presented in Table App. 3. All the mentioned  $D_{\text{trans}}$ ,  $D_{\text{rot}}$  calculations pertain to the temperature  $10^3\text{K}/T = 3.3$ . The rotational diffusion constant available for some of the compounds are quoted in the last column of the Table App. 3.

The agreement between the diffusion coefficient values theoretically estimated and experimentally determined is quite

TABLE APP. 3

## DIFFUSION COEFFICIENTS IN SOME MOLECULAR LIQUIDS

Compound	Cubic Cell, $D_{\text{trans}} \times 10^9$ $\text{m}^2 \text{s}^{-1}$	HCP cum $D_{\text{trans}} \times 10^9$ $\text{m}^2 \text{s}^{-1}$	Exptl. $D_{\text{trans}} \times 10^9$ $\text{m}^2 \text{s}^{-1}$	$D_{\text{rot-SF}}$ $\times 10^{-11} \text{s}$	HCP cum $D_{\text{rot-SF}}$ $\times 10^{-11} \text{s}$	Other reported $D_{\text{rot}} \times 10^{-11} \text{s}$
$\text{H}_2\text{O}$	2.58	3.14	2.46	2.36	2.30	
$\text{C}_6\text{H}_6$	2.21	2.54	2.15	0.49	0.66	
$\text{CH}_3\text{I}$	3.00	3.64	3.30	1.37	1.19	1.17 <sup>a</sup> , 1.07 <sup>b</sup> , 1.1 <sup>c</sup> , 1.4 <sup>d</sup>
$\text{CH}_3\text{CN}$	4.32	2.57	5.05	6.51	1.89	1.35 <sup>e</sup> , 1.4 <sup>f</sup> , 1.5 <sup>d</sup> , 1.51 <sup>b</sup> , 1.1 <sup>c</sup>
$\text{CH}_3\text{NO}_2$	2.49	3.00	2.30	0.74	1.09	
$\text{CH}_3\text{COCH}_3$	4.56	5.32	4.71	1.43	1.56	1.68
$\text{CH}_3\text{SOCH}_3$	0.65	0.80	0.80	0.14	0.24	0.35 <sup>g</sup>
$\text{CH}_2\text{Cl}_2$	3.51	4.10	3.41	2.23	1.32	2.2 <sup>c</sup>
$\text{CH}_2\text{I}_2$	0.56	0.64	0.56	0.12	0.18	
$\text{C}_6\text{H}_5\text{OCH}_3$	0.98	1.42	1.49	0.45	0.32	
$\text{C}_6\text{H}_5\text{CF}_3$	2.21	2.60	2.62	0.61	0.55	

<sup>a</sup>Gillen *et al* (1971), <sup>b</sup>Griffiths (1973), <sup>c</sup>Heatley (1974), <sup>d</sup>Lyerla and Levy (1974), <sup>e</sup>Bopp (1974), <sup>f</sup>Zeidler (1971), <sup>g</sup>Lyerla and Grant (1972).

good in all except the linear molecule  $\text{CH}_3\text{CN}$ . It could also be seen from Table App. 3 that this fast variation of  $D$  compared to  $\eta$  (see the corresponding activation energies in Table 4.1) gave rise to a large variation of  $D\eta/T$  over the temperature range and a quite small  $a_{\text{SE}}$  compared to  $\text{CH}_3\text{I}$  etc.. Assuming  $\text{CH}_3\text{CN}$  molecular radius to be same as the  $\text{CH}_3\text{I}$  radius ( $1.38 \text{ \AA}$ ) the calculated value of HCP cum  $\mu$  visc.  $D_{\text{trans}}$  is  $5.14 \times 10^{-9} \text{ m}^2 \text{ s}^{-1}$  and  $D_{\text{rot SE}}$  is  $1.82 \times 10^{11} \text{ s}^{-1}$  which compare favourably with the respective experimental values:  $5.08 \times 10^{-9} \text{ m}^2 \text{ s}^{-1}$  and  $1.89 \times 10^{11} \text{ s}^{-1}$ .

It suffices to conclude that if the Stokes-Einstein radii for the molecules are consistently used in the Torrey's relation for the intermolecular relaxation rates and the Debye's relation for the rotational diffusion constants, agreeable estimates of the corresponding parameters are obtained.

-\*-

*Bliss was it in that dawn to be alive*

*-Wordsworth*

# LIST OF REFERENCES

- ABRAGAM, A. (1961) *The Principle of Nuclear Magnetism* (Oxford University Press, London)
- AHN, MYONG-KU, JENSEN, S.J.K., and KIVELSON, D. (1972) *J. Chem. Phys.* 57 2940
- ANDERSON, J.E. (1969) *J. Chem. Phys.* 50 1474
- ASSINK, R.A., and JONAS, J. (1969) *J. Phys. Chem.* 73 2445
- ASSINK, R.A., and JONAS, J. (1972) *J. Chem. Phys.* 56 4975
- ATKINS, P.W. (1967) *Mol. Phys.* 12 133
- ATKINS, P.W. (1969) *Mol. Phys.* 12 321
- ATKINS, P.W., LOEWENSTEIN, A., and MARGALIT, Y.E. (1969) *Mol. Phys.* 17 329
- BARTOLI, F.J., and LITOVITZ, T.A. (1972) *J. Chem. Phys.* 56 413
- BAUER, D.R., BRAUMAN, J.I., and PECORA, R. (1974) *J. Am. Chem. Soc.* 96 6840
- BAUER, D.R., OPELLA, S.J., NELSON, D.J., and PECORA, R. (1975) *ibid.* 97 2580
- BERNE, B.J., and PECORA, R. (1976) *Dynamic Light Scattering* (John Wiley) p. 144
- BLOEMBERGEN, N., PURCELL, E.M., and POUND, R.V. (1948) *Phys. Rev.* 73 679
- BLOOM, M. BRIDGES, F., and HARDY, W. (1971) *Can. J. Phys.* 45 3533
- BLUME, R.J. (1961) *Rev. Sci. Instrum.* 32 554
- BONDI, A. (1968) *Physical Properties of Molecular Crystals, Liquids and Gases* (Wiley)
- BONERA, G., and RIGAMONTI, A. (1965) *J. Chem. Phys.* 42 171
- BOPP, T.T. (1967) *J. Chem. Phys.* 47 3621
- BROOKS, A.A., CUTNELL, J.D., STEJSKAL, E.O., and WEISS, V.W. (1968) *J. Chem. Phys.* 49 1571

- BROWN, R.J.C., GUTOWSKY, H.S., and SHIMOMURA, K. (1963) *J. Chem. Phys.* 38 76
- BULL, T.E., BARTHEL, J.S., and JONAS, J. (1971) *J. Chem. Phys.* 54 3663
- BULL, T.E., and JONAS, J. (1970) *J. Chem. Phys.* 52 4553
- CARR, H.Y., and PURCELL, E.M. (1954) *Phys. Rev.* 94 930
- CHANDLER, D. (1975) *J. Chem. Phys.* 62 1358
- CHESTER, G. (1963) *Rep. Prog. Phys.* 26 411
- CLARK, W.G. (1964) *Rev. Sci. Instrum.* 35 316
- CONSTANT, M., and FAUQUEMBERGUE, R. (1973a) *J. Chem. Phys.* 58 40
- CONSTANT, M., and FAUQUEMBERGUE, R. (1973b) *ibid.* 58 4031
- COX, A.P., and WARING, S. (1972) *J. Chem. Soc. Faraday Trans. II* 68 1060
- CUCKIER, R.I., and LAKATOS-LINDENBERG, K. (1972) *J. Chem. Phys.* 57 3427
- CUTNELL, J.D., ROEDER, S.B.W., TIGNOR, S.L., and SMITH, R.S. (1975) *J. Chem. Phys.* 62 879
- DEBYE, P. (1929) *Polar Molecules* (Dover Publications Incorporated New York)
- DEUTCH, J.M., and OPPENHEIM, I. (1968) *Advances in Magnetic Resonance*, Ed. Waugh, J.S. (Academic Press) 3 43
- DEVERELL, C. (1970) *Mol. Phys.* 18 319
- EDWARDS, J.T. (1970) *J. Chem. Educ.* 47 261
- EGELSTAFF, P.A. (1967) *An Introduction to the Liquid State* (Academic Press)
- EISNER, M., and MITCHELL, R.W. (1961) *J. Chem. Phys.* 34 651
- EVANS, G.J., and MYRON, M.W. (1976) *J. Chem. Soc. Faraday Trans. II* 72 727
- FARRAR, T.C., and BECKER, E.D. (1971) *Pulse and Fourier Transforms for NMR* (Academic Press)
- FAVELUKES, C.E., CLIFFORD, A.A., and CRAWFORD, B. JR. (1968) *J. Phys. Chem.* 72 962

- FAVRO, L.D. (1960) *Phys. Rev.* 119 53
- FEDER, W., DREIZLER, H., RUDOLPH, H.D., and TYPKE, V. (1969) *Z. Naturforsch.* 24A 266
- FLOWERS, B.H., and MENDOZA, E. (1970) *Properties of Matter* (John Wiley)
- FLYGARE, W.H., and GOODISMAN, J. (1968) *J. Chem. Phys.* 49 3122
- FRANCK, E.U., HERTZ, H.G., and RÄDLE, C. (1970) *Z. Phys. Chem. (Frankf. a. M.)* 73 18
- FUNG, B.M., and MCGAUGHY, T.W. (1976) *J. Chem. Phys.* 65 2970
- FURY, M., and JONAS, J. (1976) *J. Chem. Phys.* 65 2206
- FURY, W.H. (1957) *Phys. Rev.* 107 7
- GIERER, A., and WIRTZ, K. (1953) *Z. Naturforsch.* 8A 532
- GILLEN, K.T., and NOGGLE, J.H. (1970) *J. Chem. Phys.* 53 801
- GILLEN, K.T., SCHWARTZ, M., and NOGGLE, J.H. (1971) *Mol. Phys.* 20 899
- GILLEN, K.T., DOUGLASS, D.C., MALMBERG, M.S., and MARYOTT, A.A. (1972) *J. Chem. Phys.* 57 5170
- GORDON, R.G. (1968) *Advances in Magnetic Resonance*, Ed. Waugh, J.S. (Academic Press) Vol. 3 1
- GORDON, R.G., ARMSTRONG, R.L., and TWARD, E. (1968) *J. Chem. Phys.* 48 2655
- GREEN, D.K., and POWLES, J.G. (1965) *Proc. Phys. Soc. Lond.* 85 87
- GRIFFING, V., CARGYLE, M.A., CORVESE, L., and EBY, D. (1954) *J. Phys. Chem.* 58 1054
- GRIFFITHS, J.E. (1973) *Chem. Phys. Lett.* 21 354
- GRIFFITHS, J.E. (1974) *Molecular Motions in Liquids*, Ed. Lascombe (D. Reidel Publishing Company) p. 327
- GUTOWSKY, H.S., LAWRENSON, I.J., and SHIMOMURA, K. (1961) *Phys. Rev. Lett.* 6 349
- GUTOWSKY, H.S., and WOESSNER, D.E. (1956) *Phys. Rev.* 104 843
- HACKLEMAN, W.R., and HUBBARD, P.S. (1963) *J. Chem. Phys.* 39 2688

- HAHN, E.L. (1950) *Phys. Rev.* 80 580
- Handbook of Chemistry and Physics* (1962) Ed. in Chief Hodgman, C.D.  
(Chemical Rubber Publishing Co.) 43rd Edition
- HARMON, J.F., and MULLER, B.H. (1969) *Phys. Rev.* 182 400
- HEATLEY, F. (1974) *J. Chem. Soc. Faraday. Trans. II* 70 148
- HENNEL, J.W., and WALUGA, T. (1962) *Spectroscopy and Relaxation at Radio Frequency* (North-Holland Publishing Co.) 365
- HERTZ, H.G. (1967) *Progress in Nuclear Magnetic Resonance Spectroscopy* Eds. Emsley, J.W., Feeney, J., and Sutcliffe, L.H. (Pergamon Press) 3 158
- HERZBERG, G. (1950) *Molecular Spectra and Molecular Structure, Vol. 1. Spectra of Diatomic Molecules* (D. Van Nostrand Co. Inc.) 124
- HILL, N. (1954) *Proc. Phys. Soc. Lond.* B67 149
- HILL, N. (1955) *ibid.* B68 209
- HOUGHTON, G. (1964) *J. Chem. Phys.* 40 1628
- HU, C., and ZWANZIG, R. (1974) *J. Chem. Phys.* 60 4354
- HUBBARD, P.S. (1958a) *Phys. Rev.* 109 1153
- HUBBARD, P.S. (1958b) *ibid.* 111 1746
- HUBBARD, P.S. (1963a) *ibid.* 131 275
- HUBBARD, P.S. (1963b) *ibid.* 131 1155
- HUBBARD, P.S. (1969) *J. Chem. Phys.* 51 1647
- HUBBARD, P.S. (1972) *Phys. Rev.* A6 2421
- HUNTRESS, W.T., JR. (1968) *J. Chem. Phys.* 48 3524
- HUNTRESS, W.T., JR. (1969) *J. Phys. Chem.* 73 101
- HUNTRESS, W.T., JR. (1970) *Advances in Magnetic Resonance*,  
Ed. Waugh, J.S. (Academic Press) Vol. 4 1
- HWANG, L.P., and FREED, J.H. (1975) *J. Chem. Phys.* 63 4017
- International Critical Tables* (1928a) Ed. in Chief Washburn, E.W.  
(National Research Council, McGraw-Hill) Vol. 3 27
- ibid.* (1928b) 3 28

*ibid.* (1930a) 7 213

*ibid.* (1930b) 7 214

IVANOV, E.N. (1964) *Zhurnal Eksperimental' noi i Teoreticheskoi Fiziki* [Soviet Physics - JETP 18 1041]

JONAS, J. (1973) *Advances in Magnetic Resonance*, Ed. Waugh, J.S. (Academic Press) 6 73

KITCHLEW, A. (1971) *Ph.D. Thesis* (Indian Institute of Technology Kanpur)

KITCHLEW, A., and NAGESWARA RAO, B.D. (1972a) *J. Chem. Phys.* 56 649

KITCHLEW, A., and NAGESWARA RAO, B.D. (1972b) *ibid.* 57 3568

KITCHLEW, A., and NAGESWARA RAO, B.D. (1973a) *ibid.* 58 4033

KITCHLEW, A., and NAGESWARA RAO, B.D. (1973b) *Chem. Phys. Lett.* 18 123

KIVELSON, D., and OGAN, K. (1974) *Advances in Magnetic Resonance*, Ed. Waugh, J.S. (Academic Press) Vol. 7 72

KOGA, K., KANAZAWA, Y., and SHIMIZU, H. (1973) *J. Mol. Spectrosc.* 47 107

KOSFELD, R. (1968) *Texas A & M University N.M.R. Newsletter* No. 120 (September) 44

KRISHNA, N.R., and GORDON, S.L. (1974) *The Fifth International Symposium on Magnetic Resonance*, Bombay, India.

KRÜGER, G.J., and WEISS, R. (1970) *Z. Naturforsch.* 25A 777

KRYNICKI, K., and POWLES, J.G. (1965) *Proc. Phys. Soc. Lond.* 86 549

KUBO, R. (1957a) *J. Phys. Soc. Japan* 12 570

KUBO, R. (1957a) *ibid.* 12 1203

KUBO, R. (1966) *Rep. Prog. Phys.* 29 255

Landolt-Börnstein (1955) Vol. 4 Part 1 *Stoffwerte und Mechanische Verhalten von Nichtmetallen* 613 (Springer, Berlin)

*ibid.* (1969a) Vol. 2, Part 5a *Transport phänomene I* 246

*ibid.* (1969b) Vol. 2, Part 5a *Transport phänomene I* 195

- ibid.* (1969c) Vol. 2, Part 5a Transport phänomene I 224
- ibid.* (1971a) vol. 2, Part 1 Mechanisch-Thermische Zustandsgrößen 651
- ibid.* (1971b) vol. 2, Part 1 Mechanisch-Thermische Zustandsgrößen 674
- LEBLOND, J., UEBERSFELD, J., and KORRINGA, J. (1971) *Phys. Rev.* A4 1532
- LEIPERT, T.K., NOGGLE, J.H., and GILLEN, K.T. (1974) *J. Magn. Resonance* 13 158
- LONGUET-HIGGINS, H.C., and POPL, J.A. (1956) *J. Chem. Phys.* 25 884
- LYERLA, J.R., JR., and GRANT, D.M. (1972) *J. Phys. Chem.* 76 3213
- LYERLA, J.R., JR., GRANT, D.M., and WANG, C.H. (1971) *J. Chem. Phys.* 55 4676
- LYERLA, J.R., JR., and LEVY, G.C. (1974) *Topics in C-13 NMR Spectroscopy* (John Wiley) Vol. 1 79
- MCCALL, D.W., DOUGLASS, D.C., and ANDERSON, E.W. (1959) *J. Chem. Phys.* 31 1555
- MCCLELLAN, A.L. (1963) *Tables of Experimental Dipole Moments* (Freeman, San Francisco)
- MCCLUNG, R.E.D. (1969) *J. Chem. Phys.* 51 3842
- MCCLUNG, R.E.D. (1972) *ibid.* 57 4578
- MCCLUNG, R.E.D., and KIVELSON, D. (1968) *J. Chem. Phys.* 49 3380
- MCCOOL, M.A., COOLINGS, A.F., and WOOLF, L.A. (1972) *J. Chem. Soc. Faraday Trans. I* 68 1489
- MANSFIELD, P., and POWLES, J.G. (1963) *J. Sci. Instrum.* 40 232
- MARYOTT, A.A., FARRAR, T.C., and MALMBERG, M.S. (1971) *J. Chem. Phys.* 54 64
- MARYOTT, A.A., MALMBERG, M.S., and GILLEN, K.T. (1974) *Chem. Phys. Lett.* 25 169
- MASOOD, A.K.M., PETHRICK, R.A., BARLOW, A.J., KIM, M.G., PLOWIEC, R.P., BARRACLOUGH, D., and LADD, J.A. (1976) *Adv. Mol. Relaxation Processes* 9 29

- MILLER, C.R., and GORDON, S.L. (1970) *J. Chem. Phys.* 53 2531
- MILLS, R. (1971) *Ber. Bunsenges. Phys. Chem.* 75 195
- MILLS, R. (1973) *J. Phys. Chem.* 77 685
- MISHRA, P.K., and NAGESWARA RAO, B.D. (1974) *The Fifth International Symposium on Magnetic Resonance, Bombay, India*
- MITCHELL, R.W., and EISNER, M. (1960) *J. Chem. Phys.* 33 86
- MONIZ, W.B., and GUTOWSKY, H.S. (1963) *J. Chem. Phys.* 38 1155
- MONIZ, W.B., STEELE, W.A., and DIXON, J.A. (1963) *J. Chem. Phys.* 38 2418
- MULLER, B.H. (1966) *Phys. Lett.* A22 123
- MYERS, R.J., and GWINN, W.D. (1952) *J. Chem. Phys.* 20 1420
- NAGESWARA RAO, B.D., and MISHRA, P.K. (1974) *Chem. Phys. Lett.* 27 592
- NOACK, F. (1971) *NMR: Basic Principle and Progress*, Eds. Diehl, P. Fluck, E., and Kosfeld, R. (Springer-Verlag) Vol. 3 83
- OGATA, T., and COX, A.P. (1976) *J. Mol. Spectrosc.* 61 265
- OPPENHEIM, I. (1971) *Ber. Bunsenges. Phys. Chem.* 75 385
- O'REILLY, D.E., and PETERSON, E.M. (1971) *J. Chem. Phys.* 55 2155
- O'REILLY, D.E., PETERSON, E.M., and YASAITIS, E.L. (1972) *J. Chem Phys.* 57 890
- PAJAK, Z., ANGERER, J., SZCESŃIAK, E., WRÓŻ, and MIELNICZUK, L. (1970) *Acta Phys. Pol.* A38 91
- PARKHURST, H.J., JR., and JONAS, J. (1975) *J. Chem. Phys.* 63 2698, 2705
- PENDRED, T.L., PRITCHARD, A.M., and RICHARDS, R.E. (1966) *J. Am. Chem. Soc. (A)* 1009
- POWLES, J.G. (1966) *Molecular Relaxation Processes (The Chemical Society Special Publication No. 20, London)*
- POWLES, J.G. (1974) *Contemp. Phys.* 15 409
- POWLES, J.G., and FIGGINS, R. (1965) *Mol. Phys.* 10 155

- POWLES, J.G., and FIGGINS, R. (1967) *Annalen der Physik (Leipzig)* 19 84
- RAHMAN, A., and STILLINGER, F.H. (1971) *J. Chem. Phys.* 55 3336
- REDFIELD, A.G. (1965) *Advances in Magnetic Resonance*,  
Ed. Waugh, J.S. (Academic Press) Vol. 1 1
- ROSE, M.E. (1957) *Elementary Theory of Angular Momentum*  
(John-Wiley)
- ROTHSCHILD, W.G. (1969) *J. Chem. Phys.* 51 5187
- ROTHSCHILD, W.G. (1970a) *ibid.* 52 6543
- ROTHSCHILD, W.G. (1970b) *ibid.* 53 3265
- RUGHEIMER, J.H., and HUBBARD, P.S. (1963) *J. Chem. Phys.* 39  
552
- SANDHU, H.S. (1971) *Can. J. Phys.* 49 1069
- SANDHU, H.S. (1975) *J. Magn. Resonance* 17 34
- SANDHU, H.S. (1977) *ibid.* 26 7
- SANDHU, H.S., and PEEMOELLER, H. (1976) *J. Magn. Resonance*  
21 349
- SCHLÄFER, H.L., and SCHAFFERNICHT, W. (1960) *Angew. Chem.*  
72 618
- SHIMIZU, H. (1962) *J. Chem. Phys.* 37 765
- SHIMIZU, H. (1964) *ibid.* 40 754
- SIMPSON, J.M., and CARR, H.Y. (1958) *Phys. Rev.* 111 1201
- STEELE, W.A. (1963a) *J. Chem. Phys.* 38 2404
- STEELE, W.A. (1963b) *ibid.* 38 2411
- STEELE, W.A. (1969) *Transport Phenomena in Fluids*,  
Ed. Hanley, H.J.M. (Marcel Dekker, New York) 209
- SVEHLA, R.A. (1962) N.A.S.A. Technical Report No. R-132 p.34
- Tables of Interatomic Distances and Configurations in Molecules and  
Ions (1958) Spl. Publ. No. 11 and Supplement (1965) Spl. Publ.  
No. 18 (The Chemical Society, London)
- TORREY, H.C. (1953) *Phys. Rev.* 92 962
- TYN, M.T., and CALUS, W.F. (1975) *Processing* (April) 16

- VAN LOEF, J.J. (1975) *Physica* B79 86
- VARGAFTIK, N.B. (1975) *Tables on the Thermophysical Properties of Liquids and Gases in Normal and Dissociated States* (John Wiley) 30
- WALFORD, G., CLARKE, J.H., and DORE, J.C. (1977) *Mol. Phys.* 33 25
- WALLACH, D., and HUNTRESS, W.T. JR. (1969) *J. Chem. Phys.* 50 1219
- WANG, C.H., JONES, D.R., and CHRISTENSEN, D.H. (1976) *J. Chem. Phys.* 64 2820
- WANGSNESS, R.K., and BLOCH, F. (1953) *Phys. Rev.* 89 728
- WAUGH, J.S. (1966) *Molecular Relaxation Processes* (The Chemical Society Special Publication No. 20 London) 113
- WOESSNER, D.E. (1960) *Rev. Sci. Instrum.* 31 1146
- WOESSNER, D.E. (1962) *J. Chem. Phys.* 36 1, *ibid.* 37 647
- WOESSNER, D.E., SNOWDEN, B.S., and STROM, E.T. (1968) *Mol. Phys.* 14 265
- WOLRAB, J.E. (1967) *Rotational Spectra and Molecular Structure*, (Academic Press) pp. 418, 419
- WRIGHT, R.B., SCHWARTZ, M., and WANG, C.H. (1973) *J. Chem. Phys.* 58 5125
- YARWOOD, J. (1973) *Adv. Mol. Relaxation Processes* 5 375
- ZEIDLER, M.D. (1965) *Ber. Bunsenges. Phys. Chem.* 69 659
- ZEIDLER, M.D. (1971a) *ibid.* 75 229
- ZEIDLER, M.D. (1971b) *ibid.* 75 769
- ZEIDLER, M.D. (1975) *Mol. Phys.* 30 1441
- ZENS, A.P., and ELLIS, P.D. (1975) *J. Am. Chem. Soc.* 97 5685
- ZWANZIG, R. (1965) *Ann. Rev. Phys. Chem.* Eds. Eyring, H., Christensen, C.J., and Johnston, H.S. (Annual Reviews Inc., Palo Alto, California) Vol. 16 67